RELACIONES HÍDRICAS E INTERCAMBIO GASEOSO EN ENCINAS (QUERCUS ILEX L.) DE DEHESAS DEL SUDOESTE DE ESPAÑA

WATER RELATIONS AND GAS EXCHANGE OF HOLM-OAKS (QUERCUS ILEX L.) IN OAK-SAVANNAHS OF SW SPAIN

J.M. Infante Vázquez

Mayo de 1999

UNIVERSIDAD DE SEVILLA
DEPARTAMENTO DE BIOLOGÍA VEGETAL Y ECOLOGÍA

TD-1

UNIVERSIDAD DE SEVILLA

FACULTAD DE BIOLOGIA
BIBLIOTECA

Doy mi autorización a la Biblioteca de esta Facultad para que mi Tesis Doctoral "Relaciones hídricas e intercambio gaseoso en encinas (Quercus ilex L.) in oak-savannas of SW Spain"
sea consultada, según la modalidad/es indicadas:

- Consulta en depósito.
- (X) Préstamo interbibliotecario.
- Reproducción parcial.
- (X) Reproducción total.
- Tipo de Usuarios. (Todo tipo!)
- Otros términos.

Firmado: Juan Manuel Dufour

Sevilla, a 21 de Diciembre de 1999

UNIVERSIDAD DE SEVILLA
DEPARTAMENTO DE BIOLOGÍA VEGETAL Y ECOLOGÍA

RELACIONES HÍDRICAS E INTERCAMBIO GASEOSO EN ENCINAS (QUERCUS ILEX L.) DE DEHESAS DEL SUDOESTE DE ESPAÑA

WATER RELATIONS AND GAS EXCHANGE OF HOLM-OAKS (QUERCUS ILEX L.) IN OAK-SAVANNAHS OF SW SPAIN

Memoria para optar al grado de Doctor en Biología por la Universidad de Sevilla que presenta y firma el licenciado Juan Manuel Infante Vázquez.

Sevilla, 31 de mayo de 1999

Fdo.: J.M. Infante Vázquez

UNIVERSIDAD DE SEVILLA
DEPARTAMENTO DE BIOLOGÍA VEGETAL Y ECOLOGÍA

RELACIONES HÍDRICAS E INTERCAMBIO GASEOSO EN ENCINAS (QUERCUS ILEX L.) DE DEHESAS DEL SUDOESTE DE ESPAÑA

WATER RELATIONS AND GAS EXCHANGE OF HOLM-OAKS (QUERCUS ILEX L.) IN OAK-SAVANNAHS OF SW SPAIN

Memoria para optar al grado de Doctor en Biología por la Universidad de Sevilla que presenta Juan Manuel Infante Vázquez y que firman los Doctores Richard Joffre y Rocío Fernández Alés.

Sevilla, 31 de mayo de 1999

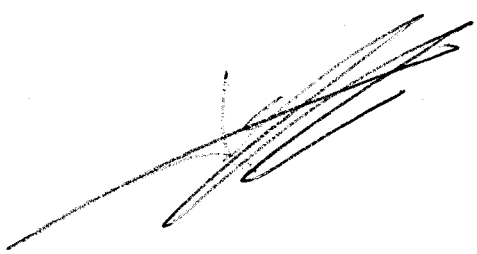

Fdo.: Richard Joffre

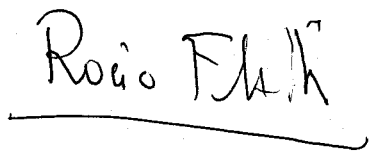

Fdo.: Rocío Fernández Alés

AGRADECIMIENTOS

En primer lugar quiero expresar mis más sincero agradecimiento a D. Richard Joffre y Dña. Rocío Fernández Alés, directores de este trabajo, sin cuyo apoyo y dedicación no habría sido posible su realización. Su trabajo, consejos y comprensión has resultado fundamentales para el desarrollo de esta tarea.

A D. Angel Martín Vicente por sus comentarios sobre el texto, así como su apoyo y buen humor, imprescindible para poder desarrollar este tipo de trabajo.

A D. José Merino y su equipo por el prestarno de material diverso.

A todos aquellos que me han echado una mano, que me han acompañado al campo, que han discutido conmigo sobre lo divino y lo humano; a todos aquellos que de alguna manera me han facilitado este, a veces, penoso trabajo: Julio, Marta, Juan, Popi, José Carlos, Chari, Juanba, Fernando, Diego, y a todo el resto del personal del Departamento de Biología Vegetal y Ecología.

A Cristina y Pablo por su apoyo incondicional, su cariño y su fe en mi trabajo. Sin ellos este trabajo no habría visto la luz.

Al resto de mi familia por apoyarme y animarme en todo momento aún sin saber exactamente lo que estaba haciendo.

A todas aquellas que saben aprovechar este apartado leyendo entre líneas, así como a aquellos que haya podido olvidar.

Los datos meteorológicos fueron amablemente cedidos por D. A. Saez Rivilla del Centro Meteorológico Territorial de Andalucía Occidental (Sevilla), y por D. S. Ruiz Hernández de la Escuala Técnica Superior de Ingenieros Industriales de Sevilla.

Este trabajo ha sido financiado por el Ministerio de Educación y Ciencia español con una beca de FPI en el extranjero (nº 91-28.719.583) y por el Programa de Medio Ambiente de la Unión Europea (MOST project, contract nº EV5V-CT92-0210).

MES REMERCIEMENTS VONT:

A M. Serge Rambal qui m'a accueilli dans son laboratoire du Centre d'Ecologie Fonctionnelle et Evolutive de Montpellier, qui a suivi avec intérêt l'évolution de ce travail, qui a permis que les travaux de recherche se déroulent dans très bonnes conditions matérielles; merci pour ses conseils, sa confiance et sa sympathie.

A Ibrahima pour son amitié et les discussions, heureusement pas toujours scientifiques.

A Claire Damesin, André Mauchamp, Jean-Marc Ourcival et Gerardo Moreno pour leur bonne humeur, leur amitié et leur discussions scientifiques toujours très fructifères.

A Dominique Guillon et Maurice Methy pour leur aide toujour sympathique et sa disponibilité.

A Christian Collin pour son aide sur le T.E., sa disposition et sa bonne humeur.

A tous ceux du terrain d'experience, les secrétaires (D. Jeanjean, O. Caggia, M. Gautier, J. Tronchessec, merci pour sa sympathie et sa patiente), les bibliothécaires (M. Bonnet, E. Gaussen et V. Nau, merci pour sa sympathie, ses bonbones et cerises), les dessinateurs, et les persones de autres équipes du CEFE (merci a J. Fabreguettes pour son aide avec les aguilles du flux de sève), qui mónt aidé à un moment ou à un autre.

A tous ceux qui mónt donné des petits ou gros coups de main, ceux qui mónt accompagné sur le terrain sans hésiter, ceux qui par leur bonne humeur et leur sourire ont rendu agréables ces quatre années de recherche au CEFE...: Luz, Claire, Rebeca, Germán, Corine, Annie, José, Elvira, Laurence, Roger....

A toutes les personnes permanentes ou de passage de l'equipe DREAM, pour leur aide.

A tous mes amies hors-CEFE, qui m'ont permis de m'evader des occupations et ont rendu agréable et inolvidâble mon sejour à Montpellier: Luz, Marife, María Jesús, Juan, Manolo, Sandino, Ade, Kerstin, Nuria (mi querida vecina), Niki, Patrice, Rocío, Teresa, Juan Carlos...

A tous ceux que jái pu oublié lors de la redaction de ces remerciements.

ACKNOWLEDGEMENTS

I thank Michael Hugues for permission to work on his farm.

I wish to thank B. Clothier, J. Stewart and anonymous reviewers for their valuable comments on the manuscript.

AGRADECIMENTOS

Á Doutora Otília Correia pelo interesse com que se dedicou à revisão deste manuscrito.

A Cristina

A mis padres

ÍNDICE

RESUMEN

Las dehesas del sur de España son unos ecosistemas caracterizados por unas densidades arbóreas bastante bajas, entre 30 y 90 árboles por hectárea, lo que da lugar a un paisaje formado por árboles completamente aislados unos de otros. Se trata de explotaciones agrosilvopastorales que se asientan en zonas de baja potencialidad agrícola. Una limitación importante a la producción de estos sistemas es la disponibilidad hídrica, debido a las fuertes fluctuaciones de la precipitación, tanto intranual (veranos secos) como interanual (sequías de varios años), características del clima mediterráneo.

El presente trabajo tiene por objetivo el estudio de las relaciones hídricas del estrato arbóreo de estos ecosistemas. Para ello se ha elegido una parcela representativa de las dehesas del sudoeste español, dominada en el estrato arbóreo por la encina (Quercus ilex L.). En ella se ha estimado el consumo de agua de los árboles, medido a través del flujo de savia, durante dieciocho meses consecutivos. También se ha medido el intercambio gaseoso foliar periódicamente a lo largo de un año. De otra parte, se ha modelizado la transpiración y la asimilación neta de la planta, con el objeto de conocer en detalle las variables ambientales que determinan estos procesos, así como poderlas integrar en el tiempo. Se discute también el papel del estrés hídrico en estos procesos.

Las encinas estudiadas poseen una dinámica de transpiración estacional bastante marcada, en particular durante el periodo seco que se extiende de junio a septiembre, y en el cual transpiran la mitad del total anual.. Se observa un ecosistema cuya vegetación arbórea posee un consumo de agua bastante bajo, un 13% de la lluvia caída para el año 1993-94, con respecto a bosques cerrados de la misma especie. El consumo anual medio fue de aproximadamente 200 mm; lo que representa entre 13.000 y 20.000 L.año^{-1}, según el tamaño de los árboles. El cociente mensual entre transpiración y evapotranspiración potencial osciló entre 0,05 y 0,27 a lo largo del año, lo que muestra una gran resistencia de la vegetación a la pérdida del agua. De otra parte, las medidas de agua en el suelo demuestran que no existen diferencias significativas entre el agua consumida por los

árboles dentro y fuera de la copa de éstos, es decir las raíces de los árboles se extienden efectivamente fuera del área de influencia de la copa.

Si se comparan los árboles aislados con los bosques cerrados de Q. ilex catalanes estudiados por Sala (1992), se observa que ambos poseen una transpiración por unidad de índice foliar (LAI) similar, y sin embargo la relación superficie xilemática-LAI es tres veces superior en los árboles aislados con respecto a los bosques cerrados.

La conductancia estomática se ha modelizado como una función de la demanda evaporativa del aire (D_a), a una escala temporal horaria y diaria. La respuesta de la apertura estomática a D_a sigue una función exponencial negativa. La misma respuesta se encontró para la conductancia del árbol entero. Dos características de la vegetación en estudio nos permiten obtener un modelo simplificado de transpiración; éstas son: un coeficiente de desconexión ("decoupling coefficient") entre la hoja y el aire circundante (Ω), próximo a cero, y una conductancia gobernada por la demanda evaporativa del aire. El modelo de transpiración se mostró apropiado a los dos niveles analizados: la hoja y el árbol. El comportamiento de este modelo es sensible al estado hídrico de la planta.

El análisis del flujo de savia muestra diferencias significativas en la densidad de flujo de savia entre distintas orientaciones del tronco analizadas; en concreto entre la orientación sur (S) y las orientaciones noreste (NE) y noroeste (NW). Estas diferencias se aprecian a una escala de tiempo diaria y estacional. La orientación NE muestra una mayor actividad a lo largo de la mañana, mientras que la orientación NW la presenta a la largo de la tarde. La orientación S muestra una menor actividad que las otras dos orientaciones, con una disminución mas o menos acusada al mediodía. Las diferencias en la dinámica fueron menos acusadas en días nublados y hacia el final del periodo de sequía, cuando la disponibilidad hídrica de la planta fue menor. Las orientaciones NE y NW presentan un flujo de savia mayor que la orientación S, exceptuando el final del periodo seco, en el cual se hacen comparables.

La teoría del "Pipe-Model" propuesta por Shinozaki, *implica un flujo sectorial en el tronco que conecta cada sector del tronco con una rama o sector de una rama diferente. En*

este sentido, la variabilidad en el flujo de savia encontrado en el tronco no puede ser explicada unicamente a través de la cantidad de radiación interceptada por la copa del árbol. Otros factores, como la arquitectura del árbol (conductividad xilemática, índice foliar) o el intercambio gaseoso foliar deben ser considerados.

Farquhar et al. (1980) y Farquhar y von Caemmerer (1982) desarrollaron un modelo mecanicista de asimilación de CO_2 en plantas C_3. El modelo ha sido recientemente utilizado en Quercus ilex por Sala y Tenhunen (1996). Este modelo, adaptado a Q. ilex, ha sido combinado con un modelo empírico de conductancia estomática y transpiración propio de las encinas de dehesa, lo que ha permitido modelizar el intercambio gaseoso de estas plantas, la eficiencia en la utilización del agua, e integrar todo ello en el tiempo. El modelo describe con precisión el intercambio gaseoso, cuando se comparan los valores modelizados con los medidos. En general, el patrón diario de intercambio gaseoso varia entre periodos secos y húmedos, siguiendo la dinámica encontrada en el flujo de savia. A nivel estacional, la mayor tasa de asimilación se da en el mes de junio, coincidiendo con la mayor tasa de transpiración. La misma relación se encuentra para las tasas mínimas que se observan en los meses más fríos, diciembre y enero.

Las bajas densidades arbóreas en los ecosistemas estudiados les proporcionan la ventaja competitiva de una mayor disponibilidad hídrica. Pero al mismo tiempo, se enfrentan a la desventaja de un mayor control climático sobre el funcionamiento de estos árboles aislados, si los comparamos con los bosques cerrados de la misma especie.

SUMMARY

Savannah ecosystems of SW Spain (dehesas) are characterised by an open tree stratum at low density, between 30 and 90 trees per hectare. The relatively low tree density gives rise to isolated trees. These agroforestry systems occupy areas of low agricultural productivity, where water availability is one of the main constrains of productivity. Water regimen is characterised by high rainfall fluctuations within the year (i.e., dry summers) as well as drought periods of several years, according to the Mediterranean regimen.

The aim of our study is to analyse the water relations of tree stratum in the dehesa ecosystems. In this way, it has been chosen a representative stand of SW Spain oak-savannahs. The tree stratum of the stand is dominated by holm oaks (Quercus ilex L.). Tree water consumption has been estimated from sap flow measurements. These measurements were recorded continuously during eighteen months. Leaf gas exchange was measured periodically during a year. Leaf transpiration and net assimilation has been modelled in order to provide a description of both, diurnal and seasonal patterns of leaf gas exchange to different environmental conditions and how these variables are affected by water availability.

The studied trees show a strong seasonal transpiration dynamics, particularly during the dry period, from June to September. During this period the tree consumed half of the annual tree water consumption. The tree stratum shows lower water consumption than dense canopies of this species, only the 13% of the annual precipitation in the hydrological year 1993-94. Annual water consumption was approximately of 200 mm (between 13,000 and 20,000 L year^{-1}, depending of the tree size). Monthly values of tree transpiration and potential evapotranspiration rate changed from 0.05 to 0.27. These results show a strong vegetation resistance to water loss. On the other hand, the measurements of water soil contents under and outside of the tree canopy showed no significant differences. Consequently we can assume a root system extended beneath of the tree canopy.

We found that transpiration per leaf area index (LAI) unit on isolated trees was comparable to dense canopies of the same species. However the xylematic surface/LAI rate is three times higher in isolated trees than in dense canopies.

The air water vapour pressure deficit (D_a) was found to be the best predictor of stomatal conductance (g_s) behaviour, at both hourly and daily time scales, in the oak-savannah ecosystem under study. The response of stomatal aperture to D_a follows a negative exponential. The same response was found for the tree conductance (g_c). Here, D_a exhibited a feedback control on g_s, that is, D_a controls stomatal aperture via leaf water flow. Two main characteristics of the vegetation under study allowed us to obtain a simplified model of transpiration: a near zero decoupling coefficient (Ω), and a surface conductance modelled by D_a. This model was found appropriate at both leaf and tree levels, with a different behaviour as a function of plant water status.

The sap flow analysis demonstrated significant differences in sap flow density among tree orientations, particularly between S orientation and NE and NW orientations. These differences have been noted at daily and seasonal time scale. The NE oriented sector showed a diurnal sap flow density course with main activity in the morning. In the NW oriented sector the main activity was in the afternoon. And the S oriented sector showed a lower activity than other sectors, with a more or less accentuated midday decrease. The diurnal differences were less pronounced in cloudy days and at the end of the drought period, when leaf water request was strongly low. Similar differences among orientations were found in daily sap flow density. The NE and NW orientations showed higher sap flow density than S orientation, excepting to the end of the drought period were values become comparable among orientations.

Shinozaki´s form of pipe model implies a sectorial flow in the trunk connecting each trunk sector with a different branch or sector of the branch. In this way, the within-tree transpiration variability founded can not be explained only by the amount of radiation intercepted by the canopy. Other factors, such as tree architecture (xylem conductivity, leaf area index) or leaf gas exchanges have to be considered.

Farquhar et al. (1980) and Farquhar & von Caemmerer (1982) developed a mechanistic model of leaf CO_2 assimilation in C_3 plants. Recently, Sala & Tenhunen (1996) used this model in Quercus ilex species. We have linked this model to our stomatal conductance and transpiration empirical models, in order to evaluate and integrate the leaf gas exchange and water use efficiency under different environmental conditions and time-levels. The modelling approach, compared to field measurements, provided a realistic description of diurnal and seasonal patterns of leaf gas-exchange response to different environmental conditions, and as affected by water availability. In general, the diurnal patterns of leaf gas exchange changed between humid and drought periods, following the sap flow dynamics. At seasonal level, the maximum leaf assimilation rate was found in June, according to the maximum transpiration rate. The same relationships were found in relation to the minimum rates, which were found in cooler months (December to January).

The low densities of trees in this ecosystem give oaks the competitive advantage of greater water availability. But at the same time, there is the disadvantage of a greater control by climatic conditions over the functioning of these isolated trees, when compared to dense forests.

RÉSUMÉ

Les "dehesas" du sud de l'Espagne sont des écosystèmes caractérisés par densités d'arbres assez basses, de 30–90 arbres à l'hectare. Ces caracteristiques donnent un paysage avec des arbres complètement isolés les uns des autres. Il s'agit d'explotations agro-sylvo-pastoraux placés en zones d'un bas potentiel agricole. Une limitation importante pour la production de ces systèmes est la disponibilité hydrique, étant donnés les fortes fluctuations des précipitations, tant intra-annuelle (étés secs) que inter-annuelle (sécheresse pendant plusieurs années), determinants du climat méditerranéen.

Le but de ce travail est l'étude des relations hydriques de le strate arborée de ces écosystèmes. Pour y arriver on a choisi une parcelle représentative des "dehesas" du sud ouest espagnol, où le strate arborée est dominé par le chêne vert (Quercus ilex L.). Dans ce parcelle on a estimé l'usage de l'eau par des arbres, mesurée avec l'aide du flux de sève pendant dix-huit mois consécutives. On a aussi mesuré de façon périodique l'échange gazeux foliaire tout au long d'un an. D'ailleurs, ou est arrivé á un modéle de transpiration et assimilation nette de la plant, pour connaître au détail quels sont les variables de l'environnement qui déterminent ces procèses áinsi que arriver à les intégrer dans le temps. On discute aussi le rôle de la contrainte hydrique dans ses mecanismes.

Les chênes verts étudiés ont une dynamique de transpiration saisonnière assez marquée, en particulier pendant la période séche de juin à septembre, où la transpiration atteinds la moitié du total annuel. Nous avons un écosystème dont la végétation arborée a une consommation d'eau assez basse, un 13% de la pluie tombée l'ánnée 1993-94, par rapport aux bois dense de la même espèce. La consommation annuelle moyenne était à peu près 200 mm; ceci représente entre 13.000 et 20.000 L.an^{-1}, selon la taille des arbres. Le quotient mensuel entre transpiration et evapotranspiration potentielle ont oscillé entre 0,05 et 0,27 au long de l'année, montrant une grande résistance de la végétation à la perte d'eau. Par ailleurs, les mesures de la teneur en eau du sol ne montrent pas des différences

significatives entre l'eau consommée par les arbre sous la canopée et hors d'elle, c'est à dire, les racines des arbres s'étendent hors de la surface d'influence de la canopée.

Si l'on compare des arbres isolés avec des bois dense de Q. ilex catalans étudies par Sala (1992), on constate une transpiration par unité de indice foliaire (LAI) similaire, cependant le rapport surface xylematique-LAI est trois fois supérieur pour les arbres isolés que pour les bois denses.

La conductance stomatique est déterminé par la demande evaporative de l'air (D_a). La réponse de l'ouverture stomatique a D_a suives une fonction exponentielle négative. Deux caracteristiques de la végétation objet d'étude nous permettent d'obtenir un modéle simplifié de transpiration; celles son: un coefficient de decouplage ("decoupling coefficient") entre la feuille et l'air environnant (Ω) près de zéro, ainsi que une conductance dirigé par la demande evaporative de l'air. Le modéle de transpiration s'a montré réussi à ces deux niveaux étudiés: la feuille et l'arbre. La conduite de ce modéle est sensible à l'état hydrique de la plante.

L'analyse du flux de sève met en évidence differences significatives pour la densité de flux de sève entre differents orientations du tronc analysés; en somme entre l'orientation sud (S) et les orientations nord est (NE) et nord ouest (NW). Ces differences son observées pour une échelle de temps journalière et seasonnière. L'orientation NE montre une majeure activité tout au long de la matinée, tandis que pour l'orientation NW une majeur activité est atteinte au long de l'aprés-midi. L'orientation S présente une activité plus petit que toutes les autres deux orientations, avec une chute plus o moins forte à midi. Les differences dans cette dynamique ont été moins marquées les jours nuageux et à la fin de la période séche, quand la disponibilité hydrique de la plante était moindre. Les orientations NE et NW presentent un flux de sève plus élevé que l'orientation S, sauf pour la période séche, où ils sont comparables.

La théorie du "Pipe-Model" proposée par Shinozaki, indique un flux sectoriel dans le tronc, que connecte chaque secteur du tronc avec une branche ou un secteur d'une branche differente. A cet égar, la variabilité du flux de sève trouvé dans le tronc ne peut pas être

expliquée uniquement par la quantité de radiation interceptée par la canopée de l'arbre. Autres facteurs comme l'architecture de l'arbre (conductivité xylematique, indice foliaire), ou l'échange gazeux des feuilles doivent être considerés.

Farquhar et al. (1980) et Farquhar et von Caemmerer (1982) ont développé un modéle mecaniciste d'assimilation de CO_2 en plants C_3. Ce modéle a été récemment utilisé en Quercus ilex par Sala et Tenhunen (1996). Il a été adapté pour Q. ilex, et combiné avec un modèle empirique de conductance stomatique et transpiration caracteristique des chênes verts de "dehesa", permettant ainsi de modéliser l'échange gazeux de ces plants, l'efficience pour l'utilisation de l'eau, ainsi q'integrer tous ces variables dans le temps. Le modèle décrit avec précision l'échanges gaseux lorsque l'on compare les valeurs modélises avec ceux mesurés. En general, le patron journalier d'échange gazeux est different entre périods séches et humides, en suivant la dynamique décrite par le flux de sève. Au niveau saisonier le taux d'assimilation plus forte est pour le mois de juin en concordance avec le taux plus elevée de transpiration. La même relation est trouvée pour les taux minimales observés pendant les mois plus froids, decembre et janvier.

Les basses densités arborées des écosystémes étudiés leur donnet l'avantage competitive d'avoir une disponibilité hydrique plus elevée. Mais au même temps ont l'inconvénient d'être plus controlés par le climat quant au functionnement de ces arbres isolés, comparés avec de bois dense de la même espéce.

I. INTRODUCTION

In the western part of Mediterranean basin, oak forests and woodlands cover about 10 million hectares. Two main types of structure can be distinguished. First, the coppices of southern France, Italy and Eastern Spain dominated by *Quercus ilex* and *Q. pubescens*, whose main products in the past were firewood and charcoal; second, the savannah-like landscapes of the Iberian Peninsula known as "dehesas" (in Spain) and "montados" (in Portugal) where *Q. ilex* (holm oak) and *Q. suber* (cork-oak) are a dominant part of the agroforestry systems and produce fodder for livestock as well as cork and firewood (Joffre et al., 1988; 1991).

Traditionally it has been considered that the holm oaks of coppices and dehesas were different species: *Quercus ilex* in coppices and *Q. rotundifolia* in dehesas. Recently, studies about the genetic of the *Quercus* genus, and particularly of *Q. ilex* species, shown that *Q. rotundifolia* and *Q. ilex* are the same species (Michaud et al., 1992). The holm oak is classified as *Quercus rotundifolia* Lam. according to the European Flora (Tutin et al., 1964), but is classified as *Quercus ilex* subsp. *ballota* according to the Iberian Flora (Castroviejo et al., 1990). In this way, we have used the name *Quercus ilex*, as the name commonly used in scientific literature.

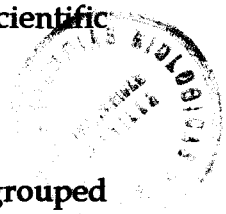

The main ecological constraints acting on these ecosystems can be grouped under three headings: (1) water availability -in terms of the length of the dry season and the high variability in annual precipitation-, (2) nutrient availability -due to low levels of nitrogen and phosphorus-, and (3) human activity. Understanding the role of these constraints will improve the prediction of the response of these ecosystems to future environmental changes.

The scope of this work will be centred on water relations, concerning ecological constraints, and dehesas ecosystems, concerning vegetation structure.

1.1. STATE OF THE ART

The Mediterranean vegetation shows adaptations to strong seasonality in climatic conditions (Schulze et al., 1987; Abrams, 1990; Salleo & Lo Gullo, 1990; Acherar & Rambal, 1992), in order to optimise plant production and water use efficiency (Tenhunen et al, 1990; Rambal, 1993; Sala & Tenhunen, 1994). In order to cope with such temporal variability, holm oak species react principally by changes in opening stomata, and this has an effect on net CO_2 assimilation.

The water relations in *Quercus ilex* have been studied in detail in dense coppices of Cataluña (NE Spain) (Piñol et al., 1992; Terradas & Savé, 1992; Castell et al., 1994; Sala et al., 1994; Sala & Tenhunen, 1994; Sala & Tenhunen, 1996;) as well as in other forests of the Mediterranean basin (Pitacco et al., 1992; Rambal, 1992; Lo Gullo & Salleo, 1993; Chaves et al., 1995; Damesin, 1996). Among the main results of those works we can emphasise that water stress during the summer periods is strongly dependent on the precipitation during the preceding fall, winter, and spring. During the water strees period they found a strong stomatal limitation to water loss, with different sensibility of sun and shade leaves to air water vapour pressure deficit. On the other hand, low intrinsic photosynthetic rates in this species are compensated by long periods of photosynthetic activity.

The water relations in isolated trees of dehesas and montados have been poorly studied. We can point out the work of Joffre & Rambal (1993) about the water balance on the dehesas ecosystems in Sierra Norte de Sevilla (SW Spain). But this one analyses mainly the water relations between the tree and the grass components of these ecosystems. Recently, Oliveira et al. (1992) and Oliveira (1995) have worked on the ecophysiology of *Q. suber*, in montados of SW Portugal. The main conclusions of their work were that the water availability to the trees was surprisingly high; vapour pressure deficit and air temperature were the most limiting environmental factors to stomatal conductance during the warmer seasons; and that maximum daily photosynthetic rates remained constant

throughout spring and summer, although daily net carbon assimilation decreased as the dry season progressed (Oliveira, 1995).

Our working hypothesis considers that oak savannahs of southern Spain are adapted to along, dry summers and irregular annual water availability. The present study meet an important gap in the knowledge of key processes involved in the plant transpiration and CO_2 assimilation on isolated holm oaks. The results will provide an important basis for further studies on this species, and might contribute to development of models on the productivity of forest systems such as the dehesas.

1.2. OBJECTIVES

The present work has the aim of study the holm oak species, the tree species more representative of dehesas ecosystems. The objectives are: 1) To analyse transpiration on isolated trees and relate it with environmental variables: water availability and air water vapour pressure deficit; 2) To analyse leaf net CO_2 assimilation and the relationships between net assimilation and transpiration.

The result obtained have been assembled in different chapters as follows:

In **chapter II**, we describe the material and methods used in this work. This section includes the description of the study site, and the methods used for estimating transpiration at tree and leaf level, leaf net CO_2 assimilation and environmental conditions through the studied period.

Chapter III describes water consumption of trees, estimated from sap flow measurements, monitored continuously from May 1993 to October 1994. The

water consumption is then contrasted with soil water content measurements beneath the tree canopy, and outside the tree canopy projected area..

In **chapter IV,** the transpiration processes both at leaf and tree scale are analysed and modelled. The main steps are the identification of all parameters and assumptions involved in the modelling procedure. The results of the model have been tested against experimental data.

The aim of **chapter V** is to show the within-crown differences in transpiration rates on isolated trees, in relation with the tree-crown orientation. The patterns of water consumption in different tree orientations are described. We discuss four possible mechanisms to explain the different diurnal and seasonal patterns in sap flow on the different plant sides.

In **chapter VI,** leaf gas exchange is modelled and evaluated in order to integrate this gas exchange under different environmental conditions and time-levels. For this purpose, we used a modified version of the Farquhar's model of C_3 leaf CO_2 assimilation. This model is combined with the empirical models of stomatal conductance and transpiration developed in this study. The effect of water stress on leaf water loss and carbon assimilation is evaluated.

In the final **chapter (VII),** the main conclusions derived from this work are exposed.

II. MATERIAL Y MÉTODOS

2.1. ZONA DE ESTUDIO

El trabajo de campo se llevó a cabo en una parcela localizada en el término municipal de Castilblanco de los Arroyos (37° 41' N, 5° 55' W, 280 m sobre el nivel del mar), 40 km al norte de Sevilla (Foto 2.1). Se trata de una dehesa de encinas (*Quercus ilex* L.) con una densidad de 40 árboles.ha^{-1}, lo que permite el desarrollo de un estrato herbáceo importante (única vegetación acompañante) compuesto fundamentalmente por especies anuales. La pendiente de la parcela es inferior al 0.5%.

La zona de estudio fue elegida por dos motivos principales: es representativa de lo que son las dehesas de la Sierra Norte de Sevilla, y se dispone de un amplio conocimiento del funcionamiento de su suelo (Joffre, 1987; Joffre & Rambal, 1988), del estrato herbáceo (Vacher, 1984; Joffre, 1987; Joffre et al., 1987; Ortega, 1987; Leiva, 1991; Roldan, 1993) y de la interacción pasto-árbol (Joffre, 1987; Joffre & Rambal, 1993).

2.1.1. Climatología

El clima es típico mediterráneo, de tipo Csb según la clasificación de Köppen (Strahler, 1986), con inviernos templados y veranos secos y cálidos. La precipitación media anual es de 720 mm (periodo 1960-92), repartiéndose el 90% de la lluvia entre octubre y mayo. El periodo estival, con una media de 120 días al año (Joffre, 1987), se caracteriza por la ausencia total de lluvias.

El trabajo de campo se realizó entre los años 1993 y 1995, en los que la precipitación fue inferior a la media anual (Fig. 2.1). El reparto de la lluvia también fue diferente, con mucha menos precipitación en invierno en ambos años y mayor en otoño (Fig. 2.2).

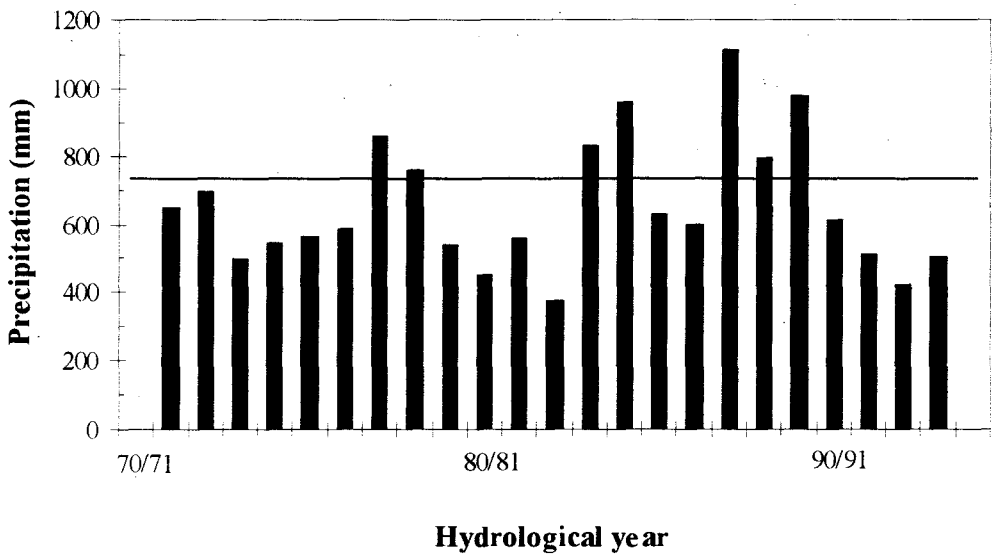

Figure 2.1. Annual (hydrological year) rainfall distribution in the study site (histogram) between 1971 and 1994. The solid line represents the value of the mean annual precipitation (720 mm) at Castilblanco (period 1960-92).

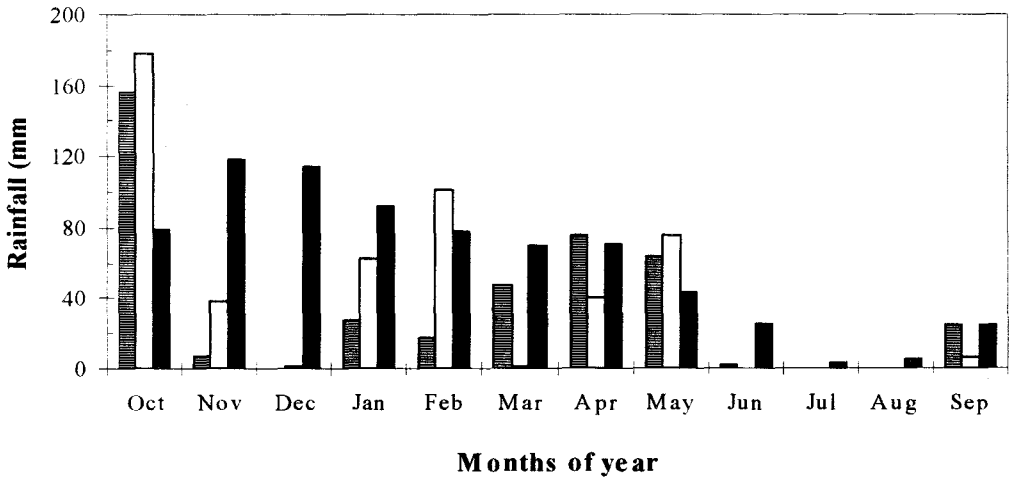

Figure 2.2. Monthly rainfall distribution in the study site. The histograms represent the year 1992-93 (horizontal lines), year 1993-94 (unfilled histogram) and the mean of the site for the period 1960-92 (filled histogram).

2.1.2. *Suelo*

El sustrato litológico corresponde a granitos sienitas pórfidos (Mapas provinciales de suelos, 1975). El suelo es pardo, muy profundo (> 80 cm) y con textura franco-arenosa en superficie (0–20 cm), y de franco a franco-arcillosa en profundidad (20 cm en adelante) (Tabla 2.1). Tanto la textura como el contenido de nutrientes que se da en esta parcela es característica de los suelos de la Sierra Norte.

Table 2.1. Some physical characteristics of the soils in the studied site. *Outside* refers to soil samples located outside the tree crown, and *Under* to soil samples located under the trees. *d* is the dry bulk density, in g cm^{-3}, *s* and *c* are the percentages of sand and clay respectively and *Tc* the textural class (from Joffre & Rambal, 1988).

	Outside				*Under*			
Depth (cm)	*d*	*s*	*c*	*Tc*	*d*	*s*	*c*	*Tc*
0-20	1.61	57.6	12.7	Sandy Loam	1.53	53.6	10.9	Sandy Loam
20-40	1.65	48.8	22.4	Loam	1.65	36.1	29.4	Clay Loam
40-80	1.77	41.1	30.7	Clay Loam	1.77	28.6	33.7	Clay Loam
> 80	1.67	42.8	13.1	Loam	1.67	43.3	13.7	Loam

2.1.3. *Vegetación*

El estudio se ha realizado dentro de una parcela de 50 x 50 m protegida del pastoreo. Dentro de la parcela se escogieron tres árboles (1, 3, 5) sobre los que se realizaron los diferentes experimentos. Los árboles son representativos del área de estudio. Las características de los tres árboles estudiados se detalla en la Tabla 2.2. El área de xilema referido en la tabla corresponde al utilizado en los cálculos del

volumen de flujo de savia. La altura del tronco se midió desde el suelo hasta el punto de bifurcación de las ramas principales. Los árboles 1 y 3 tienen dos ramas principales, y el árbol 5 tiene tres.

Table 2.2. Structural characteristics of the studied trees. Sapwood area corresponds to which used in sap flow calculations. The trunk height is the height from which the trunk divides into principal branches.

	Tree 1	Tree 3	Tree 5
Tree height (m)	7	8	8
Trunk height (cm)	165	190	255
Diameter at breast height (cm)	36.6	44.6	54.2
Sapwood area (cm^2)	201	251	308
Projected canopy surface (m^2)	66.3	75.3	119.2

2.2. *METODOLOGÍA*

2.2.1. *Variables climáticas*

La temperatura del aire, la humedad relativa del aire, la radiación global, el *PAR* (radiación fotosintéticamente activa, 400-700 nm), la velocidad del viento y la precipitación fueron medidas automáticamente por medio de una estación meteorológica automática (Campbell Scientific Ltd., Leicestershire, UK) localizada a unos 200 m de la parcela de estudio. Esta estación funcionó midiendo dichas variables climáticas desde el 15 de febrero de 1994 hasta el 31 de enero de 1995. Igualmente midió la temperatura del aire y la radiación global del 30 de julio al 30 de septiembre de 1993. Todas las medidas se registraron con una frecuencia de media hora.

De mayo a octubre de 1993 los datos de temperatura del aire, humedad relativa del aire y radiación global fueron medidos en dos estaciones automáticas de la ciudad de Sevilla; temperatura y humedad en la estación de Tablada (37° 21′ N, 6° 00′ W, 9 m sobre el nivel del mar), y radiación global en la ETSII (Escuela Técnica Superior de Ingenieros Industriales; 37° 22′ N, 5° 59′ W, 30 m sobre el nivel del mar).

La evopotranspiración potencial y la precipitación fueron medidas diariamente, entre marzo de 1993 y enero de 1995, en el pantano de Cala y en Castilblanco de los Arroyos (estaciones de la Confederación del Guadalquivir), a 12 y 2 km de distancia de la zona de estudio respectivamente.

2.2.2. *Flujo de savia*

Los diferentes métodos de medición del flujo de savia proporcionan una estima bastante precisa de la transpiración tanto de bosques (Schulze et al., 1985; Granier, 1987; Köstner et al., 1992; Heiman & Strickan, 1993; Farrington et al., 1994) como de árboles aislados (Green, 1993). Existen varios métodos de medida basados en el intercambio de calor; Swanson (1994) y Biron (1994) hacen una síntesis detallada de la evolución histórica de los métodos de medición de flujo de savia basados en intercambio de calor. En este estudio se ha utilizado el método de Granier (Granier, 1985; 1987), que se ha revelado como un método preciso para la estimación de la transpiración del árbol entero (Granier, 1987; Granier et al., 1990; Biron, 1994; Goulden & Field, 1994; Granier & Loustau, 1994).

El método consiste en dos agujas de 20 mm de longitud y 2 mm de diámetro, las cuales se insertan en el xilema del tronco, a una altura de 1,5 m, una encima de la otra con una distancia entre ellas de 150 mm aproximadamente. Ambas agujas están equipadas con un termopar que mide la temperatura media de los 20 mm de aguja, y tienen una resistencia enrollada (Fig. 2.3). La aguja superior se calienta a una temperatura constante con la resistencia, sirviendo la inferior para medir la

temperatura del tronco (temperatura de referencia). Lo que mide el sensor es la diferencia de temperatura entre ambas agujas; la diferencia de temperatura entre sensores será máxima cuando el flujo de savia sea cero, y disminuirá a medida que aumente este flujo. El tronco del árbol es aislado térmicamente con lana de vidrio, la cual sobrepasa a los sensores unos 35 cm por arriba y por abajo de éstos.

La densidad media de flujo ($m^3.m^{-2}.h^{-1}$) o velocidad ($m.h^{-1}$) v a lo largo de un radio dado fue calculada por Granier (1985) mediante la calibración con diferentes especies:

$$v = 119 \cdot 10^{-6} K^{1,231} \qquad \text{(Eqn. 2.1)}$$

donde K es una variable adimensional, que se calcula como:

$$K = \Delta Tm - \Delta T / \Delta T \qquad \text{(Eqn. 2.2)}$$

donde ΔTm y ΔT son las diferencias de temperatura entre las dos agujas del sensor, en condiciones de ausencia de flujo ($v = 0$) y para un flujo de savia positivo ($v > 0$), respectivamente.

El consumo en litros se calcula multiplicando la velocidad o densidad de flujo por la superficie que atraviesa dicho flujo. En nuestro caso será una corona de xilema de 20 mm de ancho, que es la longitud de las agujas utilizadas. Esta longitud se considera suficiente para medir más del 90% del flujo de savia que atraviesa el tejido conductor, como ponen de manifiesto Granier et al. (1994). Medidas del grosor del xilema realizada en nuestros árboles así lo avalan.

Cada árbol fue equipado con tres sensores que midieron el flujo de savia en tres sectores diferentes del tronco: 0-120°, 120-240° y 240-360° (denominadas NE, S y NW, respectivamente). Las medidas se realizaron con un intervalo de 2 minutos, registrándose valores medios cada media hora en un Data Logger (modelo 21X, Campbell Scientific Ltd., Leicestershire, UK). Las medidas de flujo de savia se

realizaron continuamente desde el 19 de mayo de 1993 hasta el 21 de octubre de 1994, en los árboles 1 y 3, y desde el 15 de agosto de 1993 hasta el 21 de octubre de 1994, en el árbol 5.

2.2.3. *Intercambio gaseoso*

Las medidas de intercambio gaseoso (conductancia estomática, transpiración y fotosíntesis) se realizaron en hojas aisladas con una cámara de intercambio gaseoso (modelo DL-2 Leaf Chamber Analyser; ADC Ltd., Hoddesdon, England), que mide con un analizador en infrarrojo del CO_2 (Infrared gas analyser, IRGA) que estima el intercambio de este gas entre la hoja y el aire que la circunda. Mide igualmente la temperatura de la hoja y el *PAR* (Photosynthetically active radiation, 400-700 nm) incidente sobre ésta. Más detalles de la metodología empleada han sido dados por Field et al. (1991).

Se llevaron a cabo entre junio de 1994 y enero de 1995. En junio los días 15, 16 y 17; en agosto los días 18 y 24; en septiembre los días 5, 21, 28 y 30; en noviembre los días 29 y 30; y en enero los días 4 y 9.

Se realizaron en hojas aisladas, dispuestas en ramas orientadas al sur, eligiendo esta orientación por disponer de más horas de sol al día. Se utilizó siempre la misma rama para un día dado, pero diferentes hojas a lo largo del día con el fin de no dañarlas excesivamente con las medidas sucesivas. El tiempo medio de estancia de la hoja en la cámara de medida fue de 45 segundos. Las medidas se realizaron con una frecuencia de una hora, desde la salida del sol hasta su puesta. En cada medida se midieron entre 5 y 7 hojas.

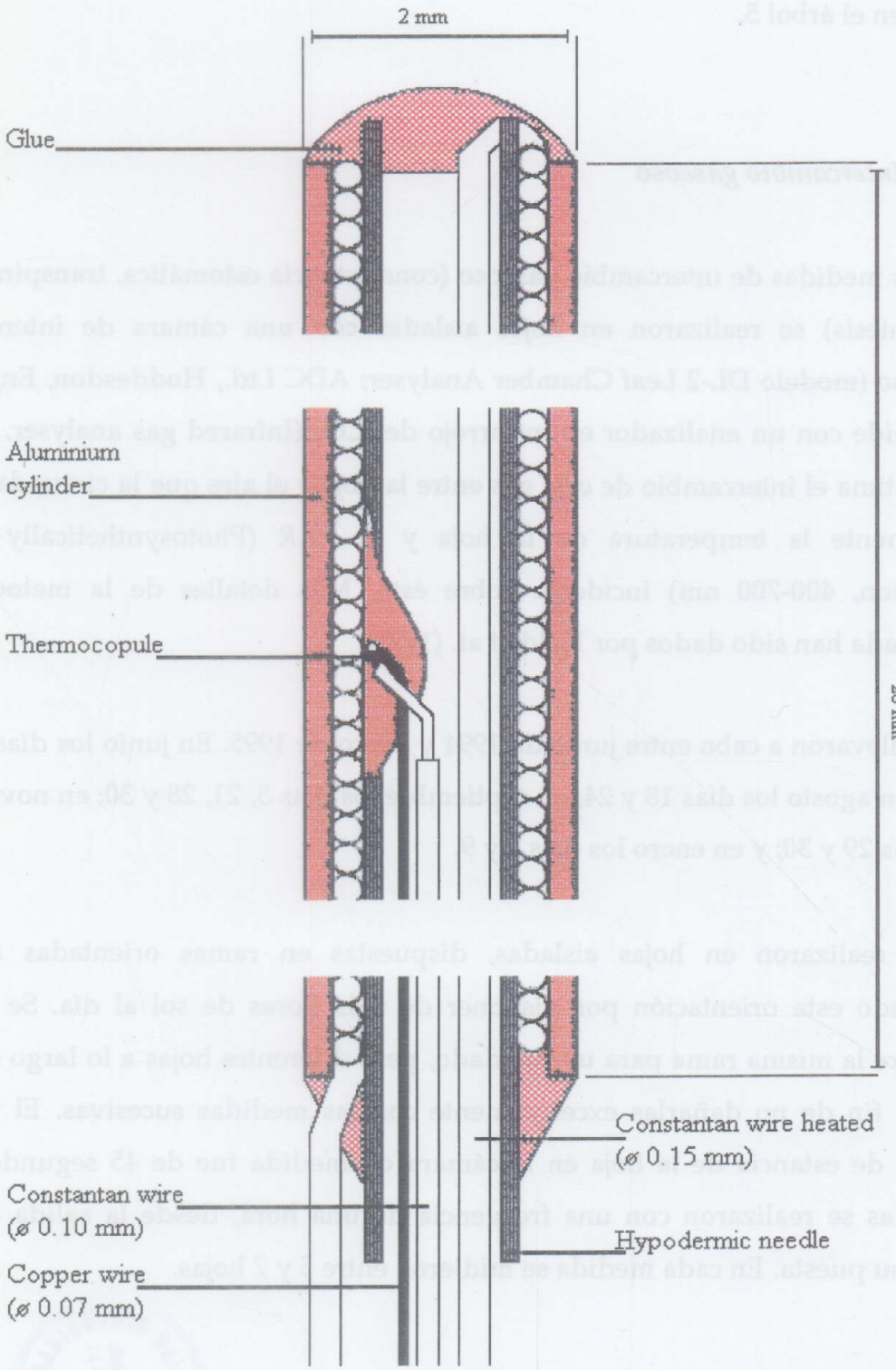

Figure 2.3. Longitudinal sectional view of the heating probe (from Granier, 1985).

2.2.4. *Índice foliar*

El índice foliar (*LAI*) de los árboles fue medido de forma instantánea con el Line Quantum Sensor (LI-COR 191SB, LI-COR, Ltd., Nebraska, USA) de 1 m de longitud. Este método estima el índice foliar de la copa de los árboles por medio de la extinción del *PAR* a través de la copa del árbol. La transmitancia de la copa es convertida en *LAI* usando la ley de Beer-Lambert:

$$LAI = -Ln\ (Q_i/Q_o) / k \qquad \text{(Eqn. 2.3)}$$

donde Q_i es el *PAR* medido bajo la copa, Q_o es el *PAR* total incidente sobre la planta, y k es el coeficiente de extinción de la luz, característico de la vegetación en estudio. En este caso se utilizó una k de 0,732 propuesta por Baldocchi et al. (1984). Este método ha sido utilizado con éxito en la estimación indirecta del índice foliar en muy diversos ecosistemas forestales (Marshall & Waring, 1986; Burton et al., 1991; Nel & Wessman, 1993; Brown & Parker, 1994).

Las medidas de *LAI* se llevaron siempre a cabo en días soleados y próximas al mediodía solar, entre las 11:00 y las 13:00 horas solar. Se midieron aproximadamente 30 puntos por árbol (Q_i), con diferentes puntos intermedios medidos fuera de la copa de los árboles (Q_o). Las medidas bajo la copa se hicieron siguiendo una cuadrícula regular con un marco de 1 x 1 m.

2.2.5. *Potencial hídrico foliar*

El potencial hídrico de la planta fue medido según el método desarrollado por Scholander et al. (1965). Para ello se utilizó una bomba de presión (modelo PMS 1000, Corvallis, Oregon, USA), conocida también como bomba de Scholander, con un manómetro que podía soportar hasta 7 MPa de presión. Para cada medida se seleccionó una rama pequeña (con unas 5-10 hojas) orientada al sur, la cual se

medía inmediatamente después de ser cortada del árbol. La orientación elegida fue la misma que para el intercambio gaseoso con el fin de homogeneizar las condiciones de estudio para las diferentes variables fisiológicas.

El potencial de la mañana (Ψ_p) se corresponde con el potencial hídrico foliar de la planta antes de la salida del sol, y el potencial mínimo (Ψ_m) se corresponde con el potencial hídrico foliar de la planta al mediodía solar. El Ψ_p y el Ψ_m fueron medidos en 1993 los días 22 de junio, 10 de agosto y 29 de septiembre. En 1994 se midieron los días 26 de marzo, 27 de abril, 15, 16 y 17 de junio, 18 de julio, 12, 18 y 24 de agosto, 5, 7, 21, 28 y 30 de septiembre, y 29 y 30 de noviembre. En 1995 se midieron los días 4 y 9 de enero.

2.2.6. *Contenido de agua en el suelo*

Se midió la cantidad de agua en el suelo bajo la copa de los árboles en estudio, y fuera de ella. Para ello fueron utilizados tubos de aluminio instalados por Joffre (1987) a una profundidad de 160 cm. Estos tubos han sido utilizados en diferentes ocasiones para estimar la cantidad de agua en el suelo de la parcela en la que se encuentran (Joffre, 1987; Joffre & Rambal, 1988; 1993). La cantidad de agua en el suelo se midió con una sonda de neutrones (Ronly Electronic Limited, D.M.G. 11, source 3700 Mbq ^{241} Am-Be, neutron detector $^{10}BF_3$, detector length 18 cm). Las medidas se realizaron en los tubos cada 10 cm hasta los 50 cm, y cada 20 cm hasta los 150 cm de profundidad. Un reflector hemisférico de poliestireno fue usado para corregir la medida realizada a los 10 cm de profundidad.

La cantidad de agua almacenada en el suelo fue calculada mediante una integración numérica de la cantidad de agua medida en cada uno de los perfiles (tubos). Para un perfil dado, el agua media contenida en el perfil fue considerada igual al agua almacenada (en cm) dividida por la profundidad del perfil, expresada en la misma unidad. Para más detalles sobre la textura de cada estrato y el método de calibración ver Joffre (1987) y Joffre & Rambal (1988). Se utilizaron

sus curvas de calibración –la de los autores mencionados- de cada estrato para el cálculo del contenido de agua en los perfiles.

La distribución de los tubos medidos fue la siguiente: fuera de la copa de los árboles se utilizaron tres tubos a una distancia media de 8 m al tronco del árbol más próximo. Bajo los árboles 1 y 3 se midió un sólo tubo. Bajo el árbol 5 se midieron tres tubos. La distancia de los tubos bajo los árboles al tronco fue la mitad del radio de la proyección de la copa.

Las medidas de la cantidad de agua en el suelo fueron realizadas los días 28 de julio, 10 de agosto y 29 de septiembre de 1993. En 1994 se llevaron a cabo dichas medidas los días 27 de marzo, 26 de abril, 10 y 25 de mayo, 9 y 20 de junio, 7 y 19 de julio, 12 de agosto, 5 y 20 de septiembre, y 30 de noviembre.

2.2.7. *Otros dispositivos experimentales: estrés hídrico artificial*

Con el fin de provocar un cierto estrés hídrico adicional en uno de los árboles, entre marzo y noviembre de 1994 se instaló un plástico sobre el suelo del árbol 3, que impermeabilizó totalmente la superficie cubierta (Foto 2.2). Con ello se evitó tanto la precipitación sobre el suelo de la planta como la evapotranspiración de dicho suelo. El plástico tenía una superficie de 150 m^2, y cubría aproximadamente un metro y medio más allá de la proyección de la copa del árbol.

Bajo el plástico se puso una capa de polietileno como aislante térmico, con el fin de evitar el calentamiento de la capa más superficial del suelo. Igualmente, sobre el plástico se esparcieron ramas y hojas de un árbol contiguo con el fin de reducir substancialmente el albedo provocado por el plástico y el polietileno.

Foto 2.1. Vista general de la parcela de experimentación de Navalagrulla (Castilblanco de los Arroyos, Sevilla).

Foto 2.2. Detalle del plástico instalado bajo el Árbol 3, aún no se había cubierto el plástico con ramas de otro árbol para disminuir el albedo del plástico.

III. TRANSPIRACIÓN DEL ÁRBOL MEDIDA A TRAVÉS DEL FLUJO DE SAVIA: PATRONES DIARIOS Y ESTACIONALES

3.1. INTRODUCCIÓN

Numerosos estudios sobre las relaciones hídricas en plantas se llevan a cabo a partir del análisis de la transpiración de hojas individuales o grupos reducidos de éstas, medidas por porometría. Las respuestas de las hojas han sido a menudo utilizadas para realizar predicciones a nivel de la planta entera e incluso de ecosistemas. Sin embargo, la respuesta de una hoja no es paralela a la de toda la planta bajo todo tipo de situaciones, debido a la variabilidad de las condiciones que se pueden encontrar en el interior de la copa. Para estudiar las relaciones hídricas de los árboles de las dehesas, se hace necesario conocer la transpiración de toda la planta, teniendo en consideración la variabilidad intrínseca de los elementos que forman la copa. La estima de la transpiración a nivel del árbol se puede hacer midiendo el flujo de savia en el tronco en diferentes orientaciones.

Los objetivos del presente capítulo son 1) describir la dinámica temporal del flujo de savia; 2) cuantificar el consumo de agua por los árboles; y 3) relacionar transpiración y disponibilidad hídrica.

Dentro de este tercer objetivo, se pretendió estudiar la respuesta de la transpiración a un estrés hídrico severo, y para ello se evitó toda precipitación sobre el suelo de uno de los árboles mediante la instalación de un plástico aislante. Este plástico también impidió la evaporación del agua del suelo cubierto.

3.2. *MATERIAL Y MÉTODOS*

3.2.1. *Flujo de savia*

Las medidas de flujo de savia se realizaron continuamente desde el 19 de mayo de 1993 hasta el 21 de octubre de 1994, en los árboles 1 y 3. El árbol 5 se comenzó a medir a partir del 15 de agosto de 1993, finalizándose en la misma fecha que los otros dos. El valor del flujo de savia por árbol corresponde a la media de los tres sensores instalados en cada árbol.

Para comparar la transpiración con la evapotranspiración potencial (*ETP*) o la precipitación se debe convertir en litros por metro cuadrado, o lo que es lo mismo mm. Para pasar de litros a mm se divide por una superficie; así se pueden obtener dos medidas de transpiración: una a nivel de individuo, y otra a nivel de parcela (por hectárea). En el cálculo de la transpiración, en mm, de un individuo se considera la superficie de la proyección de la copa, y se obtiene la transpiración real por árbol (*TRt*) o por m^2 de superficie cubierta. En el caso de la transpiración por hectárea (*TRh*) se calcula el consumo medio por árbol, y se multiplica por la densidad arbórea. En este último caso se obtiene un valor meramente orientativo, ya que se extrapola el consumo de tres árboles a toda una hectárea sin tener en cuenta la variabilidad de árboles en esta superficie. El único fin de este cálculo es el tener un orden de magnitud del consumo por hectárea, con el objeto de comparar con otros ecosistemas.

3.2.2. *Medidas fisiológicas*

Las medidas de Ψ_p, Ψ_m y ciclos diraios de potencial hídrico e llevaron a cabo entre junio y septiembre de 1993, y de marzo de 1994 a enero de 1995.

En los árboles 1y 3 se realizó un ciclo diario de conductancia estomática y transpiración de las hojas el 10 de agosto de 1993.

3.2.3. *Medidas de contenido de agua en el suelo*

El contenido de agua en los 160 cm de suelo se midió entre julio y septiembre de 1993, y de marzo a noviembre de 1994 bajo los árboles 1 y 5, así como fuera de los árboles. Las fechas exactas se detallan en el capítulo II. El agua en el suelo fuera de la influencia de la copa de los árboles se ha estimado promediando las medidas en los tres tubos fuera de la copa de los árboles. El agua en el suelo bajo la copa del árbol 5 es el promedio de las medidas de los tres tubos situados allí; y bajo la copa del árbol 1 son las medidas de un solo tubo.

No han sido utilizados los datos referentes a los tubos bajo el árbol 3 ya que presentaron una serie de problemas a lo largo del verano de 1994, y no han aportado ninguna información sobre el contenido de agua bajo este árbol.

3.3. *Resultados*

3.3.1. *Climatología del periodo de estudio*

En la Figura 3.1 se representa la *ETP* mensual ($mm.mes^{-1}$), la precipitación diaria ($mm.día^{-1}$) y radiación global acumulada diaria (H_g, $MJ.m^{-2}.día^{-1}$) para el periodo de estudio. La *ETP* total para el año hidrológico 1993-94 fue de 1318 mm; alcanzándose siempre los picos máximos de *ETP* en los meses de julio y agosto, con valores superiores a 200 mm por mes. En el verano de 1993 se registró la mayor *ETP* mensual, llegando a alcanzar un valor máximo de 275 mm.

Para este mismo año hidrológico (1993-94) se registraron 503 mm de precipitación en la zona, lo que representó un 30% menos de lluvia con respecto a la media. Ésta se repartió por igual a lo largo del periodo húmedo (de principios de octubre a finales de mayo), destacando los meses de octubre y febrero con 178 y 101 mm, respectivamente. La precipitación diaria durante el periodo de estudio

nunca fue superior a los 35 mm.día^{-1}. Si consideramos un periodo seco como aquel que se extiende entre dos días con lluvias inferiores a 5 mm (Joffre & Rambal, 1993), los periodos secos tuvieron una extensión de 114 y 123 días en 1993 y 1994, respectivamente.

Para días despejados, los valores máximos diarios de H_g se midieron en el mes de junio, siendo éstos alrededor de 30 MJ.m^{-2}.día^{-1}, y los valores mínimos en los meses de noviembre y diciembre, alrededor de 10 MJ.m^{-2}.día^{-1}. Similares valores de H_g se registraron en los dos veranos estudiados.

3.3.2. Flujo de savia del árbol

3.3.2.1. Patrones diarios

En los árboles 1 y 3 se ha comparado la dinámica a lo largo del día de la transpiración de hojas orientadas al sur con la dinámica del flujo de savia en los sensores de estos árboles orientados al sur (Fig. 3.2). Esta comparación se realizó para el día 10 de agosto de 1993; un día típico de verano. La dinámica de la transpiración de la hoja presenta un pico durante la mañana, posteriormente una disminución al mediodía, y un segundo pico al final de la tarde, más grande que el de la mañana. Este patrón de transpiración foliar se repite en los dos árboles estudiados (Fig. 3.2), pero con diferente rango de valores. La transpiración máxima medida fue de 7,25 y 10,47 mmol.m^{-2}.s^{-1} para los árboles 1 y 3, respectivamente. La dinámica del flujo de savia fue comparable a la de la transpiración foliar tanto en su forma como en la duración (Fig. 3.2), pero con un pequeño desfase de una hora y media, aproximadamente. Esto se aprecia mejor en el árbol 3 (Fig. 3.2B).

Se representa en la Figura 3.3a y b la evolución a lo largo del día del flujo de savia del árbol 5 para las cuatro estaciones del año en días despejados. Los otros dos árboles mostraron la misma dinámica.

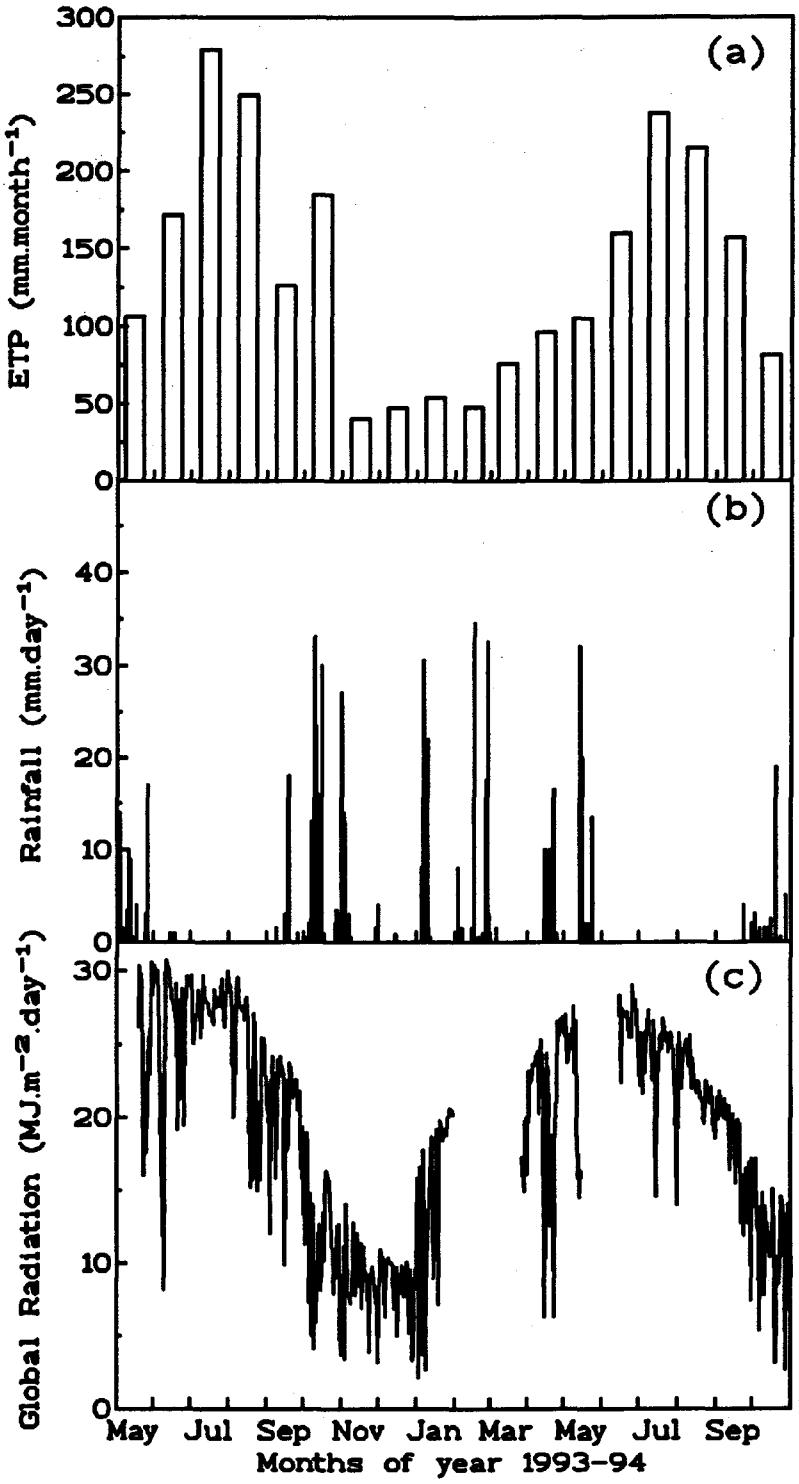

Figure 3.1. Seasonal courses of the environmental variables in the studied period. The variables correspond to **(a)** total monthly potential evapotranspiration (mm month^{-1}), **(b)** daily rainfall (mm day^{-1}), and **(c)** accumulated daily global radiation (MJ m^{-2} day^{-1}).

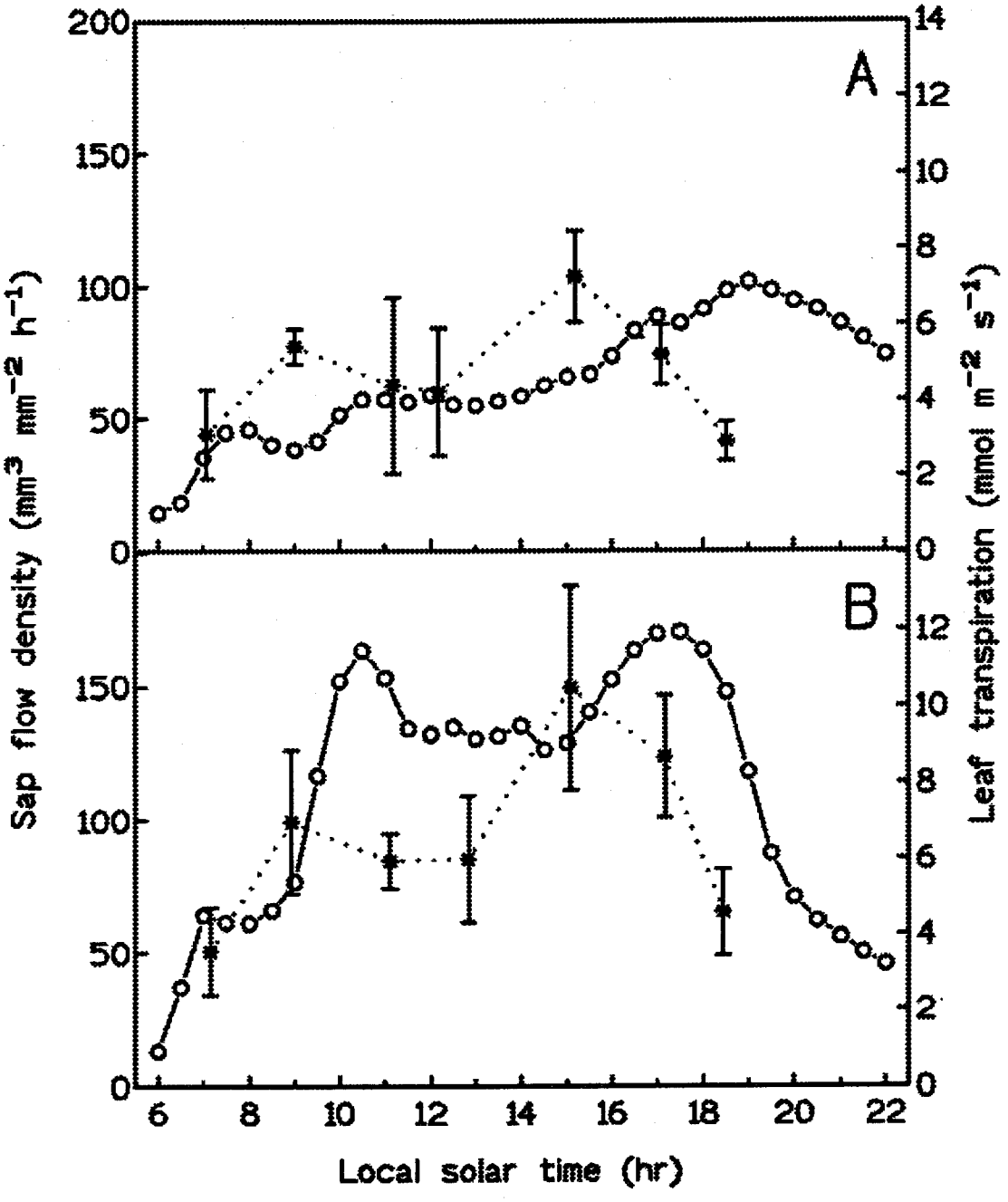

Figure 3.2. Diurnal variation of xylem sap flow density (white circles) and leaf transpiration (broken line) on 10 August 1993. The measurements were made in Tree 1 (A) and Tree 3 (B): sap flow density measurements were made in south orientation in the trunk, and leaf transpiration measurements were made in leaves exposed to the south. Vertical bars indicate standard error of the mean.

Durante el otoño e invierno (Fig. 3.3a) el flujo de savia sigue una curva en forma de campana, alcanzando los valores máximos entre las 12 y las 14 horas solar. En primavera y verano (Fig. 3.3b) los valores más altos se alcanzan por la mañana temprano -antes de las 10 horas- y justo antes de la puesta del sol (17-20 horas), con una depresión alrededor de las 12-14 horas. Hacia el final del periodo de sequía se hacen más frecuentes las curvas en forma de trapecio (por ejemplo, día 28 de septiembre) en las que la transpiración crece rápidamente por la mañana, alcanzando un valor máximo que se mantiene casi constante a lo largo del día, y disminuyendo progresivamente con la puesta del sol. Se aprecia un flujo de savia nocturno (entre 0.5 y 1 $L.h^{-1}$) correspondiente a la recarga del árbol, mayor cuanto mayor fue el consumo total diario de agua por parte del árbol.

Si bien la dinámica diaria de transpiración se difiere entre estaciones, los picos máximos horarios, que oscilan entre los 5 y los 8 $L.h^{-1}$ para el árbol 5, se pueden alcanzar en cualquier estación del año. El rango de valores máximos puntuales fue comparable entre los árboles 3 y 5, pero ligeramente inferior en el árbol 1 (4-6 $L.h^{-1}$). Durante la estación seca estos máximos disminuyen drásticamente a medida que se instala la sequía; en el verano de 1993 se alcanzaron valores máximos puntuales entre 1.5 y 3 $L.h^{-1}$, sólo comparables a días nublados de invierno. Para el mismo periodo de 1994 estos picos máximos oscilaron entre los 4 y los 8 $L.h^{-1}$

3.3.2.2. Patrones estacionales

Los valores más bajos se dan en otoño e invierno (Fig. 3.4). En el otoño-invierno existe una transpiración que oscila mucho, con valores medios entre 24 (±10) y 39 (±13) $L.día^{-1}$ de los árboles 1 y 5, respectivamente. Y los máximos entre finales de mayo y principios de junio, oscilando entre los 80 $L.día^{-1}$ del árbol 1 y los 120 $L.día^{-1}$ del árbol 5. Entre ambos periodos existen dos etapas de transición con un incremento continuo de la transpiración en primavera, y una disminución pronunciada en julio y agosto.

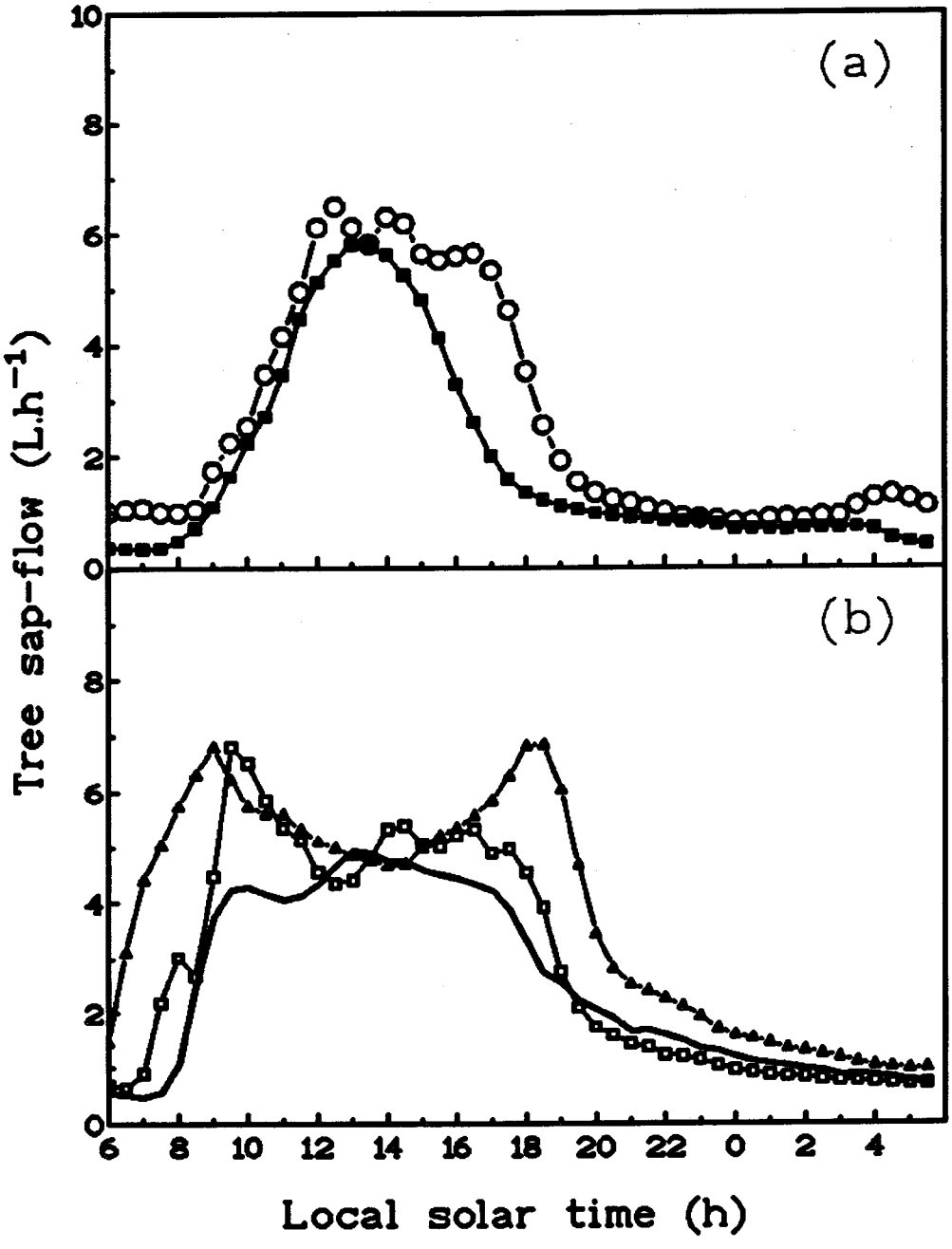

Figure 3.3. Daily variation in Tree 5 transpiration rates during sunny days in different seasons for the year 1993-94. The symbols correspond to 29 October 1993 (square filled) and 20 January 1994 (circle unfilled) in autumn-winter period (**a**) and 9 April (square unfilled), 19 July (triangle filled) and 28 September (solid line) of 1994 in spring-summer period (**b**).

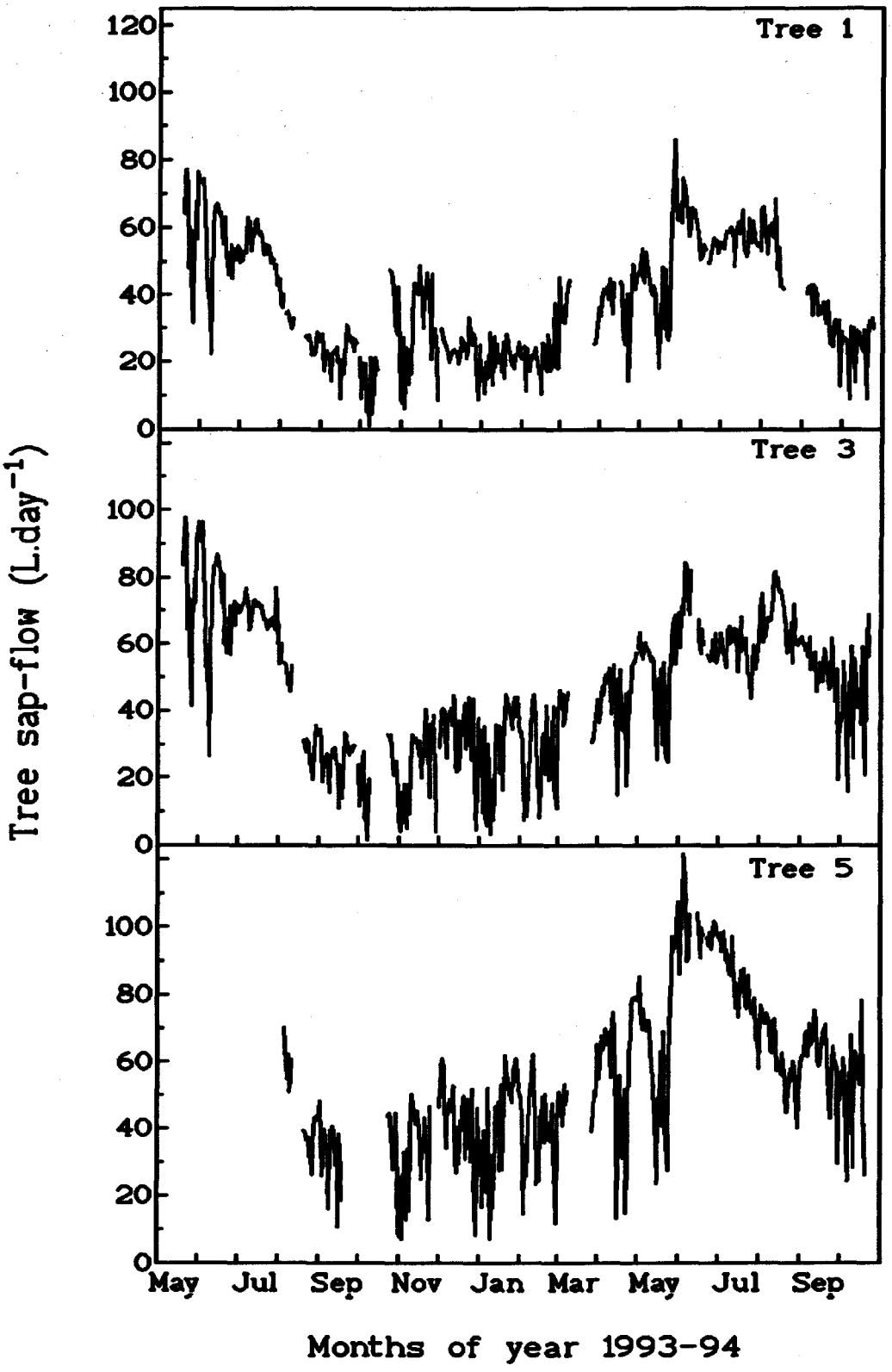

Figure 3.4. Daily tree transpiration rate (L day^{-1}) measured in three trees studied.

Comparando el verano de 1993 con el de 1994 observamos que la dinámica del flujo de savia fue similar en ambos años, exceptuando el árbol 3 que presenta una dinámica ligeramente diferente durante el verano de 1994. En este árbol no hubo un pico máximo a principios de junio con la consiguiente caída en la transpiración, sino que ésta fue más homogénea a lo largo del verano.

3.3.2.3. Consumo total del individuo y de la formación

Si consideramos el año hidrológico 1993-94, el consumo total de agua por árbol osciló entre 13.000 y 20.000 litros de los árboles 1 y 5, respectivamente. De este consumo, la mitad corresponde a los cuatro meses de la estación seca (Tabla 3.1). La otra mitad se reparte al 50% entre el periodo de otoño-invierno (octubre-febrero) y la primavera (marzo-mayo). Estos porcentajes fueron idénticos en los tres árboles. En el verano de 1993 los árboles consumieron cerca de un 20% menos de agua que en el verano de 1994. El mayor consumo de agua en el verano de 1994 se continuó en octubre si lo comparamos con el mismo periodo del año anterior (Fig. 3.4).

Table 3.1. Seasonal and annual transpiration per tree (*TRt*) in mm and litres of water consummation, estimated from tree sap flow measurements.

	Jun-Sep 1993		Jun-Sep 1994		Oct 1993-Sep 1994	
	(mm)	(Litres)	(mm)	(Litres)	(mm)	(Litres)
Tree 1	72.9	4,813	90.8	6,012	200.8	13,307
Tree 3	82.2	6,172	98.1	7,387	205.5	15,476
Tree 5	-----	-----	77.7	9,244	169.4	20,154

La *TRt* anual fue de 169, 205 y 200 mm.año^{-1} para los árboles 5, 3 y 1, respectivamente, oscilando el consumo mensual entre los 29 mm.mes^{-1} del mes de junio y los 9 mm.mes^{-1} del otoño-invierno. El árbol 5 llegó a alcanzar los 6,8 mm.mes^{-1} en el mes de septiembre de 1993. Si calculamos la transpiración de la vegetación arbórea por hectárea obtenemos una *TRh* media de 65,2 mm.año^{-1}, valor muy inferior a los obtenidos por árbol (*TRt*), debido a la baja densidad de la parcela, unos 40 árboles.ha^{-1}.

3.3.3. Relación transpiración - variables climatológicas

Se ha representado en la Figura 3.5 la *TRt* mensual de los tres árboles frente a la *ETP* mensual de la zona. Comparando este consumo mensual con la *ETP* mensual observamos cómo los picos de máxima *TRt* se alcanzan un mes antes que los picos de máxima *ETP*, manteniéndose o no, según los árboles, este consumo máximo en el mes del pico máximo de *ETP*.

Si se representa la relación mensual entre la *TRt* media de los tres árboles y la *ETP* (Fig. 3.6), se observa que los valores, en general, fueron muy bajos para todos los meses estudiados, oscilando entre 0,05 y 0,27. Los valores extremos se encontraron en dos meses consecutivos, octubre y noviembre, que separan el final de la sequía con el comienzo del periodo húmedo; estos valores fueron de 0,06 y 0,27, respectivamente. También se observa que esta relación fue inferior en el verano de 1993 que en el de 1994.

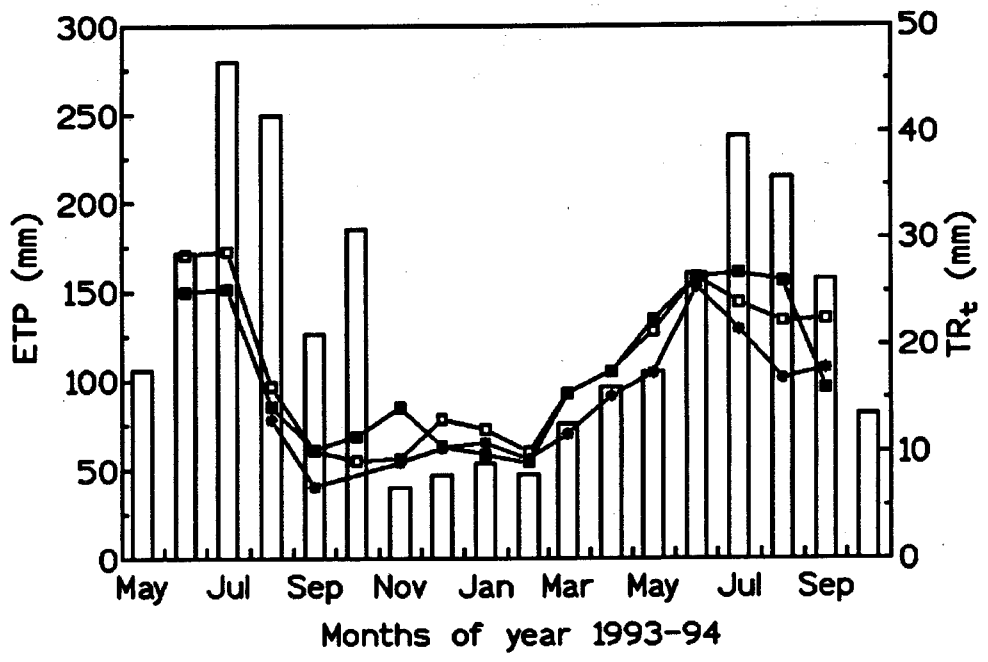

Figure 3.5. Monthly *ETP* (histogram unfilled) compared to tree transpiration (*TRt*): Trees 1 (square filled), 3 (square unfilled) and 5 (star).

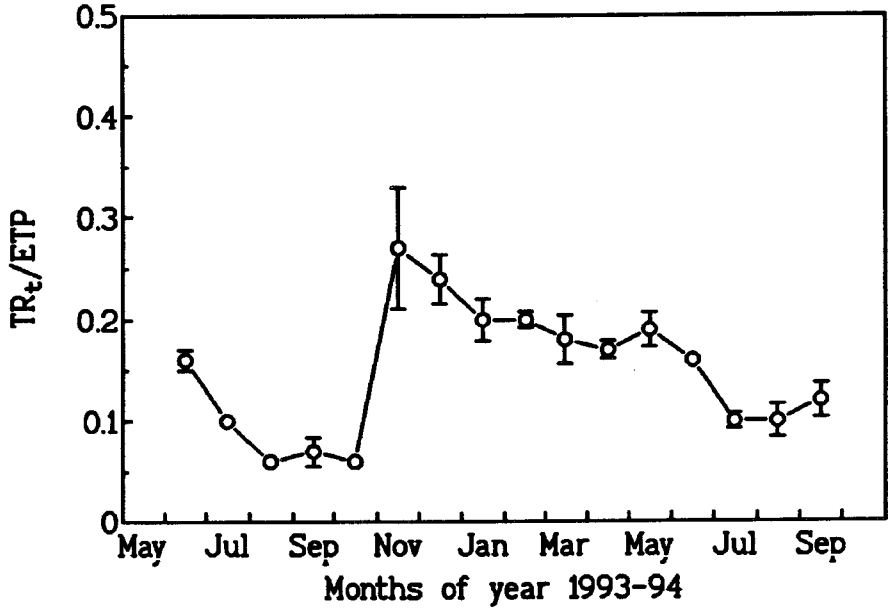

Figure 3.6. Seasonal course of the monthly ratio of mean tree transpiration (*TRt*) on potential evapotranspiration (*ETP*). Vertical bars indicate the standard error of mean.

3.3.4. Disponibilidad hídrica

3.3.4.1. Potencial hídrico de la planta

La evolución del potencial hídrico de la hoja a lo largo del día fue similar en los tres árboles estudiados, *por lo que solo se presentan los obtenidos en el árbol 5* (Fig. 3.7). La evolución de esta variable muestra una forma de uve, con un valor mínimo (el Ψ_m) al mediodía solar, que se recupera totalmente a lo largo de la tarde, tanto en el otoño-invierno como en la primavera (Fig. 3.7a y d). Sin embargo, una vez instalada la sequía, el potencial hídrico disminuye hasta alcanzar un mínimo alrededor del mediodía, que se mantiene a lo largo de la tarde, recuperándose únicamente durante la noche (Fig. 3.7b y c).

Durante el invierno y la primavera el Ψ_p se mantuvo en valores superiores a -0,5 MPa, disminuyendo progresivamente a lo largo del verano (Fig. 3.8). Los valores más negativos en 1994 se alcanzaron a finales de septiembre y fueron de -1,92 y -1,75 MPa, para los árboles 1 y 5, respectivamente. En el mismo periodo de 1993 se midieron valores algo más negativos, -2,5 y -2,2 MPa en los árboles 1 y 3, respectivamente.

Se observó un efecto del plástico en el potencial hídrico del árbol 3 durante el verano de 1994, reduciendo casi a la mitad el Ψ_p, con respecto a los otros dos árboles, en el periodo seco. Sin embargo, el Ψ_m fue comparable entre el árbol 3 y los otros dos árboles durante todo el estudio. El Ψ_p del árbol 3 fue sustancialmente más negativo durante el verano de 1993 (-2,17 MPa) que durante el verano de 1994 (-1,13 MPa).

Si comparamos el consumo diario de agua con el potencial hídrico de la hoja al amanecer (Fig. 3.9), observamos una buena correlación ($r^2 = 0,70$; $p < 0,05$) para valores inferiores a -0,5 MPa. La función encontrada que mejor correlacionó ambas variables fue una exponencial negativa de la forma:

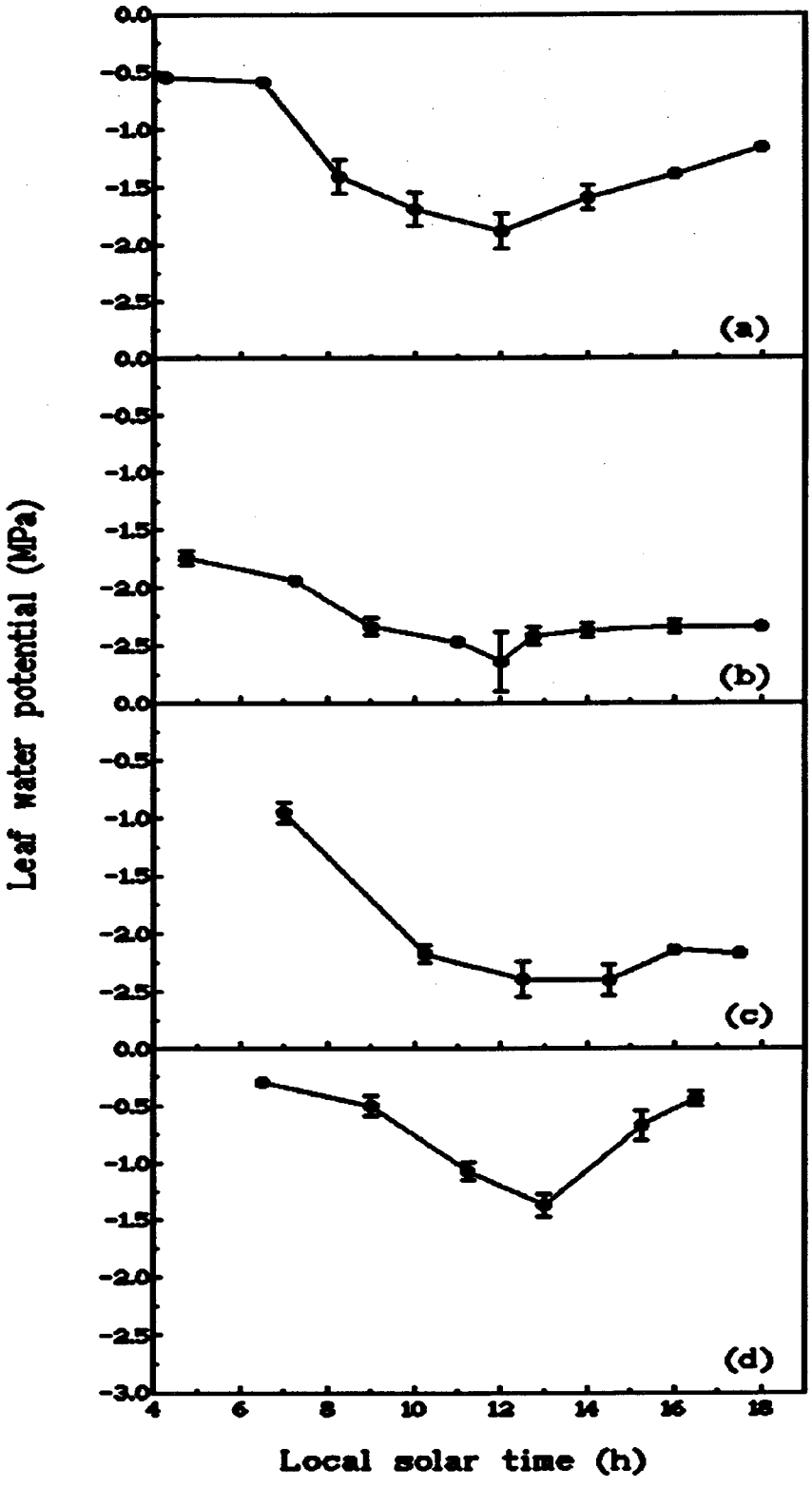

Figure 3.7. Diurnal leaf water potential course in Tree 5 on different days of the studied period: 16 June (**a**), 5 (**b**) and 30 September (**c**), and 29 November (**d**) of 1994.

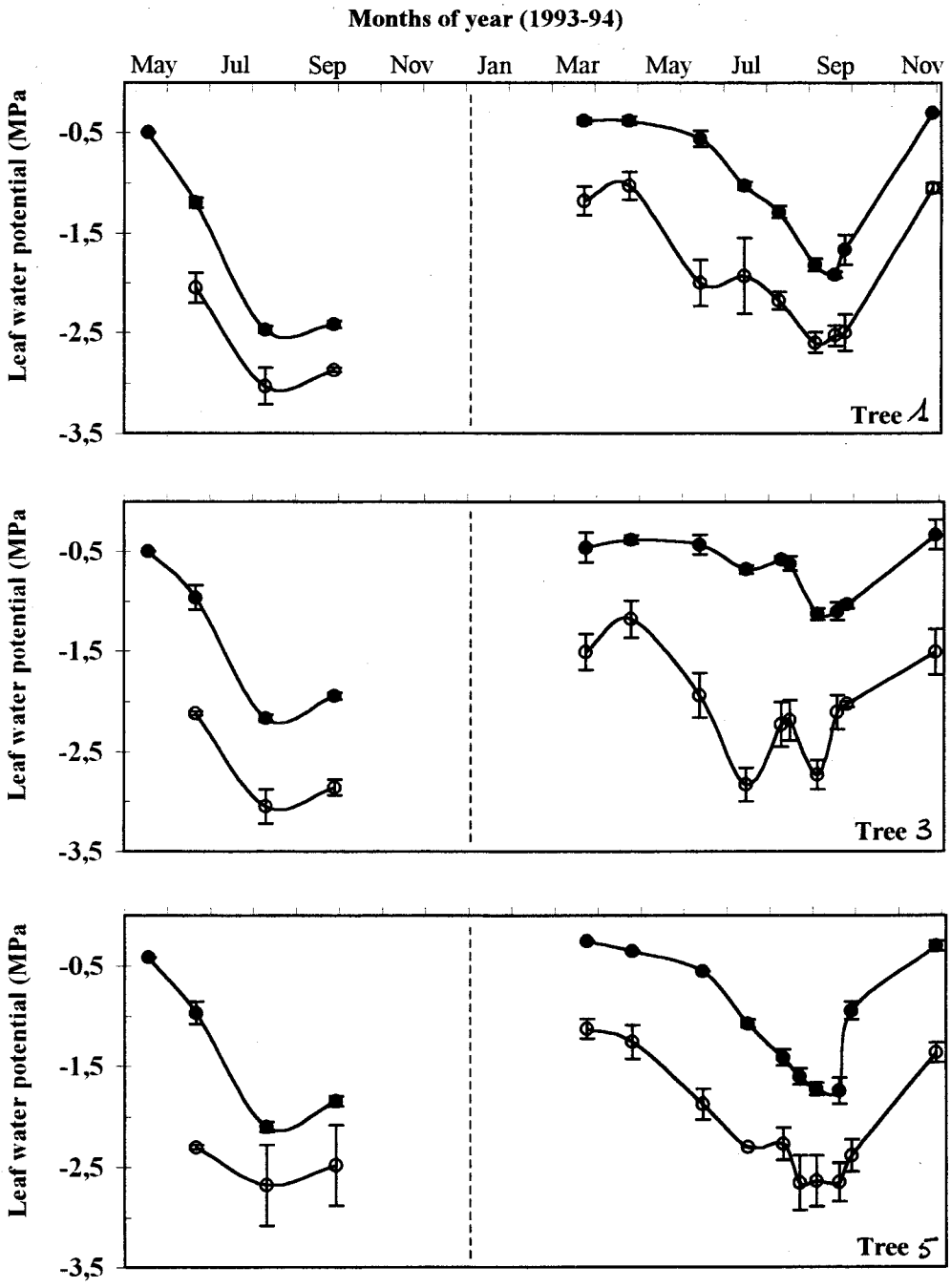

Figure 3.8. Pre-dawn (circle filled) and noon (circle unfilled) leaf water potential (MPa) for the 1994-95 period. The measurements correspond to Trees 1, 3 and 5. Vertical bars indicate the standard error of mean.

$$y = 1{,}05 \exp(1{,}2\,x) + 0{,}42 \qquad \text{(Eqn. 3.1)}$$

En la medida que el Ψ_p es mayor, la diferencia entre éste y el Ψ_m se hace mayor, tal y como se observa en la Figura 3.8. Si representamos la amplitud del potencial hídrico ($\Delta\Psi$), esto es la diferencia entre el Ψ_p y el Ψ_m, frente al Ψ_p observamos que la amplitud disminuye a medida que Ψ_p se hace más negativo (Fig. 3.10). Para esta representación hemos utilizado los valores obtenidos en los árboles en estudio durante el año 1994, junto a valores medidos en seis árboles, adyacentes a la parcela de estudio, durante el mismo periodo (datos cedidos por R. Fernández-Alés).

En esta representación se obtiene una nube de puntos dispersa, por lo que hemos trazado una línea recta por encima de los puntos más altos de dicha nube, lo que teóricamente representa la respuesta de una variable, en este caso el Ψ_p, cuando las otras no son limitantes (Rambal, 1992). En la recta trazada no se han tenido en consideración los valores aportados por el árbol 3, en la medida en que el comportamiento del potencial hídrico de este árbol ha sido modificado por el efecto del plástico. La pendiente de la recta fue de 0,75, con un punto de corte en el eje "y" de 2,6 MPa.

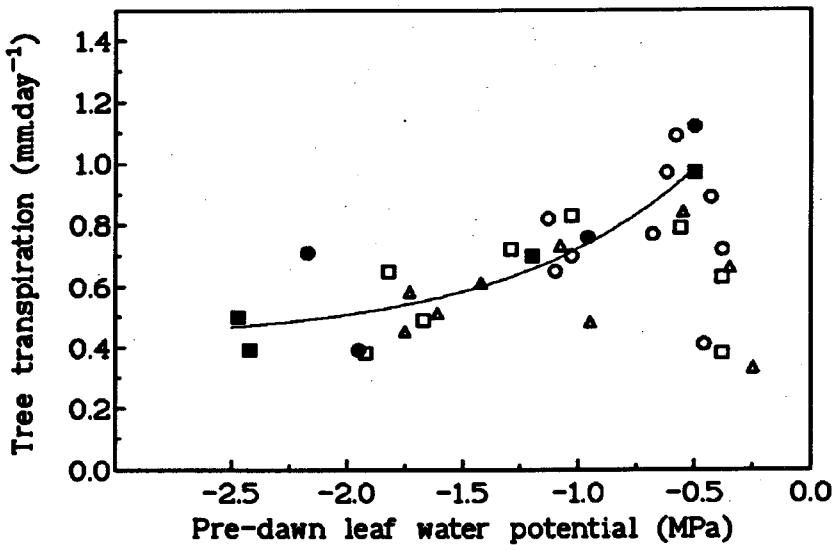

Figure 3.9. Tree transpiration rates as affected by pre-dawn leaf water potential. The measurements correspond to Trees 1 (square), 3 (circle) and 5 (triangle). Filled and unfilled symbols represent years 1993 and 1994 respectively. The solid line shown the response between both variables for a pre-dawn leaf water potential lower to -0.5 MPa ($y = 1.05 \exp(1.2 x) + 0.42$; $r^2 = 0.7$; $P < 0.05$).

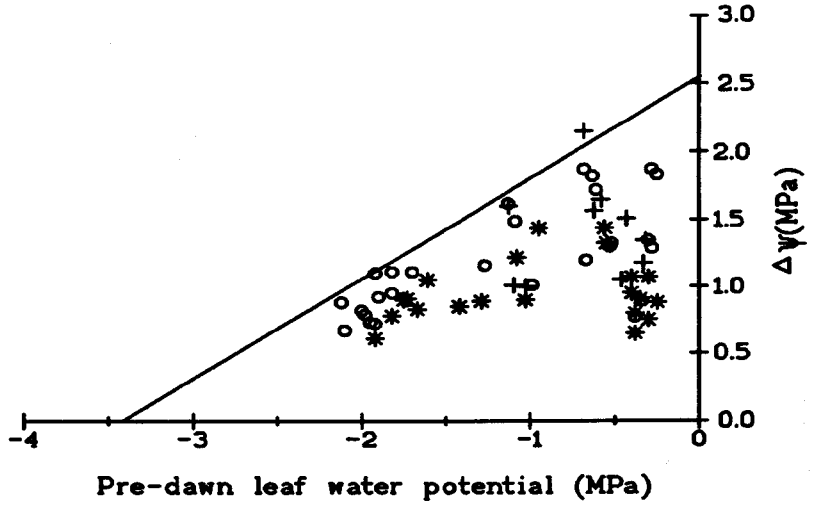

Figure 3.10. Scatter plots relating pre-dawn leaf water potential to the daily amplitude of the water potential for Trees 1 and 5 (star), Tree 3 (plus) and others trees in the same stand (circles unfilled).

3.3.4.2. Dinámica temporal y espacial del agua en el suelo

Tanto los perfiles en el interior de la copa del árbol como los que están fuera siguieron idéntica dinámica a lo largo de 1994 (Fig. 3.11). Los valores más altos se registraron en marzo, correspondiendo con la recarga invernal del suelo (Fig. 3.11). A finales de mayo hubo una recarga de agua que se explica por las precipitaciones ocurridas en este mes (75,5 mm), y que sucedieron tan sólo 15 días antes de la medida del 25 de mayo. Para el árbol 5 supuso un nivel similar al de marzo. A partir de este momento, en el que las precipitaciones cesan, la cantidad de agua en el suelo disminuye, primero bruscamente (mayo-julio), y luego más lentamente hasta alcanzar el mínimo a finales de agosto y se mantiene en ese nivel durante todo el mes de septiembre.

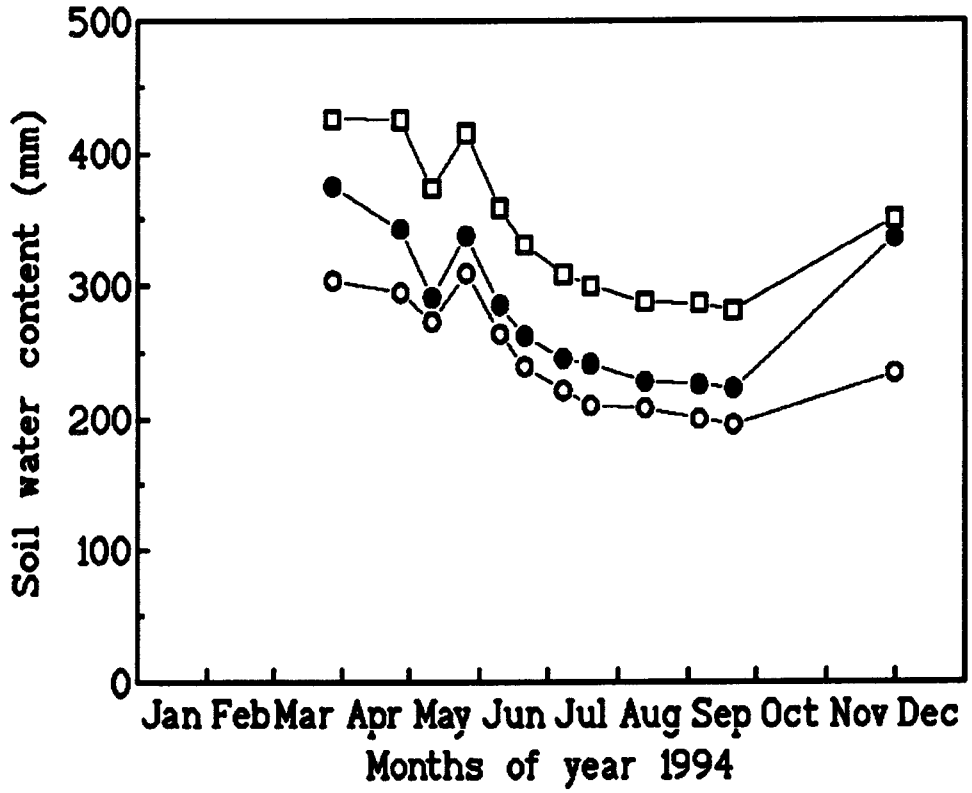

Figure 3.11. Time course of total water content for the 0-150 cm layer from Mars to November 1994. The soil profiles correspond to outside the tree crown (circle filled), and to those located under the Trees 1 (square unfilled) and 5 (circle unfilled).

Entre el final de septiembre y noviembre de 1994 cayeron unos 200 mm, lo que supuso una recarga importante del suelo, si bien ésta fue diferente para los perfiles bajo los árboles y el perfil fuera de los árboles. Este último recuperó valores similares al de final de abril -unos 115 mm-, mientras que bajo los árboles la recarga fue netamente inferior -entre 40 y 70 mm-, alcanzando niveles similares a los de finales de junio.

En la Tabla 3.2 se expresan tres variables que dan idea de la dinámica anual del agua en el suelo y el efecto del arbolado sobre ésta. Éstas son el agua máxima total medido en el perfil (*MSWS*) que se alcanza en 1994 entre marzo y mayo según los árboles, el agua mínima encontrada en el perfil al final de la sequía (*DSWS*), y la diferencia entre ambas variables que expresa el agua libre disponible para las plantas (*ASW*) durante este periodo. Se observa como *ASW*, para los árboles, oscila entre los 113,4 y los 144,4 mm, teniendo el perfil fuera de la copa un valor superior. El mayor valor de *MSWS* correspondió al árbol 1 con 426 mm, teniendo el árbol 5 un valor inferior al del perfil fuera de la copa que tuvo 375 mm. Se observa como el árbol 1 es el que tiene más agua en el perfil durante todo el periodo de estudio, y el árbol 5 el que menos. Similar relación entre perfiles se encontró durante el verano de 1993.

Con el fin de mostrar la dinámica de la desecación del suelo y su posterior recarga otoñal hemos representado en la Figura 3.12 los perfiles hídricos correspondientes a cuatro fechas representativas de 1994: comienzo de la estación seca (25 de mayo), mitad del verano (19 de julio), final de la sequía (20 de septiembre) y una vez recargado parcialmente el suelo con las lluvias otoñales (30 de noviembre). Se ha representado tanto la media de los tres perfiles fuera de la influencia de los árboles, como los correspondientes a los árboles 1 y 5. Todos los perfiles muestran una dinámica similar a lo largo de las distintas profundidades, excepto para la recarga otoñal, la cual fue mayor fuera de los árboles en los estratos intermedios, y apenas apreciable en los estratos inferiores del árbol 5.

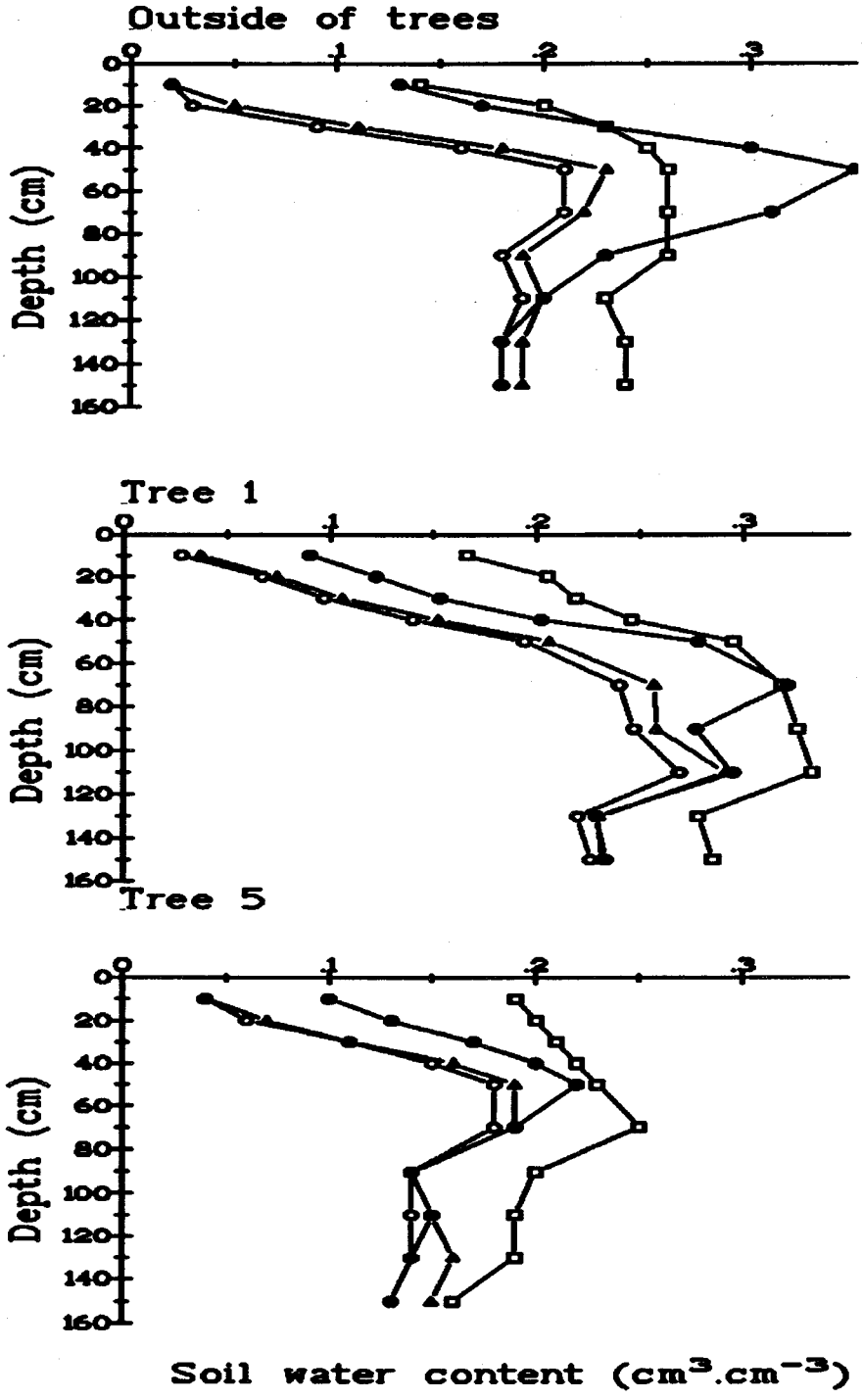

Figure 3.12. Soil water profiles located outside and under the Trees 1 and 5. The dates correspond from spring to autumn of 1994: 25 May (square unfilled), 19 July (triangle unfilled), 20 September (circle unfilled) and 30 October (circle filled).

Table 3.2. Maximum soil water storage, driest observed soil water storage and available soil water for the soil profiles located outside the tree crown, and to soil profiles located under the trees 1 and 5. The periods considered were 1993 (from July to September) and 1994 (from March to November). Values are expressed in mm and concern the 0-150 cm layer. The standard errors of the mean are shown in brackets.

	1994			1993		
	Outside	**Tree 1**	**Tree 5**	**Outside**	**Tree 1**	**Tree 5**
Maximum soil water storage (*MSWS*)	375.0 (69)	425.9	309.3 (52.3)	-----	-----	-----
Driest soil water storage (*DSWS*)	223.2 (48.8)	281.5	195.9 (49)	231.8	281.4	169.4
Available soil water (*ASW*)	151.8 (23.7)	144.4	113.4 (14)	-----	-----	-----

Podemos afirmar que la lluvia no fue suficiente para recargar los estratos inferiores del perfil en ninguno de los tres casos, aún habiendo llovido el 90% de la media para este periodo (de septiembre a noviembre). Se observa también, cómo la pérdida de agua entre julio y septiembre es mínima (alrededor de 0,02 $cm^3.cm^{-3}$) y similar entre árboles y estratos de los perfiles representados.

Para comparar la dinámica de pérdida de agua durante el periodo de sequía de 1994, hemos expresado esta pérdida (la diferencia entre la medida el 25 de mayo y la medida el 20 de septiembre), en porcentaje y en mm, por estrato medido a lo largo del perfil del suelo (Tabla 3.3). Esta pérdida de agua debería corresponder exclusivamente a la transpiración de los árboles a partir del mes de julio, ya que el pasto no se secó completamente hasta junio (obs. pers.). El mayor porcentaje de agua perdida corresponde a los 10 cm primeros del suelo, del orden del 80%, disminuyendo progresivamente a medida que se profundiza en el perfil,

para llegar a valores del 20% a los 150 cm. El consumo en mm fue variable entre estratos, consumiéndose algo menos en los últimos estratos de los perfiles (Tabla 3.3).

Table 3.3. Soil water decrease per soil layer during the dry period: between 25 May and 20 September 1994. The values are expressed in mm and percentage in relation to maximum soil water storage. The standard errors of the mean are shown in brackets.

Soil depth	Outside		Tree 1		Tree 5	
(cm)	%	mm	%	mm	%	mm
10	88.8	12.6 (0.4)	83.1	13.8	78.7	14.7 (0.7)
20	82.9	14.9 (0.9)	67.3	13.8	68.3	14.2 (1.6)
30	62.2	15.8 (1.6)	55.7	13.0	50.5	12.2 (1.6)
40	36.8	11.9 (2.8)	43.1	11.3	33.0	9.1 (2.4)
50	17.2	6.8 (2.5)	34.2	10.4	24.9	6.5 (2.7)
70	18.6	9.1 (2.4)	24.5	17.8	28.5	12.7 (4.7)
90	29.0	12.1 (2.2)	24.2	15.7	30.8	13 (4.1)
110	17.5	11.4 (2.4)	19.2	14.3	28.7	11.5 (1.6)
130	26.4	10.3 (2.1)	20.9	12.2	28.3	10.9 (1.6)
150	26.5	9.6 (2.1)	20.7	11.6	17.8	8.4 (0.6)

3.3.4.3. Relación entre pérdida de agua en el suelo y transpiración

Con el fin de relacionar el agua consumida por el árbol con la pérdida simultánea de ésta del suelo, se ha comparado transpiración y pérdida de agua en los meses de verano, cuando desaparece el pasto y el agua se pierde únicamente por transpiración de las plantas. En la Tabla 3.4 se muestra la *TRt* de los árboles 1 y 5, y la *TRh* frente a la pérdida de agua en el suelo para los meses de verano

exclusivamente (del 1 de junio al 20 de septiembre). Se puede considerar, debido a lo secos que están los perfiles superficiales del suelo (Fig. 3.12) que no existió evaporación del suelo a partir del mes de julio (F. Moreno, com. pers.).

Table 3.4. Monthly tree transpiration (*TRt* and *TRh*) in the drought period (from 1 June to 20 September) of 1994, facing the monthly soil water decrease outside and under the trees. The standard errors are shown in brackets.

	Tree transpiration (mm month^{-1})			Soil water decrease (mm month^{-1})		
	Tree 1(*TRt*)	Tree 5 (*TRt*)	*TRh*	Outside	Tree 1	Tree 5
Jun	26.3	25.4	9.6	60.5 (0.7)	75.2	60.2 (8)
Jul	26.7	21.5	8.7	17.4 (1.5)	23.8	19.0 (3.4)
Aug	26.0	16.9	7.5	8.2 (2.8)	6.8	7.8 (0.5)
Sep	16.0	17.8	6.4	3.2 (1.3)	5.1	5.4 (1.9)

Si comparamos los perfiles fuera de los árboles con aquellos que están bajo la copa de los árboles, observamos que no existen diferencias significativas ($p < 0,001$) entre el agua perdida fuera y dentro de la influencia de la copa de los árboles, para ninguno de los cuatro meses presentados en la Tabla 3.4.

Se observa una pérdida importante de agua en los 150 cm del perfil para el mes de junio, que no tiene correspondencia con el agua transpirada por los árboles ni en términos de *TRh* ni de *TRt*. Para los otros tres meses la *TRt* fue netamente mayor que el agua perdida en todos los perfiles. Sin embargo, en términos de *TRh*, en los meses de agosto y septiembre fueron comparables los valores de transpiración con los de pérdida media (de los tubos bajo los árboles) de agua en el suelo. En el mes de septiembre se transpiró más agua de la que se perdió en los 150 cm primeros de suelo.

3.4. Discusión

Los picos de densidad de flujo de savia medidos en este trabajo (alrededor de 0,5 $m.h^{-1}$) no son inconsistentes con los cálculos teóricos o las referencias de la literatura. Si estos son inferiores a los valores mínimos señalados para los vasos estrechos, se ha de tener en cuenta que el valor de 0,5 $m.h^{-1}$ es un valor medio de los 2 cm de xilema, donde se encuentran vasos conductores con muy diferente actividad. Lo Gullo & Salleo (1993) miden diámetros de vasos conductores del xilema del orden de 10 a 60 µm, en ramas de un año de edad de *Quercus ilex*. Si asumimos que el diámetro de estos vasos en ramas de 1 a 2 años de edad es tan solo la mitad o un tercio del diámetro de los mismos vasos en las ramas principales de un árbol (como ha sido puesto de manifiesto por Cochard & Tyree (1990) en algunas especies de *Quercus* caducifolios), entonces el diámetro de los vasos del xilema del tronco de *Q. ilex* puede encontrarse en un rango que va desde los 50 hasta los 150 µm, como señala Zimmermann (1983) para esta misma especie. De otra parte, árboles con vasos estrechos (50 - 150 µm de diámetro) poseen picos de densidad de flujo de savia del orden de 1 a 6 $m.h^{-1}$, tal y como ha sido señalado por diversos autores (Zimmermann, 1983; Swanson, 1994).

3.4.1. Relación entre la transpiración foliar y la de la planta entera

El almacenamiento de agua es un fenómeno común en los tejidos vivos de los árboles, los cuales juegan un papel tanto de órganos de almacenamiento de agua como de transporte (Gibbs, 1958; Zimmermann, 1983; Brough et al., 1986), difiriendo según las especies. Herzog et al. (1995) encuentran cambios diarios en el radio del tronco de los abetos (*Picea abies*), debido al agua almacenada en los tejidos vivos de la planta. De otra parte, Waring y Running (1978) sugieren que el almacenamiento de agua en el xilema es mayor durante la primavera y comienzos del verano. Este almacenamiento de agua en el tronco explica el desfase temporal entre el pico máximo de transpiración foliar y el pico máximo de flujo de savia a nivel del tronco del árbol, como se puede ver perfectamente en la Figura 3.2.

Varios autores han discutido el desfase entre la transpiración medida en el tronco del árbol y en la copa. Schulze et al. (1985) encuentran en algunas especies de *Larix* (con 12 m de altura) un desfase temporal de tres horas entre la transpiración foliar y la transpiración del árbol estimada a través del flujo de savia. Breda (1994) señala un desfase temporal entre media hora y una hora en diferentes especies de *Quercus* europeos (*Q. petraea* (Matt.) Liebl. y *Q. robur* L.), comparando medidas de flujo de savia con un modelo de conductancia estomática. Granier & Loustau (1994) estiman también un desfase temporal de una hora en *Pinus pinaster* Ait. En nuestro caso, el desfase entre el flujo de savia medido en el tronco y la transpiración foliar es de aproximadamente dos horas.

Aunque no se ha medido la cantidad de agua almacenada, sí se ha constatado de forma indirecta, a través del flujo de savia nocturno que se mide. Se observa que el flujo nocturno es mayor cuanto mayor haya sido la transpiración en el día precedente, y que puede llegar a ser significativo incluso en invierno. Nuestros árboles se encuentran en un clima en el cual son raras temperaturas bajo cero, por lo que almacenar agua en el tronco incluso en invierno no sería peligroso para las estructuras vivas de éste, de hecho esta especie se localiza en zonas de Cataluña con periodos fríos recurrentes que no limitan su distribución (Terradas & Savé, 1992). Este flujo nocturno se ve corroborado por el hecho de la existencia de una diferencia de potencial hídrico en las plantas, entre la puesta y la salida del sol al día siguiente, lo que implica una recuperación sustancial del contenido en agua de los tejidos de la planta, y para ello es necesario un flujo de savia que aporte este agua. Con esto se quiere despejar cualquier duda sobre la posibilidad de que dicho flujo de savia nocturno fuese el resultado de un artefacto experimental intrínseco al método de medición del flujo de savia.

3.4.2. Dinámica del flujo de savia

El patrón de flujo de savia diario varía según la estación del año, de forma similar a como observa Farrington et al. (1994) en dos especies de *Eucalyptus* en Australia a lo largo de dos años de estudio. Existe una disminución del flujo de savia al mediodía en algunos días de primavera y verano, que se explica por un cierre estomático, medido mediante porometría en estos árboles en muchos días de verano. Esta respuesta estomática al estrés hídrico es característica de la vegetación esclerófila mediterránea como son muchos *Quercus* (Tenhunen et al., 1981, 1982; Rhizopoulou & Mitrakos, 1990; Acherar & Rambal, 1992; Sala & Tenhunen, 1994); habiéndose puesto de manifiesto también en diversas especies arbóreas de la sabana venezolana (Bulla et al., 1995).

La transpiración diaria varía a lo largo del año, siendo notablemente superior entre mayo y agosto que entre noviembre y abril. Estas diferencias se deben sobre todo a diferencias en la dinámica diaria y duración del día, ya que los valores máximos, entre 6 y 8 $L.h^{-1}$, se alcanzan tanto en un periodo como en otro, siempre en días despejados. Si comparamos estos valores máximos con los de otras especies medidos mediante el flujo de savia encontramos que son similares a los medidos por Farrington et al. (1994) en *Eucalyptus wandoo* y *E. Salmonophloia,* o los medidos por Schulze et al. (1985) en *Picea abies* y dos especies de *Larix,* pero muy superiores a los medidos por Granier (1987) en bosques de *Pseudotsuga menziesii,* alrededor de 2 $L.h^{-1}$. Estos sólo fueron comparables a los valores medidos a finales del periodo seco de 1993.

La dinámica estacional de la transpiración de estos árboles la podríamos dividir en tres periodos, en los cuales el consumo de agua en porcentaje es similar entre árboles, a saber: un periodo invernal, de octubre a febrero, el cual se caracteriza por una transpiración media baja; un periodo de incremento continuo de la transpiración, en el que se alcanzan valores máximos de transpiración, y que iría de marzo a mayo; y un periodo de descenso continuo que va de la primera semana de junio hasta el inicio de las primeras lluvias a finales de septiembre.

Durante el periodo seco (junio-septiembre) se pierde la mitad del agua total transpirada en un año. Un patrón anual de transpiración similar encuentra Sala (1992) en bosques de *Q. ilex* en Cataluña. Este hecho se pone de relieve si comparamos los dos periodos secos estudiados. La primavera del 1993 fue más seca (mayor *ETP*) que la de 1994, y esto se apreció en el consumo de agua por parte de la planta que fue notablemente inferior (20% menos) en el verano de 1993. Esta limitación hídrica se refleja igualmente en el Ψ_p de los árboles, el cual fue de 0,5 MPa inferior en el verano de 1993.

3.4.3. Disponibilidad hídrica

3.4.3.1. Potencial hídrico de la planta

La relación entre el Ψ_p y la transpiración de la planta ha sido puesta de manifiesto por diferentes autores (Körner, 1994; Reich & Hinckley, 1989; Sala & Tenhunen, 1994). Existe un descenso continuado de la transpiración a medida que el Ψ_p se hace más negativo. En este caso, la relación sigue una función exponencial negativa que sugiere una transpiración mínima de la planta (*TRt*) de 0,42 mm.dia^{-1}, incluso para potenciales bastante negativos (inferiores a -2,5 MPa), aunque no se haya medido valores tan negativos en este estudio. Esta relación se explica por un control estomático de la pérdida de agua a través del potencial hídrico, el cual será tratado en detalle en el siguiente capítulo de modelización de la transpiración. Se observa igualmente que esta relación tiene un Ψ_p umbral de 0,5 MPa, a partir del cual se da. Esto se explica debido a que los potenciales más bajos (mayores de -0,5 MPa) se dan en el periodo húmedo (otoño-invierno), en el cual la planta se recupera totalmente durante la noche de la pérdida de agua diaria, y por lo tanto no limita el consumo de agua durante el día.

Los valores de Ψ_p y Ψ_m medidos, tanto en el otoño-invierno como durante la sequía estival, son comparables a aquellos medidos por diferentes autores en la

misma especie (Tabla A1.1) (Acherar & Rambal, 1992; Rambal, 1992; Castell et al., 1994; Sala & Tenhunen, 1994) y en otras especies de *Quercus* (Bahari et al., 1985; Abrams, 1990; Rambal, 1992).

Los valores mínimos de Ψ_p obtenidos para nuestros árboles, a pesar de haber sido medidos en años secos, son netamente inferiores a algunos descritos por Rambal (1992) para distintas especies de *Quercus*, y en particular para *Q. ilex*, en diferentes ecosistemas mediterráneos; de hecho, si comparamos el $\Delta\Psi$ y su pendiente con los de aquellos ecosistemas, observamos cómo nuestro lugar se situaría en un lugar intermedio entre mésico y xérico (Rambal, 1992; Fig. 3), lo que explicaría valores de Ψ_p intermedios entre los encontrados en la literatura, incluso cuando medimos en años bastante secos como son los considerados en este estudio.

Las diferencias de Ψ_p entre la dehesa estudiada y los ecosistemas a los que nos referimos se podría hallar en el suelo, el cual actuaría como un elemento importante en la regulación del estrés hídrico de la vegetación arbórea. En nuestro caso se trata de un suelo profundo, con una capacidad de campo importante (Joffre & Rambal, 1988), comparado con dichos ecosistemas, que haría un efecto tampón frente al estrés hídrico. Otra posible explicación se encontraría en la baja densidad arbórea que poseen nuestras dehesas, lo que permite una mayor superficie a explotar por el sistema radicular de las encinas.

3.4.3.2. Disponibilidad hídrica en el suelo

A pesar del periodo prolongado de sequía (desde 1992 hasta 1995, en esta región), el suelo bajo el árbol 1 y fuera de los árboles alcanza, en 1994, valores de *MSWS* similares a su capacidad de campo (Joffre, 1987). En cambio, el suelo bajo el árbol 5 parece resentirse más en el tercer año de un ciclo seco, sobre todo del año anterior en el que llovieron 420 mm, y no llega al nivel del árbol 1. También

se observa en este árbol como el agua disponible para la planta es inferior a la del árbol 1, tanto en el verano de 1993 como el de 1994.

Si comparamos el agua consumida por transpiración en los árboles 1 y 5 con la perdida en el sustrato observamos que en el mes de junio se pierde más de la que consumen los árboles, lo cual se podría explicar por la transpiración del pasto que aún no se ha secado totalmente. A partir del mes de julio se transpira, en términos de *TRt*, más de lo que se pierde, sin embargo como veremos más adelante no podemos aceptar la hipótesis de un desarrollo radicular restringido a la superficie de influencia de la copa, a no ser que supusiésemos raíces muy profundas que aportasen gran cantidad de agua al árbol. Pensamos que es más realista expresar la transpiración en términos de *TRh*; así encontramos que en el mes de julio se pierde más agua en el suelo de la que transpiran los árboles (en términos de *TRh*), siendo comparable en los meses de agosto y septiembre.

La diferencia de recuperación de los perfiles fuera y dentro de la influencia de los árboles pueden ser perfectamente explicadas por la intercepción de la precipitación por parte de la copa del árbol, tal y como se discute más adelante.

3.4.3.3. Desarrollo radicular

No existieron diferencias significativas entre el agua perdida en los perfiles fuera de la copa de los árboles y bajo éstas para ninguno de los cuatro meses del verano de 1994, lo que nos lleva a rechazar la hipótesis de un sistema radicular mayoritariamente concentrado en el área de influencia de la copa del árbol. A partir de estos datos podemos pensar en un sistema radicular que tiende a ocupar casi toda la superficie libre disponible. Así mismo, la gran intercepción de la precipitación por parte de la copa, que puede llegar a ser de 40% (Calabuig et al., 1978; Haworth & McPherson, 1995), nos inclina a suponer un sistema radical extendido fuera del área de influencia de la copa con el fin de aprovechar mejor la

precipitación, sobre todo en estos ecosistemas donde el agua es un recurso limitante durante ciertos periodos.

De otra parte, se observa que el árbol 5 en el mes de septiembre transpira más de lo que se pierde en los 150 cm primeros de suelo, lo que nos lleva a pensar en un sistema radicular extendido más allá de ese primer metro y medio. En este sentido, es bien conocido cómo el desarrollo radicular de los *Quercus* en general puede extenderse a profundidades mucho mayores (hasta 5-7 m de media) de la estudiada en nuestro caso (Stone & Kalisz, 1991; Lucot & Bruckert, 1992). De hecho, recientes trabajos sobre estos árboles aislados de dehesa están demostrando la existencia de un sistema radicular arbóreo importante, a más de 8 m del tronco de los árboles (fuera de la proyección de la copa), que llega a los 3 m de profundidad en el suelo (profundidad máxima a la que se ha tenido acceso) (R. Joffre, com. pers.).

3.4.3.4. Efecto del plástico sobre la disponibilidad hídrica del árbol 3

El plástico puesto sobre el suelo del árbol 3 impidió que éste se recargase de agua con las precipitaciones, y que se evaporase agua de los estratos superiores del perfil. El efecto que sobre la planta tuvo se refleja en el potencial hídrico principalmente; el Ψ_p no sobrepasa el -1 MPa en el periodo más seco, la mitad que los árboles control, siendo comparable con los otros árboles durante el resto del periodo de estudio.

El efecto del plástico sobre la transpiración no fue tan acusado como para el Ψ_p. En términos generales (balance anual) la transpiración del árbol 3 fue comparable a la de los árboles control. Únicamente cabe mencionar en la dinámica anual, que no se alcanzó el mismo pico máximo que se obtuvo en 1993 como ocurrió en el árbol 1, y que se mantuvieron valores relativamente altos a mediados del periodo seco cuando en los árboles control la transpiración decrecía continuamente.

Aunque se instalaron tubos bajo la copa del árbol 3 para medir el agua en el suelo, éstos no llegaron a funcionar bien por lo que no tenemos referencias de las variaciones de agua en el suelo para este árbol. Si bien es de suponer, a la vista del Ψ_p, que fue siempre mayor la cantidad de agua en el suelo bajo plástico, que en el suelo bajo los otros dos árboles.

3.4.4. Consumo de agua: relación con parámetros estructurales

3.4.4.1. Transpiración anual

Existen pocos trabajos en los que se haya medido la transpiración diaria en árboles a lo largo de un año, por lo que es difícil comparar con otros ecosistemas. En términos de consumo por árbol, Farrington et al. (1994) da valores de unos 12.000 $L.año^{-1}$, valores comparables a los medidos en estas encinas, si bien no son comparables en términos de densidad arbórea.

Joffre y Rambal (1993) realizan un balance hídrico en varias dehesas del sudoeste español; para ello distinguen dos componentes en estos ecosistemas. De una parte el pastizal, y de otra el sistema árbol-pasto delimitado por la superficie de la proyección de la copa del árbol. Como hipótesis de trabajo asumen que el sistema radicular del árbol no se extiende mas allá de la superficie de la proyección de la copa. En base a este balance hídrico (Joffre & Rambal, 1993), los autores estiman una evapotranspiración anual media, para la parcela objeto de estudio en este trabajo, de 398,5 mm para el componente pasto, y de 590,5 mm para el componente árbol-pasto. Podemos suponer que la diferencia de evapotranspiración entre ambos componentes corresponde a la evapotranspiración del árbol; esta diferencia sería de 192 mm. Este valor es comparable a los 200 mm estimados en este estudio.

De otra parte, Sala & Tenhunen (1996) estiman una transpiración anual, en bosques densos de *Q. ilex* en Cataluña (aprox. 9.400 $árboles.ha^{-1}$; Sala et al., 1994),

que oscila entre los 464 y los 453 mm.año^{-1}. Lo que representa entre un 87% y un 85% de la precipitación anual (534 mm) durante el año de estudio. En nuestro caso, a partir de los tres árboles medidos y considerando que las raíces ocupan todo el suelo disponible más allá de la influencia de la copa, calculamos una transpiración del estrato arbóreo (*TRh*) del orden de 65,2 mm.año^{-1}, para una densidad de 40 árboles.ha^{-1}, lo que representa tan sólo un 13% de la precipitación caída en ese año; valor muy inferior al esperado para estos ecosistemas, aún teniendo en cuenta su baja densidad.

El cociente evopotranspiración real-evapotranspiración potencial (*ETR/ETP*) representa la pérdida real de agua por parte de la vegetación frente a la pérdida potencial dada por el clima. Dicho cociente es igual o inferior a uno, y nos da idea de la resistencia que opone la vegetación a la pérdida natural de agua. Para ecosistemas de sabanas, tanto sudamericanos como africanos, Bulla et al. (1995) citan valores que oscilan entre 0,2 y 0,65. Estos ecosistemas de sabana se encuentran en latitudes tropicales o próximos a ellas, por lo que las condiciones climáticas son muy benignas y constantes, lo que hace que la transpiración sea mucho mayor y regular en el tiempo.

En los bosques densos de *Quercus ilex* estudiados por Sala (1992), Piñol (1990; in Sala & Tenhunen, 1994) estima valores muy altos, entre 0,95 y 1, para este cociente. En nuestro caso se estimó un valor anual de 0,05 (*TRh* = 65,2 mm), netamente inferior a los de otros ecosistemas de sabana. Sin embargo este valor es subestimado desde el momento que no se ha tenido en cuenta en el término evopotranspiración real, la evaporación real de la precipitación interceptada por los árboles, que podría llegar a ser del mismo orden de magnitud que la consumida por la vegetación arbórea, ya que se calculan tasas de intercepción de la precipitación por la vegetación arbórea de un 37% de media en árboles aislados de dehesas (Calabuig et al., 1978). Aunque esta intercepción depende mucho de la cantidad de agua caída por unidad de tiempo y del tamaño de los árboles (Calabuig et al., 1978; Barrantes, 1986; Haworth & McPherson, 1995). En las

sabanas de los llanos del Orinoco se han estimado tasas de intercepción del 20 % (Bulla et al., 1995).

Si consideramos una intercepción media del 37 % de la precipitación, obtendríamos valores del cociente *ETR/ETP* de 0,2, el cual se aproximaría a los valores citados para las sabanas tropicales. Aunque quedaría bastante lejos de los valores obtenidos en bosques cerrados de esta misma especie.

3.4.4.2. Relación transpiración - índice foliar a nivel de formación

Si expresamos el consumo de agua anual en función de la superficie foliar, Sala & Tenhunen (1996) obtienen, en bosques cerrados de *Quercus ilex*, entre 98,5 y 87,6 mm.año^{-1} por unidad de *LAI*. A partir de los 65,2 mm.año^{-1} observados en nuestro ecosistema, y con un *LAI* de la parcela de 0,66 m^2.m^{-2}, (*LAI* medio anual del árbol de 1,9 m^2.m^{-2}), obtenemos un consumo de 98,6 mm.año^{-1} por unidad de *LAI (TRh/LAI)*, lo que representa valores similares a los de Sala & Tenhunen (1996) para la misma especie estudiada. Valores muy superiores de *TRh/LAI*, 193 y 200 mm.año^{-1}, fueron calculados por Rambal (1993) en matorral de *Q. coccifera* y Poole & Miller (1981) en chaparral californiano, respectivamente.

Aparece el *LAI* como un factor importante en el control de la transpiración anual de estos ecosistemas, tal y como pone de relieve Rambal (1993), sobre todo para un *LAI* inferior a 2, como es nuestro caso. En la medida en que no disponemos de otros estudios anuales de transpiración, compararemos en términos de valores máximos diarios medidos en otras especies estudiadas. Los valores máximos diarios medios, encontrados en el mes de junio en nuestro caso, fueron de 90,6 L.día^{-1}, lo que representa una transpiración de la parcela de 0,55 mm.día^{-1} por unidad de *LAI*. Valor por debajo de los obtenidos en otros bosques de *Quercus*, tal y como refleja la Tabla 3.5, incluso para la misma especie (Pitacco et al., 1992).

Table 3.5. Maximum daily stand transpiration measured in different Mediterranean ecosystems, facing the stand *LAI* and stand transpiration per leaf area unit (calculated from *LAI* and stand transpiration).

Specie	Stand *LAI* ($m^2\ m^{-2}$)	Stand transpiration (mm day^{-1})	Stand transpiration LAI^{-1}	Reference
Quercus ilex	3.9	3.5	0.89	Pitacco et al. (1992)
Q. ilex	0.66	0.36	0.55	Our study
Q. durata	2.3	1.8	0.78	Goulden & Field (1994)
Q. agrifolia	5	3.6	0.72	Goulden & Field (1994)
Q. petraea	6	3.8	0.63	Breda et al. (1993b)
Q. petraea	4.3	3.3	0.77	Nizinski & Saugier (1989)

3.4.4.3. Resistencia xilemática al paso del agua

Estas diferencias en el consumo diario por unidad de *LAI* entre bosques cerrados y dehesas se podrían explicar debido a la existencia de una limitación importante al flujo de savia en los ecosistemas de dehesas. Esta limitación vendría dada por la resistencia que opondría el xilema al paso del agua, la cual se vería como el porcentaje de tejido conductor respecto al área foliar de los árboles. Si representamos el radio del tronco frente al porcentaje de xilema (considerando una corona de xilema de 2 cm) de dicho tronco, observamos que esta relación sigue una exponencial negativa ($r^2 = 0,97$; $p < 0,05$) de la forma:

$$y = 84,12 \exp(-0,08\ x) + 3,25 \qquad \text{(Eqn. 3.2)}$$

en la cual al aumento del radio de 10 a 50 cm le corresponde una disminución del porcentaje del 65 al 10% del xilema con respecto al área basal. Esto implica una disminución sustancial de tejido conductor frente a superficie foliar, en árboles aislados de grandes dimensiones, como son los de dehesas, frente a árboles pequeños -bosques cerrados- aún cuando se diese la misma área foliar por árbol en ambos casos. Es decir, a igual superficie foliar una disminución de la superficie de tejido conductor representa una resistencia al paso del agua.

Esto explicaría los valores más bajos de transpiración máxima diaria, aún cuando se alcanza en condiciones ambientales óptimas y para la misma especie (Tabla 3.5). Si comparamos los bosques cerrados estudiados por Sala & Tenhunen (1996) con nuestras dehesas, la relación superficie foliar-unidad de superficie xilemática sería de 1 a 3, es decir, los árboles de dehesas soportan tres veces más superficie foliar por unidad de superficie xilemática, con lo que se podría hablar de una resistencia física al paso del agua que sería la limitación de superficie xilemática por unidad de superficie foliar.

3.5. *CONCLUSIONES*

Nos encontramos con un ecosistema cuya vegetación arbórea posee un consumo de agua bastante bajo, un 13% de la lluvia caída para el año 1993-94, con respecto a bosques cerrados de la misma especie. En el año seco estudiado, el consumo de agua en valores absolutos y medido a través del flujo de savia, osciló entre los 13.000 y 20.000 $L.año^{-1}$. Estos árboles poseen una dinámica de la transpiración estacional bastante marcada, en particular durante el periodo seco que se extiende de junio a septiembre, y en el cual se transpira la mitad del total anual. Los picos máximos diarios de transpiración se alcanzan justo después de las últimas lluvias primaverales, siendo éstos netamente inferiores a otros medidos en bosques cerrados de *Quercus* en general, y de *Q. ilex* en particular.

Se observa un flujo de savia nocturno apreciable, que depende del agua consumida por la planta durante el día, y que se corresponde con la recarga de los tejidos conductores y de almacenamiento de la planta.

Si comparamos los árboles aislados estudiados en este trabajo con los bosques cerrados de *Q. ilex* catalanes estudiados por Sala (1992), observamos que ambos poseen una transpiración por unidad de *LAI* similar, y sin embargo la relación superficie xilemática-*LAI* es tres veces superior en los árboles aislados con respecto a los bosques cerrados. Las limitaciones a la transpiración vendrían dadas a dos niveles distintos: uno funcional que sería la regulación estomática de ésta, y que jugaría su papel a largo plazo (Sala & Tenhunen, 1994); y otro estructural que sería la relación superficie foliar por unidad de superficie xilemática. Esta relación supone una resistencia al paso del agua de forma puntual, jugando su papel a esta escala de tiempo, y explicaría el que encontrásemos picos diarios inferiores a los de bosques cerrados en condiciones óptimas de transpiración. Ambos factores podrían explicar en gran medida el bajo consumo de agua por parte de estos árboles aislados.

Comparando el agua consumida por el árbol con la perdida en el suelo, en los meses de verano, se observa que aparece más representativo del consumo de agua expresar ésta en términos de *TRh* (transpiración real por hectárea), ya que la superficie de explotación de las raíces debe extenderse por toda la superficie disponible, más allá de la proyección de la copa. Las medidas de agua en el suelo demuestran que no existen diferencias significativas entre el agua consumida por los árboles dentro y fuera de la copa de éstos, es decir las raíces de los árboles se extienden efectivamente fuera del área de influencia de la copa. Igualmente sería necesario medir más allá de los primeros 150 cm de profundidad para conocer en detalle el área de expansión de las raíces de estos árboles.

Una vez conocida la dinámica de transpiración de los árboles aislados se hace necesario conocer en detalle los factores ambientales que controlan dicha transpiración, con el fin de poder prever el funcionamiento de estos arboles y su

respuesta ante variaciones del medio físico o de manejo que pudiesen afectar a su transpiración. El estudio de estos factores a través de la modelización se aborda en el siguiente capítulo.

IV. MODELLING TRANSPIRATION: SCALING UP FROM THE LEAF TO THE CANOPY LEVEL

4.1. INTRODUCTION

The Penman-Monteith equation (Monteith, 1965) is widely used to estimate plant transpiration. This formulation considers the vegetation as a single big leaf, and calculates the latent heat flux from the known surface conductance and meteorological data. Jarvis & McNaughton (1986) expressed the formulation in terms of stomatal control of transpiration and considered scales from leaf to region. Jarvis & McNaughton (1986) rewrote the Penman-Monteith equation in a form that partitioned leaf evaporation into two components: a so-called equilibrium evaporation rate (E_{eq}) that depends only on the energy supply (radiation), and an imposed evaporation rate (E_{imp}) that depends on surface conductance, boundary layer conductance, and water vapour pressure deficit. The relative importance of these two depends on the degree of coupling of the evaporation surface (leaf, canopy, or crop) to the environment. We have modelled leaf transpiration using this approach, and set out to obtain a tree transpiration model by a similar scaling up procedure - as defined by Norman (1993).

A process of scaling up from the constituent parts to the whole tree implies an intuitive leap with respect to the process of integration. This requires complementary information about interactions between the parts, and the wide range of conditions under which the parts combine to form the whole. In this work we limited our study to the functioning parts, namely the leaf and the whole tree. Only a scaling-up process from the leaf to the tree is possible. This process was carried out at two scales; temporally from a single day to a drought period, and spatially from the leaf to the tree scale. The first step was to obtain knowledge about leaf and tree functioning to allow integration of information from the scale of the leaves that form the tree.

Characteristics were sought at leaf level, so as to set up a leaf transpiration model under the conditions appropriate for the leaf, and were inferred for the tree. The assumptions involved were tested by comparing modelled tree transpiration with tree transpiration measured by a sap flow method.

The aim of present chapter is to structure our understanding of the transpiration process at leaf scale with that at tree scale for isolated savannah trees, and to model transpiration over a drought period. The main steps are the identification of all parameters and assumptions involved in the modelling procedure. These have been tested against experimental data. Simulations have been run and the results interpreted ecologically.

4.2. *MATERIAL AND METHODS*

4.2.1. *Transpiration measurements*

The sap flow measurements were made over two periods, from 19 May to 28 September 1993; and from 27 March to 21 October 1994. In the first period two trees were used (termed Trees 1 and 3), and during the second period we added a third tree (Tree 5).

4.2.2. *Meteorological data*

Windspeed was measured at a height of 3 m. The windspeed at a height of 10 m was estimated using the semi-logarithmic expression of velocity above vegetation (Monteith & Unsworth, 1990)

$$u_z = A \ln [(z-d) / z_o] \qquad \text{(Eqn. 4.1)}$$

where u_z is the windspeed at height z, d is the apparent reference height, z_0 is the roughness length and A is the slope of this ratio. We needed to estimate the windspeed at a height of 10 m in order to calculate the tree conductance (see below in the next section). The site of the meteorological station was considered to be homogeneously covered by grass of height (h) of 0.15 m, with d equal to 0.096 m (0.64 h), and z_0 equal to 0.019 m (0.13 h) (Campbell, 1977; in Jones, 1992).

During 1994 period, air temperature and humidity were measured in the field by the automatic meteorological station. In 1993 we had to assume that the dew point temperature (T_d) did not change between Sevilla and the study site, so that the water vapour pressure in the bulk air (e_a) was estimated from the T_d recorded at Tablada. We correlated the air temperature measured in the field ($T_{a,f}$) from 30 July to 30 September 1993, with the air temperature of Tablada ($T_{a,t}$) for the same period. This correlation ($T_{a,f} = 1.013\ T_{a,t} - 2.834$; $r^2 = 0.94$, $p < 0.001$) was used for estimating air temperature for the rest of the 1993 period. That temperature was used to estimate water vapour pressure at leaf surfaces (e_s), so that D_a was calculated as e_a minus e_s.

4.2.3. *Physiological measurements*

Stomatal conductance data to be used in the modelling procedure were determined between June 1994 and January 1995. This information was collected in June (Days of month 15 to 17), August (Days 18 and 24), September (Days 5, 21, 28 and 30), November (Days 29 and 30) and January (Days 4 and 9).

Pre-dawn (Ψ_p) and noon leaf (Ψ_m) water potentials measurements were made on 22 June, 10 August and 29 September 1993. In 1994, measurements of leaf water potential were made on the same dates as the stomatal conductance measurements.

4.3. MODELLING PROCEDURE

4.3.1. Specifications

We attempted to model both the hourly leaf transpiration rate (expressed in mmol m^{-2} s^{-1}) as measured with the leaf chamber analyser, as well as the total mean daily water flow passing up the whole tree (expressed in sap flow density units: mm^3 mm^{-2} h^{-1}), as measured using the three sap flow probes at the trunk portion of the tree. The models were based upon known relationships between transpiration, stomatal conductance, weather variables and plant water status. The last variable was represented by the pre-dawn leaf water potential (Ψ_p). Field measurements of each variable used in the modelling procedure were recorded in the 1994/1995 period; sap flow and weather variables were also recorded in the 1993 period. Weather variables used for mean daily tree transpiration modelling were mean daily values. We assume, on the basis of our observations, that plant photosynthetic activity began at a solar irradiance above 50 W m^{-2}. Hence, mean daily values of the other variables were calculated during daytime, when the overall irradiance exceeded 50 W m^{-2}.

Tree transpiration was measured in terms of sap flow density, i.e., water volume transpired by the tree normalised with respect to the sapwood cross-sectional area. This allowed us to compare all trees in terms of transpiration, independently of allometric characteristics of the trees. Field measurements of sap flow density were assembled for two periods: in 1993 period for Trees 1 and 3, (19 May to 28 September) and in 1994 period for Trees 1 and 5 (27 March to 21 October). For each period, transpiration data were assigned on alternate days to one of two independent data sets: one for modelling and the other for validation of the model, except for the transpiration measurements on Tree 3 (year 1994), which were only used for modelling purposes.

4.3.2. Construction and validation of the model

Initially, plant physiological studies showed transpiration (E) to depend on stomatal conductance (g_s), net radiation (R_n), air humidity, soil moisture deficit, temperature, and windspeed (u). In general, leaf transpiration can be expressed by the Penman-Monteith equation

$$\lambda E = \frac{s\,R_n + \rho_a\,c_p D_a g_b}{s + \gamma\,(1 + \frac{g_b}{g_s})} \qquad \text{(Eqn. 4.2)}$$

where λ is the latent heat of vaporisation of water, s is the slope of the saturation vapour pressure curve with respect to temperature, ρ_a is the density of air saturated with water vapour, c_p is the molar heat capacity of dry air at constant pressure, g_b is the boundary layer conductance of the leaf, D_a is the vapour pressure deficit of the ambient air, and γ is the psychrometric constant. This expression was developed for a hypostomatus leaf. We assumed that the total transfer conductance for sensible heat and water vapour ratio is 1 (Jarvis & McNaugthon, 1986; Jones, 1992). Here, λE depends mainly on R_n, g_s, g_b, and D_a. This formulation was then expressed by Jarvis & McNaughton (1986) in terms of stomatal control of the transpiration as follows

$$E = \Omega\, E_{eq} + (1-\Omega)\, E_{imp} \qquad \text{(Eqn. 4.3)}$$

where Ω is the dimensionless decoupling coefficient, E_{eq} is the equilibrium evaporation rate that depends on net radiation, and E_{imp} is the imposed evaporation rate dependent on surface conductance, boundary layer conductance, and water vapour pressure deficit. This equation simplifies the calculation of E with regard to stomatal control, from the leaf scale to the regional scale (Jarvis & McNaughton, 1986; McNaughton & Jarvis, 1991).

The role of the stomata in transpiration control has been widely discussed in the recent literature (Meinzer & Grantz, 1989; Meinzer, 1993). Stomatal control of transpiration is strong, if g_b is high compared with g_s (Meinzer, 1993). When g_b is low, transpiration promotes a local equilibrium in the humidity near the leaf, within the boundary layer, uncoupling leaf water vapour pressure deficit (D_l) from that in the bulk air (D_a). As suggested by various authors (Aphalo & Jarvis, 1991; Mott & Parkhurst, 1991), we also used D as the most appropriate variable for describing the stomatal response to humidity. The degree to which D_a is imposed at the leaf surface (Jarvis & McNaughton, 1986) is in terms of the dimensionless decoupling coefficient, Ω (Equation 4.3), which takes a value in the range from 0 to 1. Values near 1 mean that conditions at the leaf surface are independent of those in the surrounding bulk air. Conversely values near 0 mean that conditions at the leaf surface are very strongly coupled to those in the free airstream. In the latter case, D_l can be considered effectively equal to D_a.

This decoupling coefficient was formulated by Jarvis & McNaughton (1986) in terms of the g_b/g_s ratio for the leaf scale (Ω_l) or the ratio g_a/g_c (i.e., tree boundary-layer conductance / tree stomatal conductance) for the tree scale (Ω_c). Martin (1989) points out that radiative conductance (g_r) should be included in the formulation of Ω, and proposes a modified derivation of the elasticity of evaporation to conductance. However, the role of g_r depends on the ratio of the aerodynamic conductance to the surface conductance, and is important only when the values of surface and aerodynamic conductance are close. As Figure 4.1 shows, for low values of Ω_l, Martin's correction would not contribute significantly to transpiration control. The same effect was observed for Ω_c. Consequently, we have used the Jarvis & McNaughton (1986) approximation to calculate Ω at both leaf and tree scales.

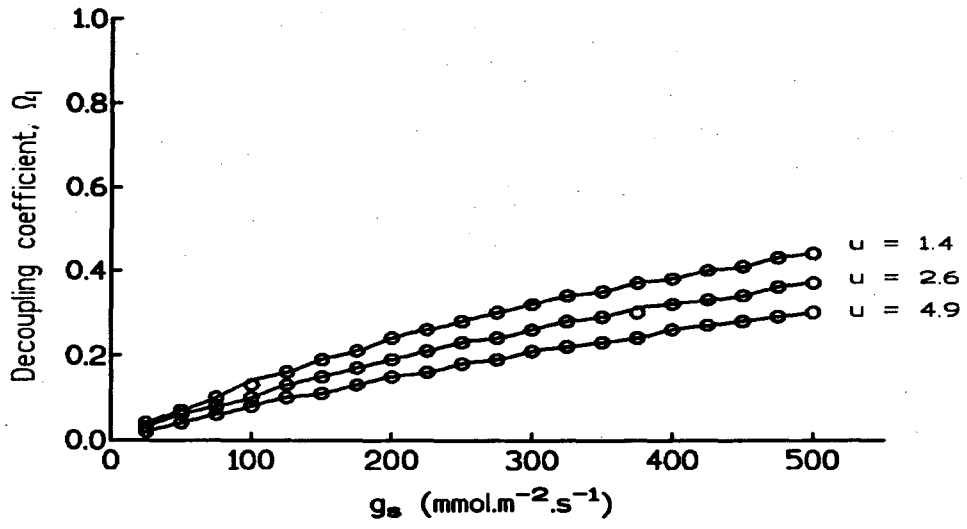

Figure 4.1. Variation of Ω_l at leaf level in relation to g_S for different values of daily windspeed (u) measured in the period of study. The solid line shows the values estimated by the Jarvis & McNaughton (1986) formulation, and the unfilled circle the values estimated by the Martin (1989) formulation (see the text). The values of u correspond to maximum (u=4.89 m s^{-1}), mean (u=2.57 m s^{-1}) and minimum (u=1.43 m s^{-1}) mean daily values recorded in the stand.

4.3.2.1. *Leaf level transpiration*

Values of g_b (mm s^{-1}) were calculated from the following expression given by Jones (1992)

$$g_b = 6.62\ (u\ /\ d_l)^{0.5} \qquad \text{(Eqn. 4.4)}$$

where u is the windspeed (m s^{-1}), and d_l is the characteristic dimension (m) of the leaf, which we found to be 2.67 ± 0.52 cm for our leaves. From the value of g_b calculated and g_s measured in the field, we estimated Ω for the leaf (Ω_l) under different environmental conditions for the range of g_s measured. Figure 4.1 shows

the variation of Ω_l in relation to g_s for different mean daily values of u measured in the present study. The three mean values of u used were the maximum (u = 4.89 m s^{-1}), average (u = 2.57 m s^{-1}), and minimum (u = 1.43 m s^{-1}) values recorded in the stand in 1994. This Figure shows a decoupling coefficient lower than 0.3 for almost all values of g_s under usual conditions of windspeed. The mean value of Ω_l over the range of stomatal conductance and windspeed is approximately 0.2, a value similar to that cited by Meinzer (1993) for temperate forests. From the low mean values of Ω_l obtained, we can consider $\Omega_l \approx 0$ and therefore, $D_l \approx D_a$. Substituting Ω_l in Equation 4.3, we found that $E_l = E_{l\,imp}$, that is

$$E_l = 0.622\ \rho_a\ g_s\ D_a\ /\ P \qquad \text{(Eqn. 4.5)}$$

where P is the atmospheric pressure (kPa), considered equal to 100 for the whole period studied. Then, this leaf-level expression is simply the general case for a non-isothermal system where the leaf temperature (T_l) and air temperature (T_a) are different (Jones, 1992).

In our study we observed that $T_l = T_a \pm 1.5$ °C and Equation 4.5 could be simplified to the case of an isothermal system around the leaf as follows

$$E_l = g_s\ D_a\ /\ P \qquad \text{(Eqn. 4.6)}$$

Thus, we obtained a simplified formulation of E_l from our leaves that depend exclusively on g_s and D_a. So in order to know all factors regulating E_l, we must now analyse the behaviour of g_s.

Various models of stomatal conductance have been described in the literature, which are based upon observed relationships between g_s and environmental variables. Jarvis (1976) outlined the general form of a non-linear model

$$g_s = g_o f_1(R_n) f_2(D_a) f_3(T_a) \ldots \quad \text{(Eqn. 4.7)}$$

where g_o is some reference value which is usually the maximum stomatal conductance. The individual functions (f_1, f_2, f_3 ...) are experimentally determined. These functions can be found at the maximum envelope of the data when plotting g_s against each variable, and represent the stomatal response to one variable when others are not limiting. However, two drawbacks to this approach need to be mentioned. Probable interactions between variables are ignored, and the response functions are normally obtained under controlled conditions where only one or two variables are varied at any time. In reality, all variables act simultaneously in interconnected ways so those interactions are to be expected. The variables used, and their role in the model, will depend both on the species and on the level of study in the plant.

In order to model g_s, we related stomatal conductance with the different environmental variables of vapour pressure deficit, air temperature, windspeed, photosynthetically active radiation, and pre-dawn leaf water potential. Figure 4.2 shows the functions of leaf stomatal conductance response to these major environmental variables. For hourly values of g_s, we found that D_a alone explained some 70% ($p < 0.05$) of stomatal conductance ($g_s = 380.9 \exp(-0.82 D_a) + 93.8$; in mmol $m^{-2} s^{-1}$) (Fig. 4.2b) by a non-linear response in the form of a negative exponential function. In contrast, pre-dawn Ψ_p contributed only an additional 3% ($p < 0.05$) to the explanation of g_s. When considering mean daily values of g_s, we obtained a function of g_s explained by mean daily D_a with a r^2 of 96.7% ($p < 0.001$) for a similar model of negative exponential response. Adding the variable of Ψ_p, the variance rose by only 0.6% ($p > 0.05$). The other variables, T_a, PAR (Fig. 4.2c and d) and u, in the range tested, had no particular impact on g_s behaviour for either time-scale. The radiation intercepted by the plant did not play an important role in control of g_s because it was not a limiting factor under the study conditions.

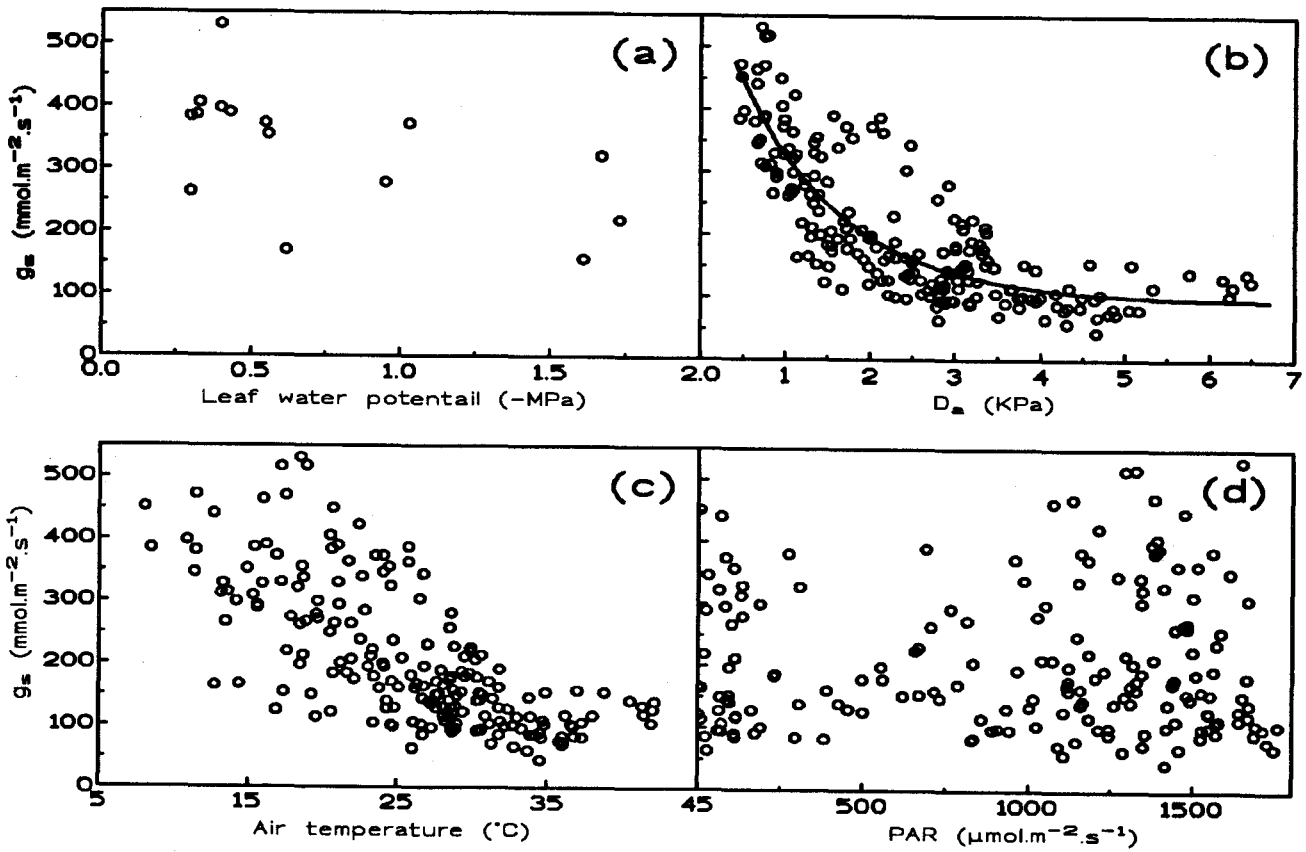

Figure 4.2. Functions of the daily maximum stomatal conductance response to pre-dawn leaf water potential (**a**), and the hourly stomatal conductance response to air water vapour pressure deficit, with the model chosen for this variable ($g_S = 380.9\ exp[-0.82\ (D_a\text{-}0.4)] + 93.8$; $r^2 = 0.697$ and $P < 0.05$), (**b**), air temperature (**c**) and photosynthetically active radiation (*PAR*) (**d**). The three last variables represent hourly values measured with the leaf chamber analyser.

Thus, to simplify the modelling procedure, we used only the variable D_a to explain the behaviour of gs. The general form we used for this function of g_s, as explained by D_a, is

$$g_s = k_0 \exp(-k_1 D_a) + k_2 \qquad \text{(Eqn. 4.8)}$$

where the parameter k_1 (kPa^{-1}) is the rate constant of the curve, k_2 (mmol m^{-2} s^{-1}) is the value of g_s at which it becomes independent of D_a. The sum of k_0 (mmol m^{-2} s^{-1}) and k_2 represents the maximum stomatal conductance (g_{sm}).

Substituting the form of g_s (Equation 4.8) into Equation 4.6, we can express E_l in the general form of

$$E_l = (k_0 \exp(-k_1 D_a) + k_2) D_a / P \qquad \text{(Eqn. 4.9)}$$

4.3.2.2. Tree level transpiration

The aerodynamic value of g_a (mm s^{-1}) was calculated from the expression (Monteith & Unsworth, 1990)

$$g_a = k^2 u_Z / \{\ln[(z-d)/z_0]\}^2 \qquad \text{(Eqn. 4.10)}$$

where k is the von Karman constant (= 0.41), z is considered at 10 m, and d and z_o were calculated using the approximation proposed by Abtew et al. (1989)

$$d = (0.71 R + X) F_c \qquad \text{(Eqn. 4.11)}$$

where R is the radius of curvature of the top of plant canopy (mean value of 5.25 m), X is the distance from the ground to the centre of curvature (mean value of 2.25 m), and F_c is the fraction of the total surface covered by roughness elements

of the tree. We considered the tree-canopy as a sphere, with a mean diameter of 10.5 m. F_c was calculated as the ratio of the total area covered by the projected tree-canopy surface in a hectare, considering a mean distance among trees of 18.5 m (mean distance between trees studied), to the surface of a hectare. Finally, we considered that (Abtew et al., 1989)

$$z_o = 0.13\ (h-d) \qquad \text{(Eqn. 4.12)}$$

where h is the maximum height of the trees (we found to be approximately 9 m).

Values of g_a calculated in this way ranged between 61 and 200 mm s^{-1} for the minimum and maximum mean daily values of windspeed, respectively. Maximum values of mean daily g_c, as estimated from the Penman-Monteith equation of Equation 4.2, were always less than 1.5 mm s^{-1}. From both g_a and g_c, the mean value of the tree decoupling coefficient (Ω_c) was calculated to be 0.035, and lower than 0.08 at the minimum windspeed (u = 1.75 m s^{-1}). Therefore, we can consider that Ω_c is essentially zero for both periods of study, such that the tree temperature (T_c) is similar to T_a. Substituting Ω_c in Equation 4.3 and considering $T_c = T_a$, we developed an expression for the E_c of these oak trees as

$$E_c = g_c D_a / P \qquad \text{(Eqn. 4.13)}$$

The E_c is represented by a similar formulation to E_l, but now at a tree level. In order to know the behaviour of E_c we must therefore model g_c. We consider our model for g_c to be a function with the same general form as that obtained for g_s (Equation 4.8). Substituting g_c in Equation 4.13 of this general form, we obtain the following expression for E_c

$$E_c = (k_0 \exp(-k_1 D_a) + k_2)\ D_a / P \qquad \text{(Eqn. 4.14)}$$

The parameters of Equations 4.9 and 4.14 all have different meaning from those in Equation 4.8. In the present case, k_0 is the slope of the E_c (D_a) curve, k_1 is the inflexion point of the curve, and k_2 is the inclination at the end of the curve.

Next, plant water status was considered in the modelling of E_c. For this, transpiration was modelled across a Ψ_p range with 0.5 MPa steps, being in agreement with the number of points measured per step and the transpiration variability within the Ψ_p step.

4.4. Results

A close accord was observed between the course of time of transpiration and Ψ_p for Trees 1 and 5 (1994) and Trees 1 and 3 (1993), respectively. However, because of experimental conditions, Tree 3 in the 1994 period exhibited a different variation with time, in both transpiration and plant water status. This, together with similar structural characteristics, makes all the trees comparable in terms of their physiological functioning.

The Ψ_p for 1994 varied between -0.25 and -1.9 MPa, except for Tree 3 which was artificially disturbed by the sheet of plastic. Tree 3 transpiration rate showed a different pattern than Trees 1 and 5 in early and mid-summer, whose Ψ_p did not exceed -1.2 MPa (Fig. 4.3). We found a jump in the Ψ_p of Tree 5, between Day 264 and Day 273 (Fig. 4.3), that could be explained by the 5 mm of rainfall that fell on the experimental site during Day 272. In 1993, Ψ_p had varied between -0.55 and -2.47 MPa, as normally expected. The decrease in Ψ_p for the 1993 period can be explained by the lower rainfall (a decrease to 16 per cent) than in 1994, because the annual precipitation distribution within the two years was comparable. Both 1993 and 1994 were unusually dry years, with only 58 and 70 per cent of the mean

total precipitation falling on the study site, respectively. The chamber vapour pressure deficit (D_{ch}) values ranged between 0.4 and 6.5 kPa (Fig. 4.2b).

4.4.1. Leaf transpiration

Measurements of g_s and E_l made from June 1994 to January 1995 covered a wide range of environmental and plant water conditions. Daily values of g_s for this period ranged between 70 and 500 mmol m^{-2} s^{-1}, with maximum values close to 530 mmol m^{-2} s^{-1} (Fig. 4.2). The measured E_l hourly values, recorded in 1994, ranged between 1.6 and 7.4 mmol m^{-2} s^{-1} (Fig. 4.4). The E_l model was validated by comparing E_l measured in the leaves with the E_l simulated using Equation 4.9. Included in this were the inherent assumptions of Equation 4.6, and those of the g_s model (Equation 4.8). The correlation between E_l measured and simulated ($Y = 0.92\ X$; $r^2 = 0.94$, $p < 0.0001$) gives a slope slightly less than 1. That is, E_l simulated is slightly greater than E_l measured. We observed, as can be seen in the Figure 4.4, that values of E_l above 6 mmol m^{-2} s^{-1} diverged from the line 1:1. These values were recorded only for Tree 3 on 15 June and 18 August. From the beginning of June to September, this Tree showed a lower sap flow course than other trees, due to the disturbance described above. On the other hand, we found a similar correlation between mean daily E_l measured and that simulated from Equation 4.6 ($Y = 0.76\ X$; $r^2 = 0.96$, $p < 0.0001$), as Jarvis (1995) pointed out for daily averaging in linear responses.

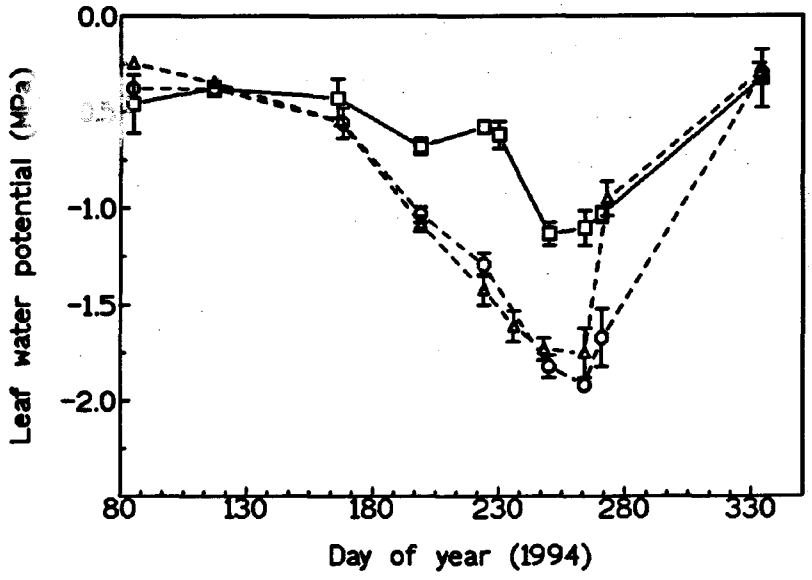

Figure 4.3. Pre-dawn leaf water potential (MPa) for the 1994 period of study: Trees 1 (o), 3 (□) and 5 (Δ). Tree 3 experienced different experimental conditions. Vertical bars indicate the standard error of mean.

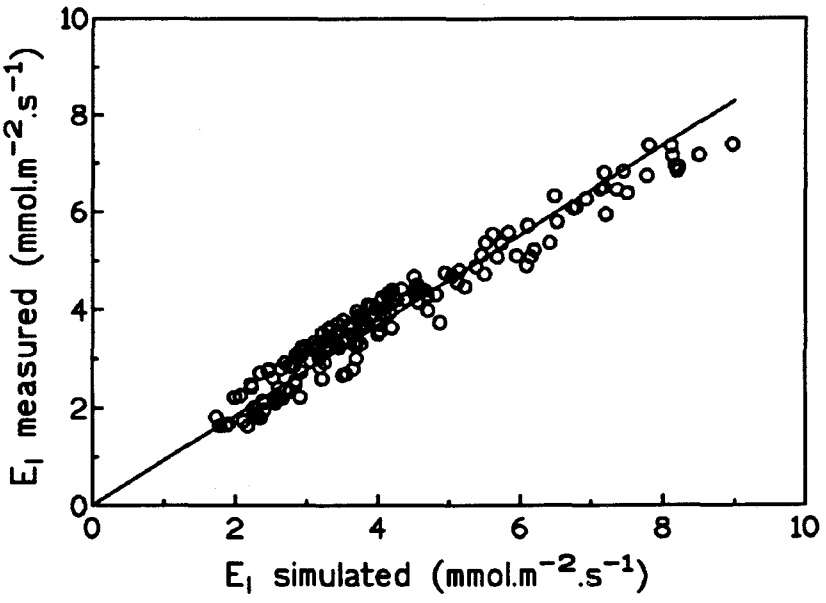

Figure 4.4. Linear regression passing through the origin between measured and simulated values of leaf transpiration (mmol m^{-2} s^{-1}) for the 1994 period ($Y = 0.92\,X$; $r^2 = 0.94$ and $P < 0.0001$).

Following Equation 4.9, E_l was modelled as a positive exponential function of D_a. The response of E_l to increasing D_a was characterised initially by a linearly increasing response between the variables, wherein transpiration is limited only by D_a. Later, stomatal closure was correlated to high values of D_a. Then, E_l approached a maximum value beyond which it was nearly constant with increasing D_a, where the increase of D_a is opposed by the stomatal closure. But from a critical value of the D_a, at the maximal stomatal closure, we found a new increase in E_l with the increase of D_a. The behaviour of the parts of this curve are represented by the parameters k_0, k_1, and k_2.

Generally, mean daily values of D_a in the periods of study ranged from 0.15 to 5.2 kPa. Although a few days did have mean daily values above 4 kPa, owing to a heat-wave in early and middle July 1994.

4.4.2. *Tree transpiration*

We have inferred the model of g_s at tree scale, and have created a model of g_c with a general form similar to that of the g_s model. From this model of g_c, we simulated E_c (Equation 4.14). Following Equation 4.14, E_c shows a similar response to D_a to that of E_l, as described above. In order to know the behaviour of the transpiration model, E_c was modelled for different periods and plant water status (Fig. 4.5A and B).

Figure 4.5 shows the response of E_c, as measured in the field, to D_a for different ranges of Ψ_p in 1993 and 1994. The mean daily E_c (considered as sap flow density) values recorded in both years ranged between 9 and 81 $mm^3\ mm^{-2}\ h^{-1}$. More points can be detected at the beginning of the curves in Figure 4.5A than in Figure 4.5B because the 1994 period was longer by several days at the start of spring and the end of drought when D_a was low. The measurements in 1993 were strictly

limited to the drought period, from the last spring rain to the beginning of autumn rains. The values of the parameters for the various models are shown in Figure 4.6. The decline of maximum values of E_c with the decrease in Ψ_p was comparable for the two years (Fig. 4.5A and B). The different range of D_a for the 1993 and 1994 periods may be due to its estimation in 1993 from the dew point temperature at Sevilla, where the humidity is generally higher than at the study area. Thus although D_a for the 1993 period might have been underestimated, it is at least proportional to that of the study site for all days of that year.

The model of E_c requires three parameters - k_0, k_1 and k_2 - as already described in the section on modelling procedure. The units of these parameters are given in Table 4.1.

Figure 4.6 shows the evolution of these parameters with decreasing Ψ_p in different periods, and under different conditions of study (Table 4.1). The parameter k_0, which represents the slope of the curve generated by the model, decreased with increasing water stress, exhibiting the same negative linear response in both years (Fig. 4.6A). The slope for the linear regression of k_0 was comparable for the three trees in 1994; however, Tree 3 displayed a slightly lower slope, for reasons already discussed. The slope for 1993 was twice that for 1994 (Table 4.2).

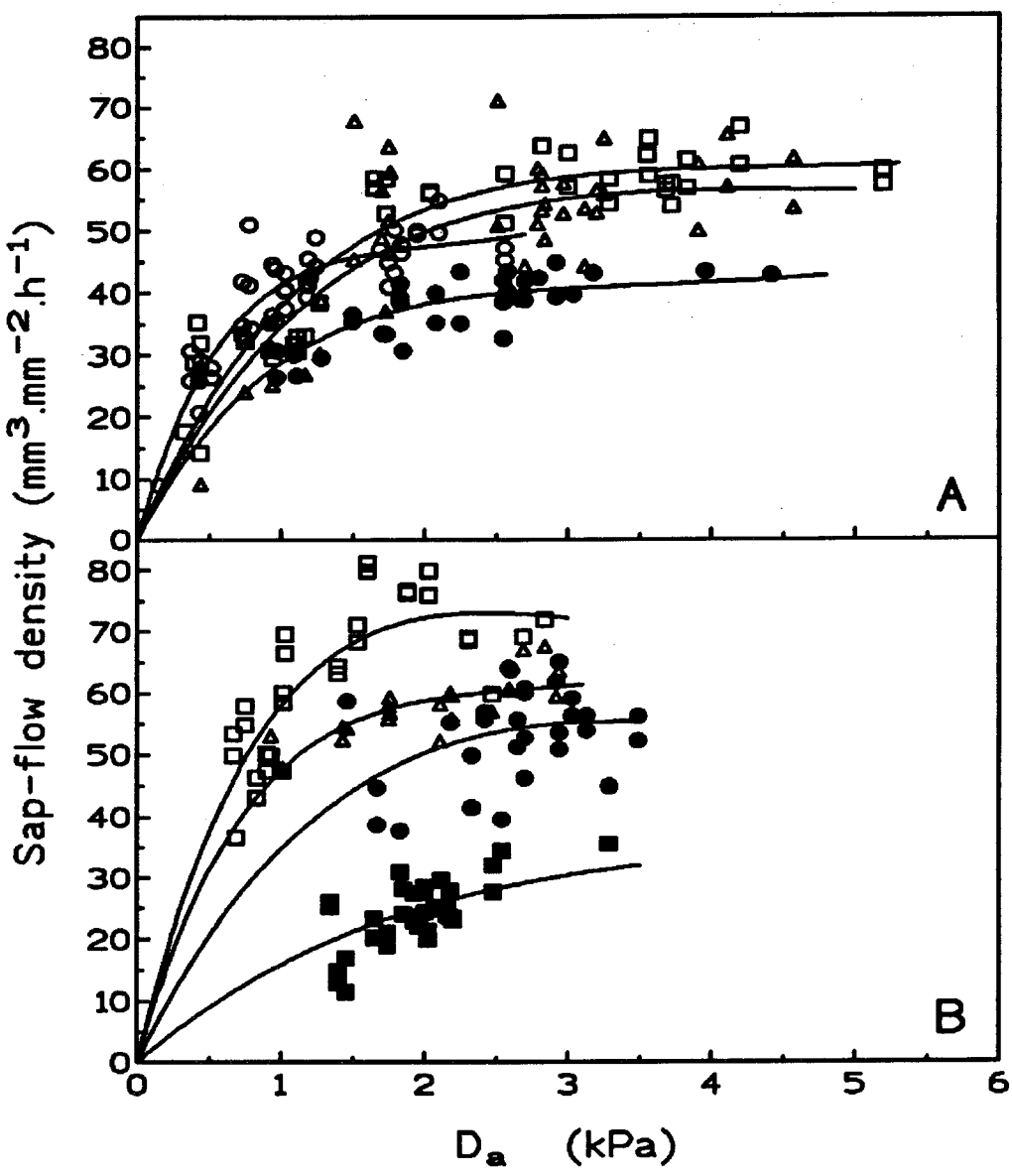

Figure 4.5. Functions of mean daily tree transpiration (mm^3 mm^{-2} h^{-1}) response to mean daily air water pressure deficit (kPa) for different ranges of pre-dawn leaf water potential (MPa), in the 1994 period (**A**) and the 1993 period (**B**). The unfilled circle shows the range between 0 and -0.5, unfilled square between -0.5 and -1.0, unfilled triangle between -1.0 and -1.5, filled circle between -1.5 and -2.0, and filled square between -2.0 and -2.5.

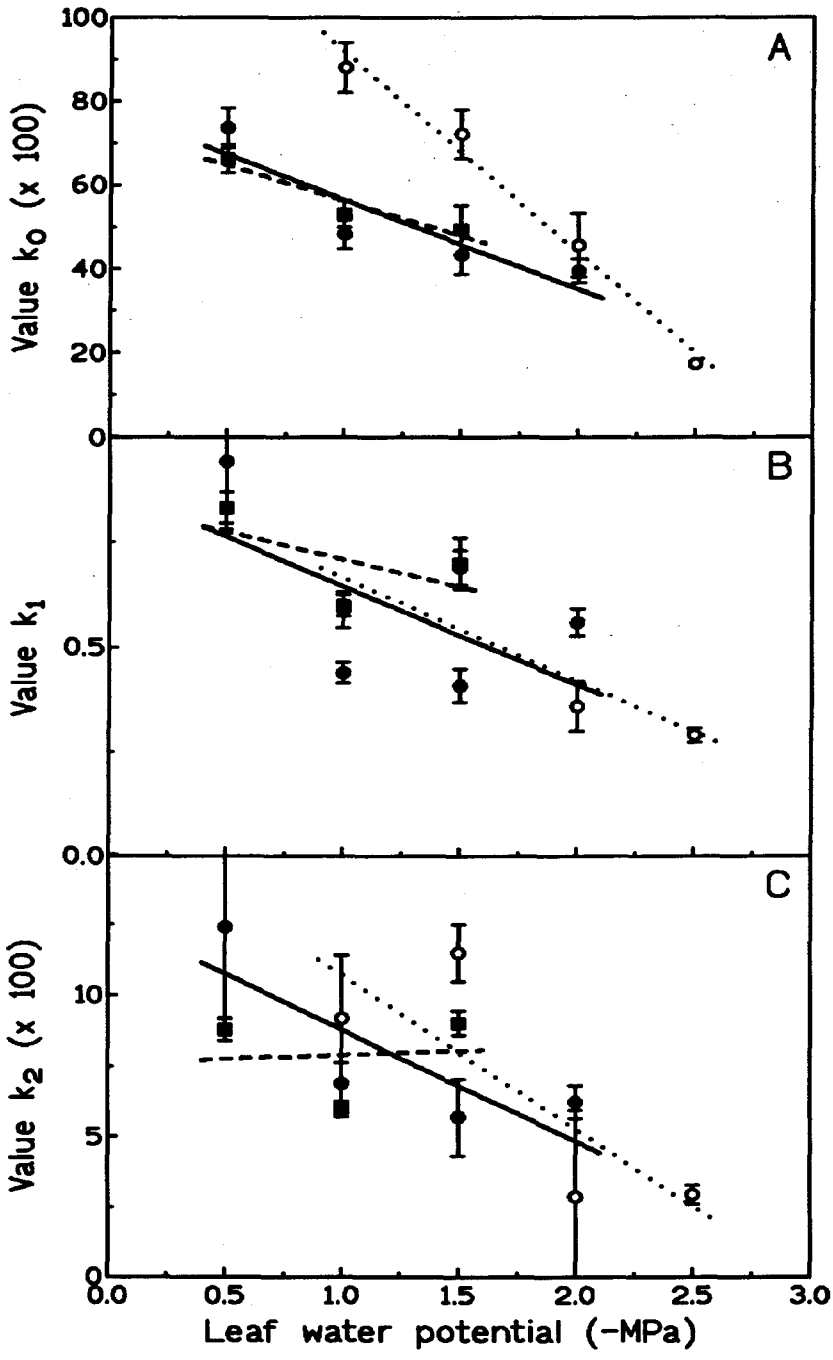

Figure 4.6. Evolution of the three parameter values used in modelling tree transpiration in relation to water stress. The value of Ψ_p shows the upper limit of the range in which it was modelled. The lines correspond to linear regressions for different periods of study: 1993 period, dashed line (unfilled circle), 1994 period, solid line (filled circle) and Tree 3 dotted line (filled square). Vertical bars indicate the standard error of mean.

Table 4.1. Parameter values (k_0 and k_2 in $mm^3\ mm^{-2}\ h^{-1}$, and k_1 in kPa^{-1}) of the curves derived from tree transpiration model (first data set); n is the number of observations used and the number in parentheses shows the standard error of the mean.

	1993 period			1994 period			Tree 3 (1994)		
Range Ψ_p (-MPa)	k_0	k_1	k_2	k_0	k_1	k_2	k_0	k_1	k_2
0.0 - 0.5	-----	-----	-----	7362	0.94	1241	6620	0.83	878
				(482)	(.16)	(321)	(329)	(.04)	(37)
0.5 - 1.0	8814	0.59	919	4829	0.44	689	5324	0.59	596
	(599)	(.04)	(222)	(341)	(.02)	(73)	(319)	(.03)	(28)
1.0 - 1.5	7222	0.70	1150	4344	0.41	569	4946	0.70	902
	(586)	(.04)	(102)	(474)	(.04)	(135)	(575)	(.06)	(43)
1.5 - 2.0	4574	0.36	289	3957	0.56	622	-----	-----	-----
	(764)	(.06)	(304)	(284)	(.03)	(58)			
2.0 - 2.5	1732	0.29	296	-----	-----	-----	-----	-----	-----
	(61)	(.02)	(33)						
	n = 118			n = 165			n = 176		

Parameter k_1 represents the inflexion point of the curve. A high value of k_1 would mean that the inflexion point is near the origin of D_a. That is, E_c quickly reaches its maximum value, and this would normally correspond to a high value of k_0. Similar slopes were observed for the two periods in the correlation between this parameter and the Ψ_p. Again, only Tree 3 (1994 period) showed some difference (Fig. 4.6B).

Parameter k_2 shows the slope at the end of the curve. This parameter is difficult to interpret in relation to Ψ_p because it attempts to explain a poorly represented part of the curve. For this reason, a large standard error is associated with this

parameter (Fig. 4.6C). In the two periods studied there was a negative correlation between this parameter and Ψ_p (Table 4.2). Except that again Tree 3 showed a poor correlation with Ψ_p, which can be explained by the similar maximum values of E_c for the three Ψ_p ranges. In terms of g_c, a decrease in the sum of k_0 and k_2 means a decrease in g_{sm}, as shown by Equation 4.8.

Table 4.2. Statistics of linear regression between the values of parameters derived from tree transpiration models and leaf water potential range which to modelled; n is the number of observations and r^2 is the coefficient of determination.

Period of study		Parameters of the model					
		($mm^3\ mm^{-2}\ h^{-1}$)		(kPa^{-1})		($mm^3\ mm^{-2}\ h^{-1}$)	
	n	k_0		k_1		k_2	
		r^2	Slope	r^2	Slope	r^2	Slope
1993	4	0.98	-4779	0.71	-0.25	0.64	-545
1994	4	0.81	-2139	0.40	-0.24	0.67	-395
Tree 3 (1994)	3	0.91	-1672	0.32	-0.13	0.01	28

The behaviour of the E_c model was validated by comparing the observations of the second data set with the transpiration simulated from the input variables, using the parameters derived from the first set of measurements. This procedure was applied across the two years of study, for each of the Ψ_p ranges. Figures 4.7A and B show the relationship between measured and simulated values of E_c, for all seasons and each period of study. The model performed well, accounting for 79-87% ($p < 0.05$) of the variation in the variable, and with the slopes of regression

lines very close to unity (Table 4.3A). The predicted values of E_c showed no-significant bias from the observed values, in both 1993 and 1994. We also analysed the performance of the model by steps of Ψ_p, but the results were somewhat different (Table 4.3B).

Table 4.3. Statistics of linear regression between measured and simulated daily values of tree transpiration throughout the season (**A**) and by range of Ψ_p (**B**): n is the number of observations and r^2 the coefficient of determination.

A:

Period of study		Transpiration (E_c)	
	n	r^2	Slope
1993	118	0.87	1.04
1994	166	0.79	1.03

B:

	1993 period			1994 period		
Range of Ψ_p (-MPa)	n	r^2	Slope	n	r^2	Slope
0.0 - 0.5	--------	--------	--------	47	0.81	1.00
0.5 - 1.0	30	0.77	1.38	40	0.75	0.89
1.0 - 1.5	21	0.24	0.81	45	0.73	1.16
1.5 - 2.0	28	0.02	0.25 *	34	0.75	1.38
2.0 - 2.5	39	0.21	0.85	--------	--------	--------

(* the slope is not significantly different from zero)

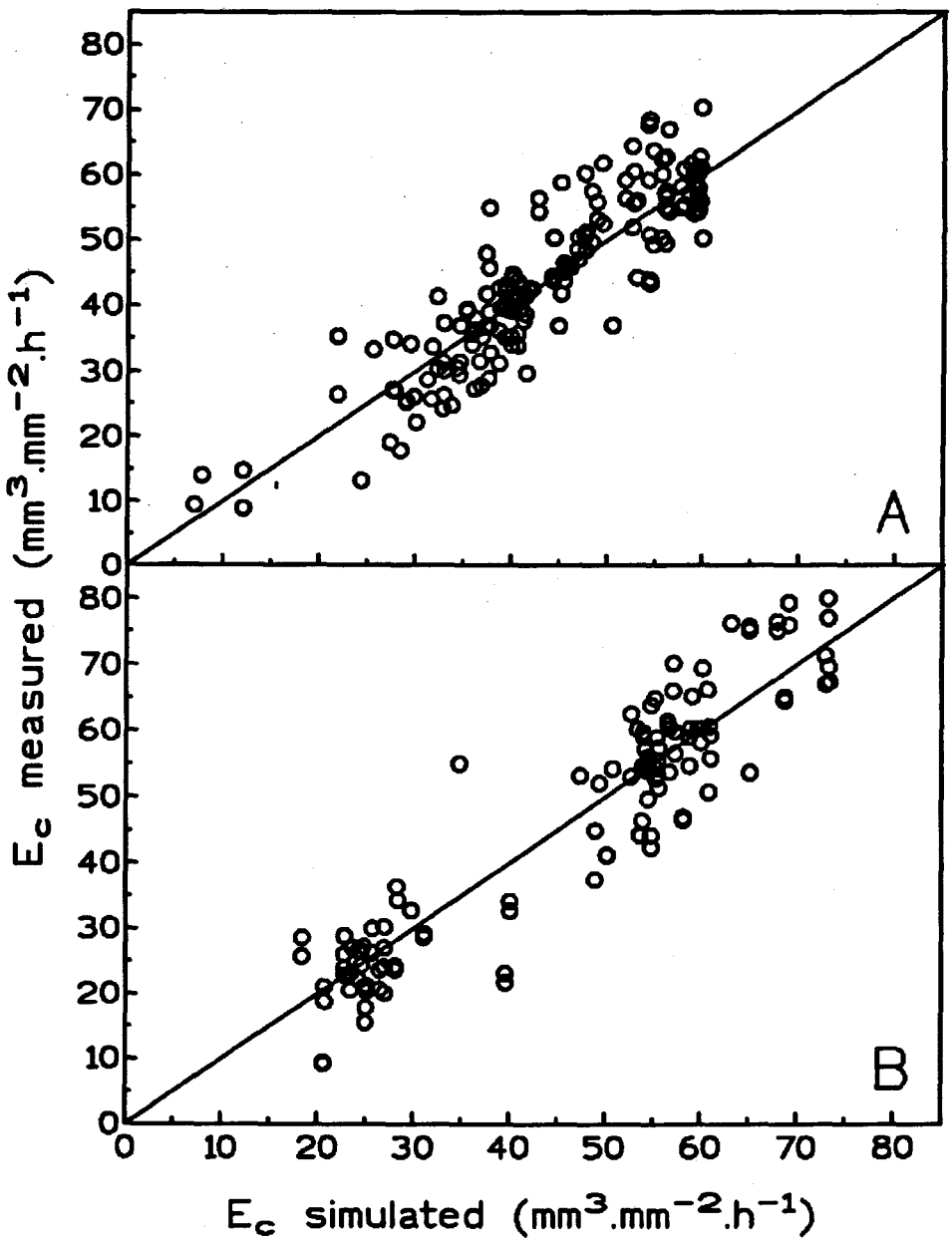

Figure 4.7. Relationships between measured and simulated values of mean daily tree transpiration (mm^3 mm^{-2} h^{-1}) for the 1994 period (A) and the 1993 period (B). The solid line represents the 1:1 value.

4.5. DISCUSSION

4.5.1. *Stomatal response to environmental conditions*

The daily patterns of g_s and E_l recorded in our study are in the range of those measured by other authors on the same species under different environmental conditions (Acherar & Rambal, 1992; Castell et al., 1994; Sala & Tenhunen, 1994).

Ambient humidity, expressed as D_a, was found to be the most significant predictor of both hourly and mean daily g_s values (Körner & Cochrane, 1985). Stewart (1988) gives different models for hourly and mean daily surface conductance, but unlike our results the hourly g_s estimates were more precise than the mean daily g_s values. This difference can be explained by the fact that the models used by Stewart (1988) in g_s modelling included several other variables, and these variables would have evolved differently throughout the day. Consequently, a mean daily model with all these variables has lower precision, both because of the interactions between variables and their evolution. In contrast, our model of g_s is based on a single variable, so that the evolution of this variable throughout the day can be stated with greater precision.

Diurnal changes in leaf water potential do not seem to exert a major influence on stomatal aperture (e.g., Tenhunen et al., 1987; Sala & Tenhunen, 1994). However, at the seasonal timescale, a good correlation of g_{sm} and g_s with Ψ_p has been found (Körner, 1994; Reich & Hinckley, 1989; Sala & Tenhunen, 1994). In our study, it does not provide significant contribution in the explanation of the hourly and mean daily g_s, respectively. The evolution of g_s, with D_a, for different Ψ_p ranges showed a direct covariation between D_a and Ψ_p. An increase in D_a through a drought period was followed by a decrease in the daily g_{sm}. Similar results were obtained by Granier & Loustau (1994) for maritime pine. This D_a-Ψ_p covariation explains the low contribution of Ψ_p to the g_s model, and furthermore, it simplifies

it. In fact, plant water status will have a significant effect on the estimates of transpiration, as was pointed out by Stewart (1988).

The main advantage of a model of surface conductance driven by a single variable is that there are no interactions or interconnected processes between variables to consider. The procedure is simplified. The wide range of D_a values that were recorded in the period of study leads to the simplification of the model based only on this variable and not involving a restriction of the knowledge of surface conductance behaviour, at least for the timescale at which we worked.

The stomatal response to humidity may be linear, or non-linear (Farquhar, 1978; Jones, 1992), depending on the system involved. Lösch & Tenhunen (1981) and Jarvis & Morison (1981) suggest a linear response of g_s to D_a. However, other authors report a non-linear response in many species such as in conifers (Lindroth, 1985; Stewart, 1988 and Johnson & Ferrell, 1983), in Eucalyptus (Körner & Cochrane, 1985; Dye & Olbrich, 1993) and Grantz & Meinzer (1990) in sugarcane. In our case, the non-linear response has the form of a negative exponential function, characterised by the parameter k_2. This response was found in hourly and mean daily measurements of g_s. The same hourly response was suggested by Sheriff (1984) in his analysis of stomatal response to humidity. Granier & Loustau (1994) describe similar behaviour, without k_2, for conifer stomatal conductance across different classes of soil moisture. But if only one soil moisture class is considered, the parameter k_2 could be included in their expression (Fig. 3 in Granier & Loustau, 1994). The fact that this parameter has not often been used in the non-linear response may be due to the lack of measurements of stomatal conductances available at high values of D_a, as occurred here in the field. Values of D_a close to 5 kPa represent a strong climate stress for the plants, which is unusual to find under temperate climates, except in Andalusia.

This negative exponential response suggests a feedback control of g_s by D_a (Farquhar, 1978). This should also be found in the transpiration behaviour. An increase in D_a will involve an increase in leaf transpiration, and consequently a decrease in local leaf water potential that will regulate the stomatal aperture. In this, case the direct controller of stomatal aperture will not be D_a, as a feedforward control, but transpiration via the local leaf water potential, preventing the development of a more-severe water stress in the leaf. This feedback control of g_s could be explained as an adaptation of these plants to long dry periods, during which the plant is forced to maintain a minimum g_s to continue its functioning. At the same time, this feedback response implies a continuous water loss during the dry period, which could promote damage to the plant under an extended drought. The problem is solved in "dehesa" ecosystems by the low tree density, which allows a higher water availability to isolated individual trees even in dry years, as is shown here by the low Ψ_p recorded in both years of study, which can be considered dry years.

4.5.2. *Transpiration modelling*

The simplified model of E_l, inferred at tree level, provides a good agreement between the E_c measured and that simulated. This is due to near zero estimated values of Ω, resulting from the small leaves and the well-ventilated canopies of these sclerophyllous trees, which create only small gradients of saturation deficit for large boundary layer conductances. The Ω explains the sensitivity of transpiration to changes in surface conductance, which we found did not change with the increased spatial-scale in our "dehesa" ecosystem. This is contrary to the thesis of Jarvis & McNaughton (1986), and McNaughton & Jarvis (1991), which suggests a diminished sensitivity of transpiration to surface conductance with increasing areal scale. Transpiration control by surface conductance at all spatial scales makes the "dehesas" more dependent on atmospheric conditions.

In the following analysis of transpiration behaviour and biological interpretation, we will use the E_c model as an example. The relationship between E_c and D_a exhibits a behaviour described by a positive exponential function at different Ψ_p levels, with transpiration tending to increase with D_a and finally approaching an asymptote. This tendency is opposed by the tendency of stomata to close with increasing D_a, which explains the asymptote of E_c at high values of D_a (Farquhar, 1978; Jarvis & McNaughton, 1986). This is in accord with the feedback hypothesis of stomatal regulation shown by g_s in Figure 4.2 (Jones, 1992; Lindroth, 1985). A similar response of E to D_a was found by Meinzer et al., (1993). Feedback control allows the plant a certain transpiration (asymptote of E_c in Fig. 4.5) at high values of D_a compared with feedforward control, which makes transpiration decrease at high values of D_a.

4.5.2.1. Response of transpiration to water stress

The pronounced limitation of E_c with decreasing Ψ_p results from progressive stomatal closure as plant water stress increases. In the relationships between E_c and D_a, seasonal hysteresis was also observed for the consecutive Ψ_p ranges. The slope of the curves decreased with decreasing Ψ_p. That is, a decline in Ψ_p involves a lower value of E_c for the same values of D_a, except for values near zero.

The hysteresis of transpiration through the drought period may be explained by an acclimation of the plant's stomatal flow to water stress conditions. A decrease in Ψ_p involves a decrease in mean daily g_s, but for a given level of water stress, a decrease in D_a involves a slower increase in E_c than when under a less-severe water stress level. This creates the advantage of increased water use efficiency at low Ψ_p during long drought periods, and an increased tolerance to dry conditions by the acclimated leaves. Furthermore, it would explain the low

stomatal conductances throughout the day as measured in July and August at the higher D_a values (see g_s, Fig. 4.2B). Lösch & Tenhunen (1981) pointed out this phenomenon in the rate of stomatal response to ambient humidity for different conditions of prevailing humidity. The same change was found by Matthews et al. (1984) during the growth of sunflower leaves at different water deficits. As the drought progresses, water storage in the sapwood decreases (Hinckley et al., 1978; Zimmermann, 1983), and this can magnify the hysteresis process. Carlson & Lynn (1991) and Waring & Running (1978) reported a similar jump in the relationship between Ψ_p and tree transpiration daily time course. They associated it with the water capacitance of the sapwood.

An alternative explanation for the hysteresis phenomenon could be xylem embolisms at low leaf water potentials. This would reduce the volume and velocity of sap flow in the plant. This would be in accord with the different gap size between curves found between 1993 and 1994, and could explain the seasonal course of Ψ_p in each year. In 1993 the pre-dawn Ψ_p was lower than in 1994, and it decreased in fewer days. Lo Gullo & Salleo (1993) showed for *Quercus ilex* L. species, that a loss in hydraulic conductivity of about 53% for values of Ψ_p close to the turgor loss point could occur during summer drought period. Breda et al. (1993a) showed, in two species of European *Quercus*, a reduction of 70% in E and g_s, at Ψ_p ranging from -1.7 to -2.0 (MPa) due to xylem cavitation. In the same study those authors show curves of vulnerability to cavitation for two species, as characterised by a drastic loss of conductivity over a small range of Ψ_p. Figure 4.5B shows a similar drastic reduction of sap flow in the Ψ_p range 2 - 2.5 (-MPa). Probably, both systems of control, namely plant response to leaf water potential and xylem dysfunction, are necessary to explain the stomatal behaviour to water stress here (Jones & Sutherland, 1991).

4.5.2.2. Behaviour of the E_c model parameters

The three parameters required by the E_c model evolve differently depending on the particular plant water limitations. As water stress becomes established, transpiration decreases for the same D_a value by the mechanism of hysteresis as described above. The slope of k_0 evolution under water stress shows the rate at which the plant responds to water limitations. The plant response also depends in the climatic conditions during the study period, as can be see comparing the slope of k_0 for the 1993 and 1994 periods. Despite climatic differences between these two study periods, all trees were exposed to a similar weather pattern during a given period.

The behaviour of parameter k_1 is better explained at the g_c level. The response of g_c to D_a showed a feedback control, whereas the increase in D_a involved an increase of leaf transpiration, and a decrease in local Ψ_p with increasing stomatal closure. If the local Ψ_p is not restored at the same rate at which D_a changes, the result is a gap between the two variables. Consequently, an increase in D_a becomes necessary to maintain the same stomatal aperture. Similar results were found by Granier & Loustau (1994) in modelling g_s for pines. In terms of E_c, as Ψ_p decreases, an increase of D_a is necessary to achieve the maximum value of E_c. This explains the decrease in the k_1 value with decreasing Ψ_p. Here, there is also a negative linear response. This region of the curve represents the start of the control of E_c by g_c, because there is a feedback control. At low levels of g_c this variable limits plant transpiration. The regression between parameter k_1 and Ψ_p could represent the specific response of the plant to water stress for a given species. The slope of this regression will be greater between different species than between trees of the same species, as it occurs in our case.

The response of transpiration to D_a is also characterised by the behaviour of the end of the curve. From higher values of D_a, there is a second inflexion point in the curve, and the transpiration can increase again, as at the beginning of the curve. The slope of this increase is represented by the parameter k_2. This part of the curve has not been represented in Figure 4.5. We have shown the model only in the range of D_a measured, which was always lower than the critical value of D_a, from where the transpiration can increase again. We found a negative correlation between the parameter k_2 and the Ψ_p, that could be explained by an adaptation of the stomatal closure to water stress. That is, as drought becomes severe the limit of the stomatal closure becomes lower (acclimation to water stress). This hypothesis is supported by the hysteresis phenomenon described above for transpiration. Also, the response could be explained by a limit to water loss through the local Ψ_p. There is less water availability in the leaf response to an air vapour pressure deficit.

We found a decrease in the sum of k_0 and k_2 when Ψ_p decreased, which means a decrease in g_{sm} with increasing water stress, as was shown by Körner (1994), Granier & Loustau (1994), and Reich & Hinckley (1989).

4.5.2.3. Validation and general behaviour of the leaf and tree models

Comparing the E_l measured with that simulated, we find a good correspondence. These results are better than those obtained with other models reported in the literature, such as that of Granier & Loustau (1994) for the hourly modelling of the transpiration of maritime pines. Also, the model of E_c gave values close to those measured. Some of the differences between the E_c measured and that simulated may be due to a combination of measurement errors in the micrometeorological properties (±10%; Stewart, 1988) and in the sap flow (±15%, Loustau et al., 1990). Nonetheless, the present E_c model does provide a very good

description of the daily transpiration changes (explaining between 79 and 87% of the variance) in isolated trees under different plant water status.

However, if we analyse the performance of the model per interval of Ψ_p, the results are somewhat different (Table 4.3B) compared with the simulations for each whole period of study (Table 4.3A). The origin of these different results is the D_a-Ψ_p covariation, which implies high values of D_a for low values of Ψ_p. This results in E_c being poorly correlated with D_a for low values of Ψ_p, as the points are on the asymptote of the curve. In general, the description of daily whole-tree transpiration provided by the model is less accurate at the drier end of the Ψ_p curve. Here, E_c becomes more independent of D_a than at the beginning, where there is a good linear relation between these variables. For this reason, the model cannot explain all the variability of in the daily E_c for short periods of high values of D_a. This effect is illustrated by the Ψ_p range of 1.5 - 2.0 (-MPa) in the 1993 period, where the slope of the regression line is not significantly different from zero. The transpiration values measured were towards the end of the curve. Also, this effect explains the differences of r^2 found in the different Ψ_p intervals between the periods studied. Further research is needed, under controlled conditions of Ψ_p and D_a, of transpiration in oak-savannah ecosystems.

4.6. CONCLUSIONS

The model used for modelling transpiration in holm oaks under a drought period was found to provide acceptable predictions of leaf transpiration and tree transpiration. Validation of the behaviour showed insignificant differences between the observed and estimated transpiration. However, a decrease was found in the precision of the model for the periods with exclusively high values of D_a. More detailed studies are necessary to elucidate the response of transpiration to high values of D_a.

Of the climatic variables studied, ambient humidity of the air- expressed as air water vapour pressure deficit (D_a)- was found to be the best predictor of stomatal conductance (g_s) behaviour, at both hourly and daily time scales, in the oak-savannah ecosystem under study. The response of stomatal aperture to D_a follows a negative exponential. The same response was found for the tree conductance (g_c). Here, D_a exhibited a feedback control on g_s, that is, D_a controls stomatal aperture via leaf water flow.

Two main characteristics of the vegetation under study allow us to obtain a simplified model of transpiration: a near zero decoupling coefficient (Ω), and a surface conductance modelled by D_a. This model was found appropriate at both leaf and tree levels, with a different behaviour as a function of plant water status. Transpiration (E) was modelled by a positive exponential function to describe the feedback control found in the g_s response. For the transpiration model, D_a and predawn leaf water potential are the main variables explaining transpiration behaviour from the leaf level to that of isolated whole trees. The transpiration model was characterised by three parameters. The parameter k_0 explains the adaptation of the plants to variations in weather conditions; k_1, the species-characteristic parameter showing the response in g_s to water stress; and k_2, explaining the behaviour of transpiration at high values of D_a.

The sensitive response of stomatal aperture to saturation deficit is probably due to an adaptation of this species to saturation deficit within the tree-canopy, which is controlled by overhead conditions (McNaughton & Jarvis, 1983) and long drought periods. At the same time, from the scientific viewpoint, these overhead conditions simplify the process of scaling-up from the leaf to the tree, due to the homogeneity of environmental conditions at the two spatial scales. We found that transpiration at both leaf and tree scales is linearly related to surface conductance, which is a particular case in the functional relationships between both variables (Jarvis, 1995).

The low densities of trees in this ecosystem give oaks the competitive advantage of a greater water availability. But at the same time, there is the disadvantage of a greater control by climatic conditions over the functioning of these isolated trees, when compared with closed forests.

V. WITHIN-TREE SAP FLOW VARIABILITY: APPLICATION OF THE PIPE-MODEL THEORY

5.1. INTRODUCTION

Major environmental factor influencing both transpiration and assimilation in plants is the amount of radiation intercepted by foliage elements (Green, 1993; Alvino et al., 1994). In general, the canopy radiation balance depends not only on the density and distribution of the foliage, but also on the amount of incoming radiation in tree canopy, that is the fractional area of sunlit and shaded leaves (Stockle, 1992; Green, 1993). In oak-savannahs of SW Spain, tree stratum is represented only by isolated trees, at low density. In these isolated trees, hemispherical crown shape can be assumed, with different radiation intercepted by the foliage according to orientation and the sun's azimuth. On the other hand, sun-shade functional differentiation of leaves has been pointed out in many works (Hollinger, 1992; Green, 1993; Alvino et al., 1994; Sala & Tenhunen, 1996). This functional differentiation between leaves implies significant differences in leaf transpiration. In this way, according to different incoming radiation regimen among tree-crown orientation, we must found a different transpiration regimen among tree-crown orientation on isolated trees.

Shinozaki et al. (1964 a, b) pointed out an explicit formulation of a pipe model of tree form: "*... A unit amount of leaves is associated with the downward continuation of non-photosynthetic tissue that has a constant cross-sectional area. Analogically speaking, a unit amount of leaves is provided with a pipe ... The pipe serves both as the vascular passage and as mechanical support, and runs from the leaves to the stem base through all of the intervening strata.*"

The outcome of this theory in physiological terms, as noted Nygren et al. (1993), is that tree transpiration rate is proportional to leaf area and the sapwood

(current sapwood in oak species) cross sectional area is a function of water requirements of the canopy. Several empirical observations in different species and environmental conditions (Waring et al., 1977; Rogers & Hinckley, 1979; Kaufmann & Troendle, 1981; Waring et al., 1982; Shelburne et al., 1993; Nygren et al., 1993) support the theory. According to the model, the annular pipes, defined as bundles of sap flow streamlines, must be formally identifiable with corresponding annual growth rings. Also, the conductivity of unit pipe will be different in different types of branches or stems (i.e., different water request). Nygren et al. (1993) noted, as the conductivity of unit pipe change among branches with different leaf area. This difference can be found between species as at tree or stand level.

Like this, and following the pipe-model theory, our hypothesis of work suppose that the functional differentiation among tree-crown orientations will be expected to reflect in different sap flow among tree-trunk orientation.

In this chapter we study the within-crown differences in transpiration rates on isolated trees, in relation with the tree-crown orientation, and analyse what are the reasons for this. We discuss four possible mechanisms (radiation intercepted by canopy, leaf area index, xylem conductivity and leaf conductance) to explain the different diurnal and seasonal patterns in sap flow on the different plant sides.

In order to determine within-tree variation in sap flow density on isolated trees, three sensor per tree were installed being in agreement with the trunk diameter of trees and the changes of sensor positions throughout the long periods of study. Trunk orientations analysed were NE, NW and S. Sap flow was monitored continuously from May to September 1993 (dry period), on two trees.

5.2. *MATERIAL AND METHODS*

5.2.1. *Sap flow measurements*

Sap flow measurements were carried out in Trees 1 and 3, with close height and diameter at breast height (Table 2.1). At that height, the trunk divided into two principal branches in both trees. The height of the lowest leaves was approximately 2 m in all the trees of the plot - being the maximum height of tree-grazing by farm animals. Data were continuously collected from 19 May to 27 September 1993 (during the drought period).

We divided the trunk into three sections each with different orientations, 0-120°, 120-240° and 240-360° (termed NE, S and NW, respectively), to allow for variation in the radiation intercepted by the tree at different periods of the day. Three sets of probes were installed in each tree, one set per section. The mean value of the three probes provides the transpiration for the whole-tree.

5.2.2. *Other measurements*

The leaf area index (*LAI*) was measured with a 1 meter line Quantum sensor (LI-COR 191SB, LI-COR, Ltd., Nebraska, USA). The method estimates the *LAI* of the tree canopy by extinction of the photosynthetically active radiation (PAR). PAR measurements were taken using two perpendicular orientations of the instrument per sample point; between 11:00 and 13:00 h local solar time in 9 September 1993. We adopted the coefficient of extinction of 0.732 proposed by Baldocchi et al (1984). The projected canopy area of each tree was divide into square with a distance of a 1 meter between sample points. The number of sample points was about 30 per tree.

5.2.3. *Statistical analysis*

The *t-test for paired comparisons* was used to show the differences in sap flow density among different tree orientations. It tests whether the mean of sample differences between pairs is significantly different from a hypothetical mean, which the null hypothesis puts at zero. The standard error over which this is tested is the standard error of the mean difference (Sokal & Rohlf, 1981).

Differences in *LAI* between sectors of the crown in each tree were tested with the Tukey-HSD test for the analysis of variance (Sokal & Rohlf, 1981).

5.3. RESULTS

Figure 5.1 shows the main climatic conditions from May to September 1993: daily rainfall and daily accumulated global radiation (H_g). The autumn 92-summer 93 period was a rather dry year. Total precipitation for this period was 422 mm, against an average of 720 mm for this station (period 1962-92), i.e., 41.5 % less rainfall for this year. Moreover, monthly precipitation distribution in the year was different, with half the total rainfall in spring.

For the analyses of differential sap flow within the tree we used the sap flow density per unit time ($mm^3\ mm^{-2}\ h^{-1}$, in daily patterns, and $mm^3\ mm^{-2}\ day^{-1}$, in seasonal patterns), since it is not possible to know the surface of water flow for the different orientations into which we divided the trunk, nor to calculate the sap flow per sector of trunk. We recorded maximum hourly values of sap flow density of about 400-500 $mm^3\ mm^{-2}\ h^{-1}$ in both trees. This maximum represents punctual peaks of sap flow early in the morning or late in the afternoon, depending on sap-flowmeter orientation in the trunk. Maximum daily values of sap flow density were about 4000-4500 $mm^3\ mm^{-2}\ day^{-1}$.

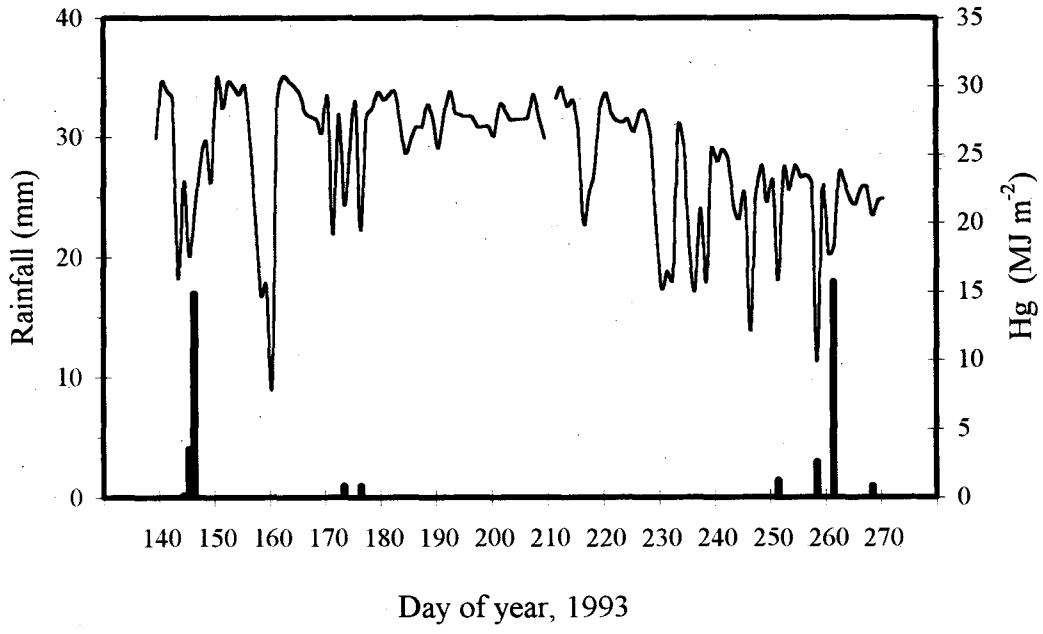

Figure 5.1. Daily rainfall (black bars; in mm), and daily accumulated global radiation (solid line; in MJ m^{-2}) in the period of study.

5.3.1. Daily sap flow

Within-tree sap flow density variations between orientations change considerably from cloudy to sunny days, as throughout the drought period. In order to show the diurnal within-tree sap flow density variation between orientations, we chose four sunny days (with H_g higher than 24 MJ m^{-2}) and four cloudy days (with H_g lower than 16 MJ m^{-2}) throughout the study period. Because similar results on within-tree sap flow density variation were found in both trees studied, Tree 1 and Tree 3, we shown the results of an only tree. Figure 5.2a shows the daily evolution of principal climatic variables (R_g and D_a) for the four sunny days studied. The days correspond to 30 May, 1 July, 8 August and 11 September 1993. Figure 5.2b shows the daily course of sap flow density in the

orientations considered in Tree 3. The graphs show daily evolution from one morning (6:00 h, local solar time) to the next morning (5:30 h, local solar time).

On sunny days (Fig. 5.2b), the NE orientation showed a rapid increase of transpiration in early morning, soon after sunrise, but often with a decrease toward midday that continued in the afternoon. On the other hand, the NW orientation showed a continuous increase through the morning, with maximum values after midday and in early afternoon, and decreased in late afternoon. The S orientation also showed an increase of transpiration in early morning soon after sunrise (but with maximum values lower than those of the other orientations), and there was a midday decrease, with a second peak in early afternoon. In all cases, there was a sap flow after sunset corresponding to water recharge of the trunk. The sap flow density of S orientation was always lower than of the other orientations, except at the end of the dry period, when values were comparable. The differences between orientations were not appreciable towards the end of the dry period (see 11 September, Fig. 5.2b), when the water deficit was severe (Fig. 3.8).

Figure 5.3a shows the daily evolution of R_g and D_a for the four cloudy days chose. The days correspond to 23 May, 9 June, 24 August and 15 September 1993. Figure 5.3b shows the daily course of sap flow density in the orientations considered in Tree 3. Again, the graphs shown daily evolution from one morning (6:00 h, local solar time) to the next morning (5:30 h, local solar time). Here, we found two marked different periods. In the beginning of drought there was not important differences between sectors, even were recorded similar values in three sectors (e.g., 9 June; Fig. 5.3b). It must be denoted that in 9 June was recorded the lower H_g value (8.2 MJ m^{-2}) of the study period. To the end of the drought period, and at low sap flow, were found noticeable differences between sectors. In Tree 3, the S orientation reach values between NW and NE orientations (Fig. 5.3b). Between the beginning and the end of the drought period we found an intermediate period as will be showed in the seasonal sap flow section.

We denote an important difference in sap flow between cloudy and sunny days. Even though we found significant differences between orientations in daily accumulated sap flow, the sap flow course throughout the day become similar for the three orientations, for example in 23 May, 24 August and 15 September (Fig. 5.3b). This fact was found independently of the period of the year.

5.3.2. *Analysis of within-tree variation in sap flow*

Figures 5.4 and 5.5 (Trees 1 and 3, respectively) shows the dynamics of daily sap flow density, in the three orientations considered, throughout the studied period. The seasonal pattern of sap flow was similar in the three orientations (Fig. 5.4 and 5.5). Daily sap flow density was lower throughout the whole period in the S orientation in both trees.

In order to analyse sap flow differences between orientations, we have considered four periods. The period named *Total* contains the whole period of study (from 19 May to 27 September). At the same time, this period was divided in another three periods in function of the seasonal sap flow dynamic (daily accumulated sap flow density, in $mm^3\ mm^{-2}\ day^{-1}$) (Fig. 5.4 and 5.5).

One first period (termed P_1; from 19 May to 9 June), where the sap flow change with climatic conditions, and corresponding to later spring. A second period (termed P_2; from 10 June to 29 July), characterised by a continuous and homogeneous decreasing of daily sap flow. It corresponds with the more severe drought period. The last period (termed P_3; from 30 July to 27 September), has been characterised by an important variability in sap flow dynamic, in the end of the drought period and the start of the autumn.

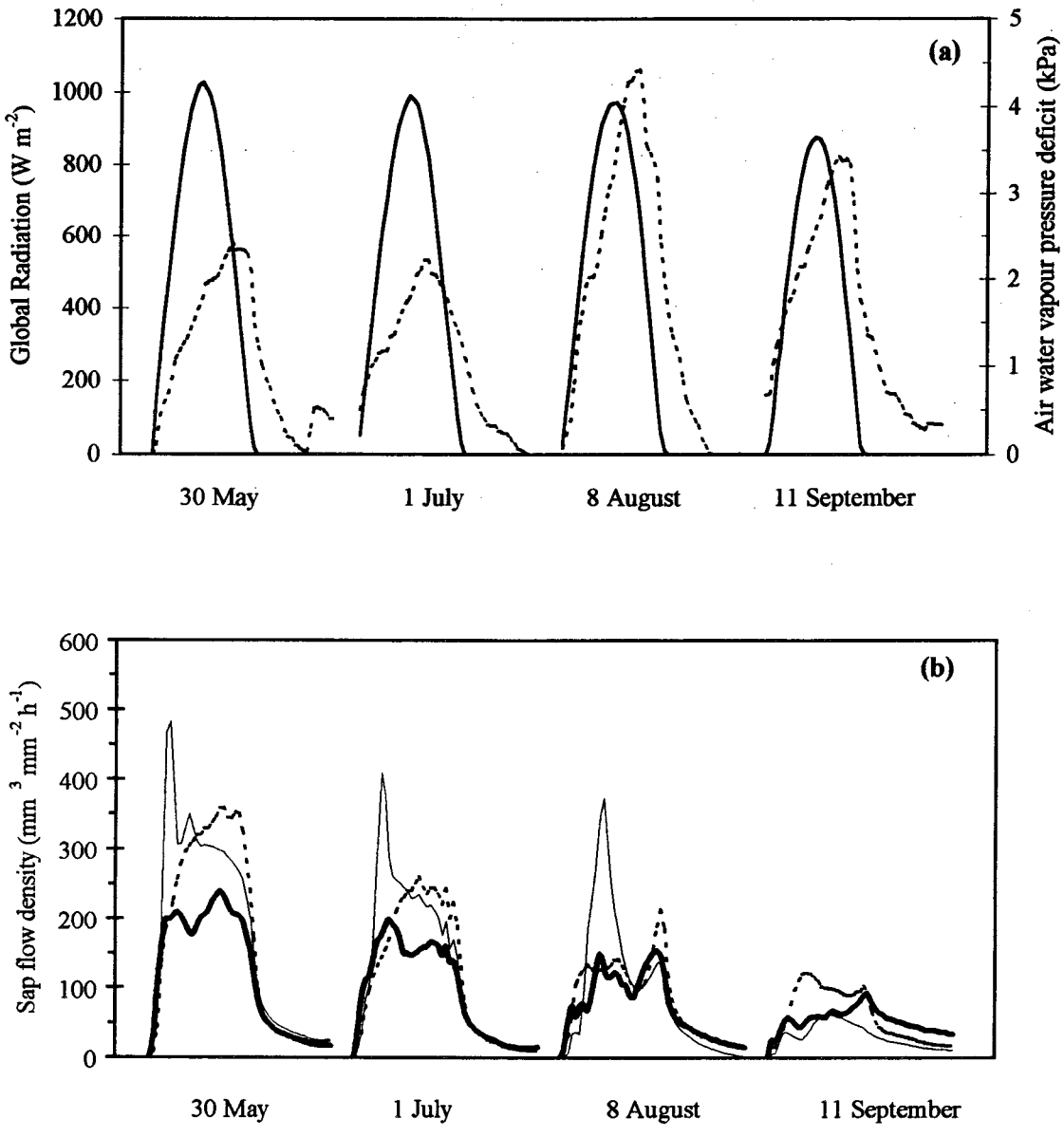

Figure 5.2. Daily variation of climatic variables: global radiation (solid line) and air water vapour pressure deficit (broken line) (**a**); and daily variation of xylem sap-flow density course in Tree 3, measured in three different orientations: NE (solid line), NW (broken line) and S (wide solid line) on sunny days (**b**). The graphs show daily variation from one morning (6:00 h, local solar time) to the next morning (5:30 h, local solar time). Days correspond to 1993 period.

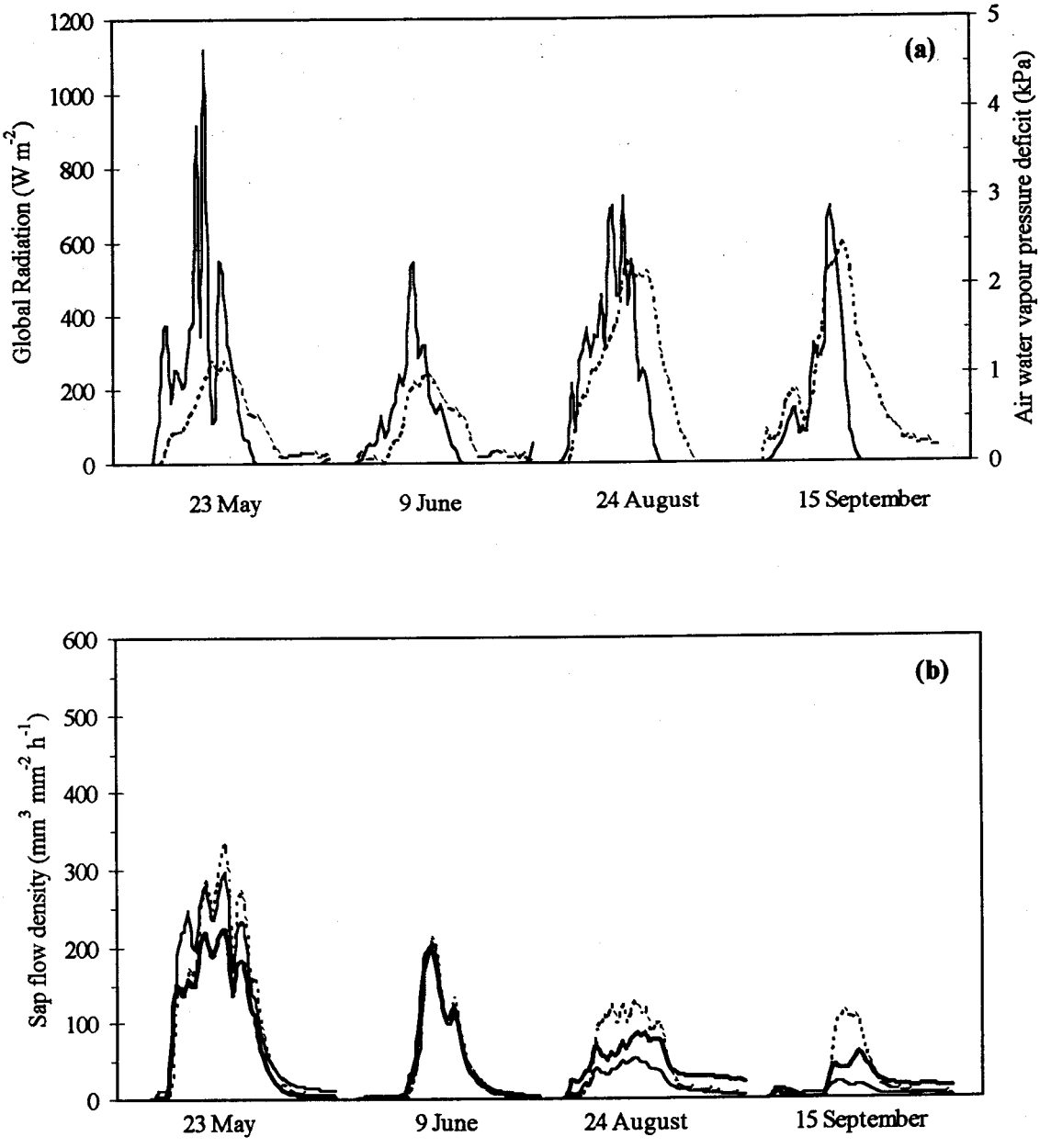

Figure 5.3. Daily variation of climatic variables: global radiation (solid line) and air water vapour pressure deficit (broken line) (**a**); and daily variation of xylem sap-flow density course in Tree 3, measured in three different orientations: NE (solid line), NW (broken line) and S (wide solid line) on cloudy days (**b**). The graphs show daily variation from one morning (6:00 h, local solar time) to the next morning (5:30 h, local solar time). Days correspond to 1993 period.

Table 5.1 shows the results of the comparisons, with the *t-test for paired comparisons*, between orientations for the different periods considered. This Table shows the mean value of the difference, and the probability of the null hypothesis. It has been considered the null hypothesis for $p > 0.01$. We found, in *Total* period, significant differences between S and the other orientations in Trees 1 and 3. However, we not found significant differences between NE and NW orientation in Tree 1. The same response was found in P_1 and P_3 in Tree 1. The other periods show significant differences between orientations in both trees.

The sign of the mean value (Table 5.1) denote that orientation show the higher sap flow. Thus, the differences between S and NW orientations were always negatives; that is, the sap flow was higher in NW than in S orientation. The sap flow values were always lower in S than in NW and NE orientations, excepting during the P_3 period in Tree 3.

Table 5.1. Mean of sample differences in sap flow density ($mm^3\ mm^{-2}\ day^{-1}$) between trunk orientation pairs. In parenthesis the probability to found the null hypothesis; *n* is the number of observations.

Sectors difference	**Tree 1**				**Tree 3**			
	Total	P_1	P_2	P_3	*Total*	P_1	P_2	P_3
NE – S	615.0	683.0	842.8	427.8	398.0	962.2	788.7	- 240.9
	($p < 0.0001$)	*($p < 0.0001$)*	*($p < 0.0001$)*	*($p < 0.0001$)*	*($p < 0.0001$)*	*($p < 0.0001$)*	*($p < 0.0001$)*	*($p < 0.0001$)*
NE – NW	39.7	- 168.7	169.2	-34.3	- 134.9	134.7	174.3	- 562.7
	($p = 0.3486$)	*($p = 0.0676$)*	*($p < 0.0001$)*	*($p = 0.6820$)*	*($p = 0.0016$)*	*($p = 0.0070$)*	*($p < 0.0001$)*	*($p < 0.0001$)*
S – NW	- 600.6	- 851.7	- 668.9	- 462.1	- 532.9	- 827.4	- 614.3	- 321.8
	($p < 0.0001$)	*($p < 0.0001$)*	*($p < 0.0001$)*	*($p < 0.0001$)*	*($p < 0.0001$)*	*($p < 0.0001$)*	*($p < 0.0001$)*	*($p < 0.0001$)*
	n = 101	n = 22	n = 29	n = 50	n = 122	n = 22	n = 50	n = 50

5.3.3. *Within canopy variation in leaf area index*

Figures 5.6 and 5.7 show the tree-canopy projection of Trees 1 and 3, respectively. Spatial variability of *LAI* has been drawn with the software package SURFER (Surface Mapping System, Version 5.00, Golden Software Inc., Colorado, USA). The measurements correspond to 9 September 1993. In these figures has been drawn also the sectors considered in sap flow analysis, and the exact trunk position.

The Tukey-HSD test for the analysis of variance, with a significance level of 0.05, indicates significant differences in *LAI* between NE and S orientations. However, were not found significant differences between the other orientations (NE-NW and S-NW). Similar results were found in both trees. Table 5.2 resumes the statistic of differences in *LAI* between sectors.

Table 5.2. Statistics of the canopy leaf area index (*LAI*, in m^2 m^{-2}) measured in Trees 1 and 3 in 9 September 1993: *Mean* is the *LAI* mean value of the sector, *SD* is the standard error of the mean, and *n* is the number of observations. The sectors of canopy have been termed as north-east (NE), south (S) and north-west (NW) (see explanation in text). Sites follow by the same letter are not significantly different ($p>0.05$).

	Tree 1			Tree 3		
Sectors	*Mean*	*SD*	*n*	*Mean*	*SD*	*n*
NE	3.3 [a]	0.8	10	2.7 [a]	0.8	18
S	2.0 [b]	1.3	9	1.7 [b]	1.1	12
NW	2.2 [b]	1.1	11	2.3 [ab]	1.0	11

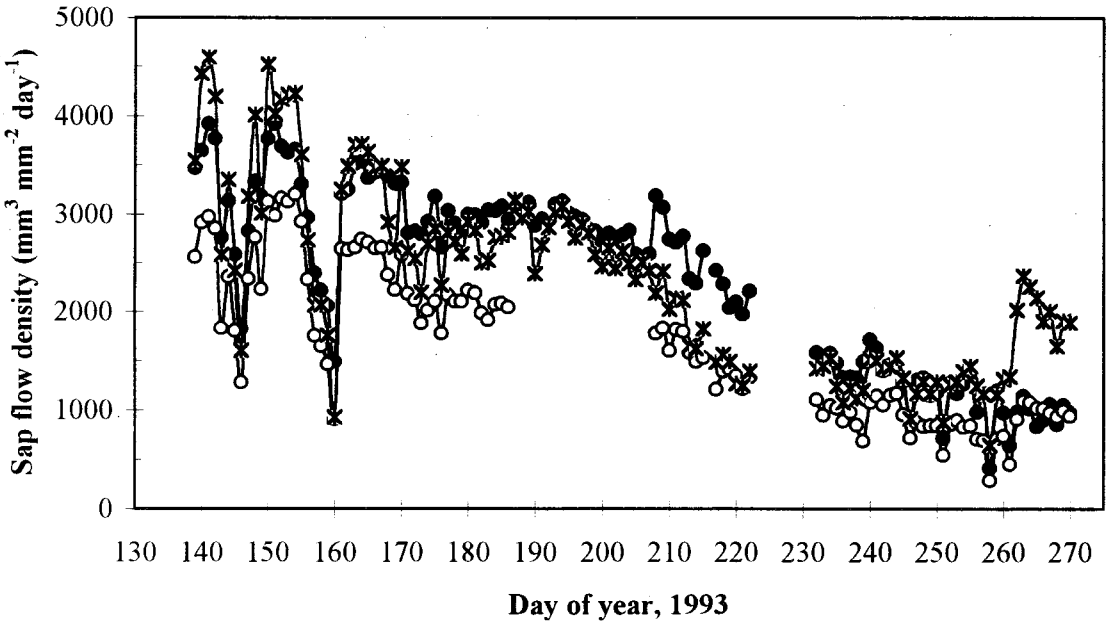

Figure 5.4. Seasonal variation in daily sap-flow density (mm^3 mm^{-2} day^{-1}) recorded in three different orientations: NE (black circle), NW (asterisk) and S (white circle) in Tree 1.

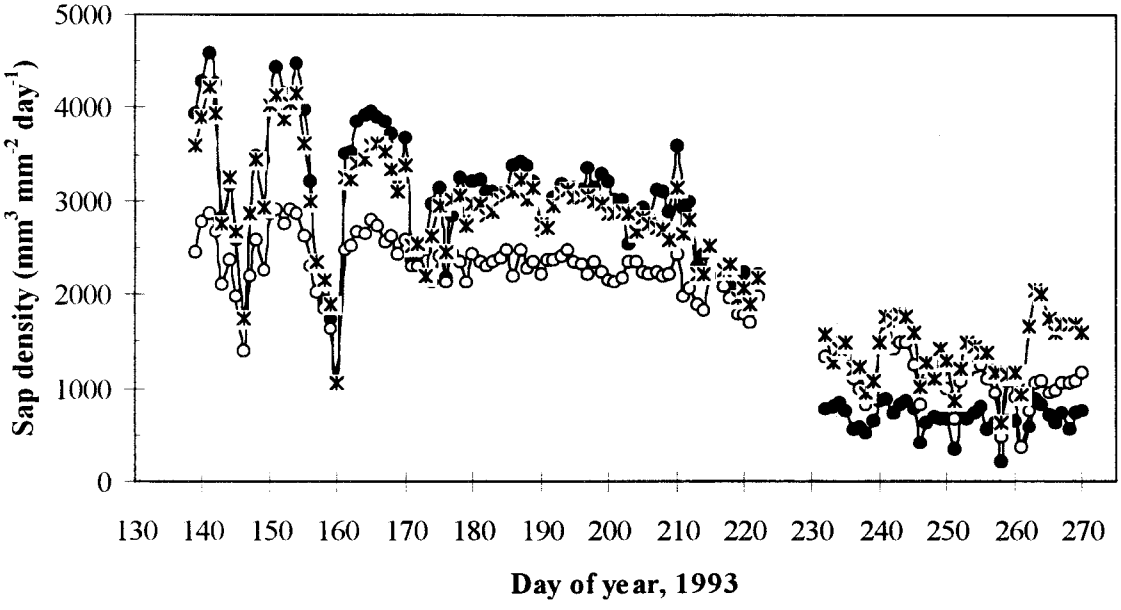

Figure 5.5. Seasonal variation in daily sap-flow density (mm^3 mm^{-2} day^{-1}) recorded in three different orientations: NE (black circle), NW (asterisk) and S (white circle) in Tree 3.

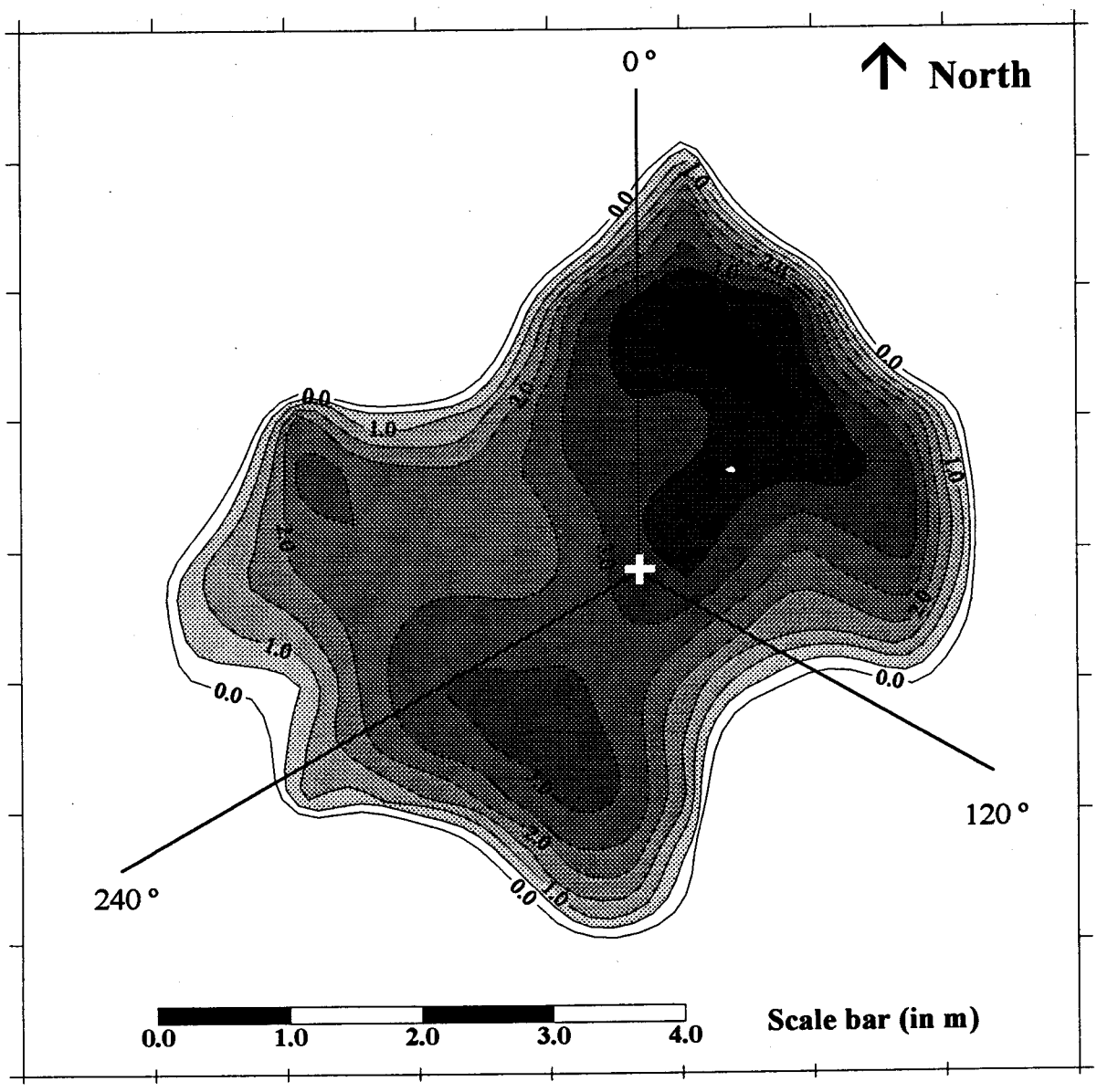

Figure 5.6. Projected tree-canopy leaf area index (m^2 m^{-2}) of Tree 1. The solid line delimits the three sections considered in sap-flow measurements. The white cross represents the tree trunk position. The date corresponds to 9 September 1993.

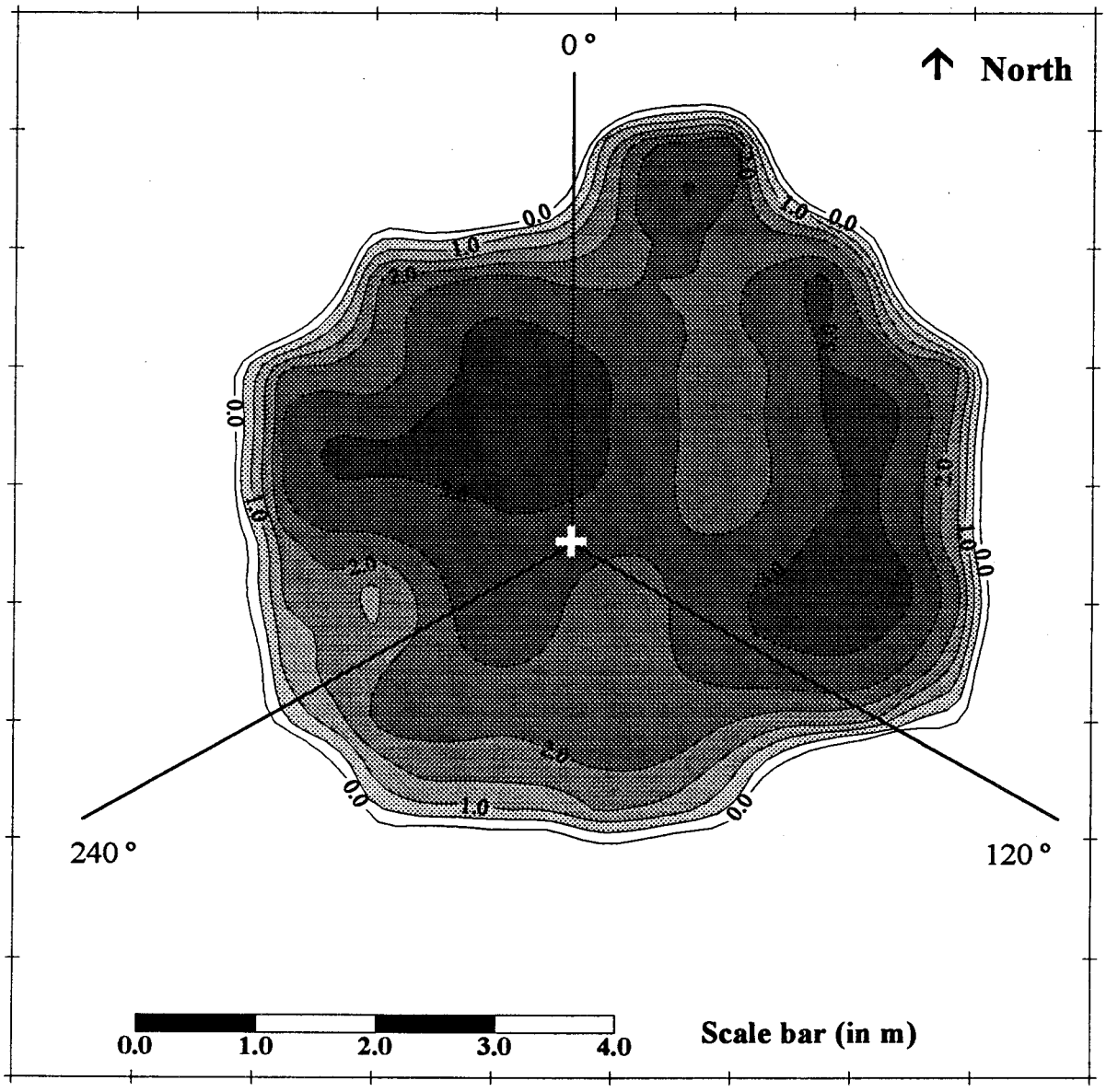

Figure 5.7. Projected tree-canopy leaf area index (m^2 m^{-2}) of Tree 3. The solid line delimits the three sections considered in sap-flow measurements. The white cross represents the tree trunk position. The date corresponds to 9 September 1993.

5.4. DISCUSSION

5.4.1. *Within-tree sap flow variability: the Pipe-model idea*

In large-porous oaks, water ascends from one particular region of the root system along a strip of young xylem to one particular portion of the crown. The independence of the various sides (sectors) of the tree has reached an extreme in ring-porous species (Zimmermann & Brown, 1971). In this way, we measured sapwood width in the trunk in various *Q. ilex* trees and in two different stands using injected dyes. In these experiments, we always found a sap flow along a strip of xylem perpendicular to the soil, and rejected a sectorial flow spiralling in the trunk of this species, or any others complex twirling paths as founded in some coniferous species (Zimmermann, 1983). From this, and the fact that the main branches of the tree extend from just above the sap-flowmeters, we can assume a sectorial flow in the trunk connecting each trunk sector with a different branch or sector of the branch (i.e., different tree-crown sector). This assumption can be considered independently of the changes in sapwood cross-sectional area and specific conductance of xylem with the tree height level, suggested by Rennolls (1994) about the pipe model theory.

On the other hand, the *t-test for paired comparisons* used to compare sap flow in different trunk orientations demonstrate significant differences among them, particularly between S orientation and NE and NW orientations. These differences have been noted at daily and seasonal time scale. In general, in the NE oriented sector we found a diurnal sap flow density course with main activity in the morning, in the NW oriented sector the main activity was in the afternoon, and the S oriented sector showed a lower activity than other sectors, with a more or less accentuated midday decrease. The differences were less pronounced in cloudy days and at the end of the drought period, when leaf water request was strongly low.

Assuming the connection between one trunk sector and one tree-crown sector given, the differences in sap flow in trunk between sectors are due to differences in functioning and structural features at tree-crown level, as will be discussed below. This observation support the original pipe-model theory (Shinozaki et al., 1964a, b). However, if we found quite different functioning sector within a tree, beyond the relationship between cross-sectional area of vascular pipes and the leaf biomass that the pipe must supply, we could infer an independent functioning of pipe units on different canopy sectors.

5.4.2. *Sap flow differences in crown orientation*

Few works have taken into account the within-tree variability in transpiration estimated by sap flow measurements. However, some authors have shown the need of measurements around the trunk to ensure a true average and accurate sap flow (Miller et al., 1980; Tyree, 1988; Steinberg et al., 1990; Heimann & Stickan, 1993). Anfodillo et al. (1993) and Granier et al. (1994) noted as infrared technique evidence large differences in sap flow among sides of a stem, for several species. Miller et al. (1980) pointed out differences in sap flow density between north and south sides in the tree trunk for two American temperate oak species (*Quercus velutina* Lam. and *Q. alba* L.). Steinberg et al. (1990), in a very well-watered pecan tree (*Carya illinoensis* 'Wichita'), showed as sap flow in the southern branch was 41% higher than in the northern branch of the same diameter.

We discuss four possible mechanisms to explain the different diurnal and seasonal patterns in sap flow on the different plant sides. Three of these -radiation intercepted by tree-canopy, leaf area index and xylem conductivity- are related to structural features. The fourth, leaf conductance, concerning the tree functioning.

As has been noted in the Introduction section, the amount of *radiation intercepted by tree-canopy* is an important environmental factor influencing transpiration in plants (Hinckley et al., 1978; Green, 1993; Alvino et al., 1994). We

can assume that the tree-crown is hemispherical, which is close to the real situation as in these isolated trees the leaves tend to form a monolayer. If we assumed that part of the crown is shaded, in terms of time, the shaded part will be mainly north-oriented sectors rather than south-oriented ones. This different radiation regimen among orientations is supported by the fact that the plant flowering is related to radiation intercepted by the crown, and in isolated *Quercus ilex* trees were found as the quantity of flowers is higher in S than N orientations, and the flower maturing period change with the orientation (Gallego-Fernández, 1989).

The different plant sectors analysed on sap flow measurements correspond approximately to different light interception sections of the tree crown. This explains why morning sap flow density peaks were in the NE sector, and afternoon sap flow density peaks in the NW sector. It also explains why on cloudy days sap flow per orientation became similar, in terms of diurnal course, because there were no differences in intercepted radiation between different crown sectors. However, the amount of radiation intercepted by tree-canopy sides do not explains the differences in daily sap flow amount between orientations, and why the sap flow on south orientation was lower.

Changes in the *leaf area index* has been considered as an adaptation of Mediterranean plants to water stress, in order to optimise water use efficiency (Tenhunen et al., 1990; Rambal, 1993). This fact has been pointed out recently by Castro-Díez et al. (1997) in *Quercus ilex* species along a steep rainfall gradient in NE Spain. We found significant differences in *LAI* between NE and S orientations, which could explain daily sap flow differences between both orientations. However, we did not found these differences in *LAI* between NE and NW or S and NW orientations, when differences in sap flow were noted.

We could think in within tree variability on plant adaptation to water stress, changing the *LAI* with the water stress of different tree-crown sectors.

Unfortunately, there is no data available describing the spatial leaf area distribution on isolated trees.

The direct relationship of *xylem conductivity* with foliage transpiration is well documented (Hinckley et al., 1978; Miller et al., 1980; Steinberg et al., 1990); this relationship also is related to environmental factors as the aridity in evergreen *Quercus* species (Castro-Díez, 1996; Villar-Salvador et al., 1997). Xylem conductivity adjustments to changes in leaf transpiration rate become given at two levels. A functional level, in short-term, through embolism process and recover of hydraulic conductivity (Cochard & Tyree, 1990; Lo Gullo & Salleo, 1993). An other structural level, in long-term, through variations in sapwood vessel diameter and density (Villar-Salvador et al., 1997). In the last case, it has also been noted that variations in sapwood vessel diameter and density can be related with the growth and ramification of branches (Aloni, 1987; in Villar-Salvador et al., 1997). In this way, no differences among orientations were found in growth and ramification of branches in isolated trees on oak-savannahs (*Quercus ilex* L.) (Fernández-Alés, unpublished).

As on a microscale, variability in water status within-tree tissues becomes a complex and difficult area to investigate, the response of xylem conductivity to changes in leaf or canopy transpiration rates has been studied at community or species scale. But, in the same way, we could think in a differential response of the xylem conductivity or xylem thickness in within-trunk of tree according a differential within-canopy transpiration. This fact could explains the lower sap flow measured in S orientation, because there was an adaptation of this part of xylem to a more severe water stress than others orientations. This idea is supported by fact that at the end of the drought period the sapwood in S orientation shown a lower sap flow/xylem dehydration rate, when the seasonal sap flow was also lowers than the others orientations. This fact is visible in the night sap flow of S orientation. Anfodillo et al. (1993) pointed out as the thickness of the conductive xylem appears to be quite different between the southern and the northern sides of the tree. The differences between orientations were noted in

coniferous (*Picea abies, Abies alba*) and hardwoods (*Fagus sylvatica*) species. Also, Nygren et al. (1993) noted that the conductivity or unit pipe is different in different types of branches for a given plant. These results support our idea of different sapwood among orientations, in vessel diameter, density or thickness.

It has been accepted that sun-exposed leaves show higher *leaf conductance* than shade-exposed leaves (Hinckley et al., 1978; Hollinger, 1992; Green, 1993; Alvino et al., 1994; Sala & Tenhunen, 1996). However, this assumption must be considered for well watered plants. In this way, Sala & Tenhunen (1996) show comparable diurnal courses of stomatal conductance and transpiration in sun and shade leaves of *Quercus ilex* species during the drier months. Oliveira (1995) found similar results on leaves of *Q. suber* species. In some cases, it has been reported lower leaf conductance associated with sun leaves (Lassoie & Chambers, 1976; in Hinckley et al., 1978).

Sun-shade functional differences of leaves implies significant differences in leaf water potential (Hinckley et al., 1978; see discussion in page 33). This author noted as soil moisture deficits increased, variations between sun and shade foliage in *Quercus alba* trees decreased. Similar results were found with *Q. ilex* species in our work; the sap flow density differences between orientations decreased as ψ_p decreased (more negatives). In these trees, leaf transpiration can be considered as a positive exponential function of D_a, and the response of leaf transpiration to D_a come driven by leaf water potential (see chapter IV). Assuming different leaf water potential among tree orientations during drought period, as was found in *Quercus* species (Hinckley et al., 1978; Oliveira, 1995; pers. obs.), it could explains the lower transpiration of the southern orientated leaves, and as the drought become severe the differences between orientations decrease, because leaf water potential among orientations becomes comparable.

5.5. CONCLUSIONS

The results demonstrate significant differences in sap flow density among tree orientations, particularly between S orientation and NE and NW orientations. These differences have been noted at daily and seasonal time scale. The NE oriented sector show a diurnal sap flow density course with main activity in the morning, in the NW oriented sector the main activity was in the afternoon, and the S oriented sector showed a lower activity than other sectors, with a more or less accentuated midday decrease. The diurnal differences were less pronounced in cloudy days and at the end of the drought period, when leaf water request was strongly low. Similar differences among orientations were found in daily sap flow density. The NE and NW orientations shown higher sap flow density than S orientation, excepting to the end of the drought period were values become comparable among orientations. Our results support the idea of the needs of measurements around the trunk to ensure a true average and accurate sap flow as has been pointed out by different authors (Miller et al., 1980; Tyree, 1988; Steinberg et al., 1990; Heimann & Stickan, 1993). However, further detailed studies on this sectorization of transpiration in isolated trees are necessary

Shinozaki´s form of pipe model implies a sectorial flow in the trunk connecting each trunk sector with a different branch or sector of the branch. In this way, the within-tree transpiration variability founded it can not be explained only by the amount of radiation intercepted by the canopy. Other factors, as tree architecture (xylem conductivity, leaf area index) or leaf gas exchanges it must be considered.

Sprugel et al. (1991) pointed out that a branch may be regarded as hydraulically autonomous only under normal diurnal conditions, and that the autonomy does not exist under seasonal or long-term conditions. From the results shows here we can to infer a hydraulic autonomy of branches under short and long-term conditions. Except that the autonomy of branches will be less noticeable under stress conditions, as we found for water stress to the end of the drought period.

VI. MODELLING LEAF GAS EXCHANGE: TIME INTEGRATION

6.1. INTRODUCTION

As has been noted in chapter I, the Mediterranean vegetation shows adaptations to a strong seasonality in climatic conditions, from leaf to whole-plant levels. We are interested in knowing the gas exchange response of *Quercus ilex* — as isolated trees — under these limitations in different seasons through a year. Simulation models are essential tools in such work, for integrating physiological information across spatial and temporal scales. In this work we have not considered spatial integration, due to problems found at tree-canopy scale. These included different radiation regimen within the canopy, functional sun-shade response, and possible leaf nitrogen content variations throughout leaf phenology. Such factors are not well studied in *Quercus*. We worked with sun leaves, the leaf population more representative of the isolated tree-canopy (due to low leaf area index, about 1.9 m^2 m^{-2} as annual mean value).

Farquhar et al. (1980) and Farquhar & von Caemmerer (1982) developed a mechanistic model of leaf CO_2 assimilation in C_3 plants, which has been used as starting point in many leaf photosynthesis simulations in different species (Harley et al., 1986, 1992; Harley & Tenhunen, 1991; Kirschbaum, 1994; McMurtrie et al., 1992), including oaks (Hollinger, 1992; Tenhunen et al., 1990). Only recently has it been used in *Quercus ilex* (Sala & Tenhunen, 1996).

However, no mechanistic stomatal conductance model has yet been developed. Frequently, Farquhar's photosynthesis model has been linked to an empirical model of stomatal conductance developed by Ball et al. (1987), though we have not found simulations using this model accurate when compared with our measurements. The use of the model also involves important problems, as pointed out by Aphalo & Jarvis (1993).

The aim of this chapter is 1) to model and evaluate leaf gas exchange in *Quercus ilex* L., 2) to integrate this gas exchange under different environmental conditions and time-levels, and 3) to evaluate the effect of water stress on leaf carbon assimilation. For this purpose, leaf gas exchange (stomatal conductance, transpiration and net photosynthesis) was measured in sun leaves, in different seasons of the year. The measurements were made in a dry year, when water availability problems were more marked.

For time integration of leaf gas exchange, we used a modified version of the model of C_3 leaf CO_2 exchange proposed by Tenhunen et al. (1990) (see also, Harley & Tenhunen, 1991) in *Quercus coccifera,* used also by Sala & Tenhunen (1996) in *Q. ilex* forests of Catalonia (Spain). We also used an empirical stomatal conductance model tested by us in these trees (see chapter IV). For leaf transpiration, we used a mechanistic model developed from the Penman-Monteith evapotranspiration equation, which was formalised by Jarvis & McNaughton (1986) and repeatedly used in different ecosystems and species, such as those studied here (see chapter IV).

6.2. *MATERIAL AND METHODS*

6.2.1. *Physiological measurements*

Leaf stomatal conductances (g_s), net CO_2 leaf assimilation (A_n), and leaf transpiration (E_l) measurements were carried out between June 1994 and January 1995, in June (Days 15 to 17), August (Days 18 and 24), September (Days 5, 21, 28 and 30), November (Days 29 and 30), and January (Days 4 and 9). Instantaneous leaf water use efficiency (*WUE*) was calculated as A_n divided by E_l. Leaf water potential measurements were made on the same date as other physiological measurements.

6.3. MODEL DESCRIPTION

In this section we describe the different sub-models (stomatal conductance, transpiration and photosynthesis) used in leaf gas exchange modelling, and briefly discuss their linkage and parameterisation. The Appendix 2 provides definitions of terms, parameter values, and equations used in modelling procedure. We developed a model whose inputs allow a temporal (from hour to year) leaf gas exchange integration. Leaf gas exchange was modelled with a half-hour frequency, which we consider representative of temporal changes in the leaf gas exchange model inputs. The time integration will be discussed at two scales: daily and seasonal levels.

Measurements for the different sub-models were made under a wide variety of environmental conditions (of D_a, D_{ch}, T_a, T_l, etc...) as shown in Table 6.1. This Table also shows the range of physiological variables measured in the study. The simulations describe the response of a single-sided (hypostomatus) leaf in free air. We will discuss the results in these terms, while acknowledging that they are not strictly valid since we do not deal with angle features or the heterogeneous environment of a real leaf.

6.3.1. *Stomatal conductance sub-model*

For stomatal conductance modelling, we used an empirical model based on the measurements made on trees through the study period. In order to model g_s, we related stomatal conductance with the different environmental variables. We considered that leaf to air water vapour pressure deficit (D_a) represents the stomatal response to humidity more appropriately than does leaf relative humidity (h_s), as has been noted by various authors (Aphalo & Jarvis, 1991; Lloyd, 1991; Mott & Parkhurst, 1991). We found the model based on D_a and Ψ_p accounted for the maximum variance of g_s measured.

Table 6.1. Range of the physiological and environmental variables recorded in the study.

Symbol	Value	Units	Description
Ψ_p	(-0.25 - -1.9)	MPa	Pre-dawn leaf water potential
A_n	(0 - 14.8)	μmol m^{-2} s^{-1}	Net CO_2 leaf assimilation
D_a	(0 - 7.1)	kPa	Leaf to air water pressure deficit
D_{ch}	(0.4 - 6.5)	kPa	Leaf to chamber water pressure deficit
E_l	(1.6 - 7.4)	mmol m^{-2} s^{-1}	Leaf transpiration
g_s	(65 - 531)	mmol m^{-2} s^{-1}	Stomatal conductance
P	1	kPa	Air pressure
PAR	(0 - 1960)	μmol m^{-2} s^{-1}	Photosynthetically active radiation
T_a	(-3.5 - 41.1)	°C	Air temperature
T_{ch}	(8 - 42)	°C	Chamber air temperature
T_l	(7.4 - 41.6)	°C	Leaf temperature

Other variables such as *PAR*, u or T_a had no impact on g_s behaviour. However, we included *PAR* in the g_s model in order to limit the high values of g_s measured at sunrise, and due to the presence of dew on the leaves at sunrise, transpiration would be suppressed. The g_s model used — explained by these three variables — was

$$g_s = g_{sm}\, f(D_a)\, f(\Psi_p)\, f(PAR) \qquad \text{(Eqn. 6.1)}$$

where g_{sm} is maximum stomatal conductance measured, and $f(D_a)$, $f(\Psi_p)$ and $f(PAR)$ are the functions of D_a, Ψ_p and *PAR* (inputs to the model), respectively. The equations are shown in the Appendix 2. Table 6.2 shows the value of parameters for the stomatal conductance model.

Table 6.2. Values of the parameters for the leaf stomatal conductance model.

Symbol	Value	Units	Description
k_0	0.85	mmol m^{-2} s^{-1}	(Eqn. A1)
k_1	0.38	kPa^{-1}	Rate constant of the curve (Eqn. A1)
k_2	0.12	mmol m^{-2} s^{-1}	(Eqn. A1)
k_3	0.38	mmol m^{-2} s^{-1}	(Eqn. A2)
k_4	1.50	MPa^{-1}	Rate constant of the curve (Eqn. A2)
k_5	0.47	mmol m^{-2} s^{-1}	(Eqn. A2)
k_6	30	mmol photons mol H_2O^{-1}	(Eqn. A3)

Stomatal conductance was modelled almost exclusively on the basis of D_a and Ψ_p. Both variables showed a non-linear response in the form of a negative exponential function, characterised by a parameter (k_2 and k_5 respectively) that results in a non-zero value for the conductance, even in severe climatological and water-limiting conditions (high values of D_a and low values of Ψ_p). On the other hand, the effect of T_a on g_s response is masked by D_a because the latter takes into account the former. The minimum and maximum limits of g_s used in the modelling procedure were respectively 10 and 530 mmol m^{-2} s^{-1} (g_{sm}).

6.3.2. *Transpiration sub-model*

We have modelled the leaf transpiration in this ecosystem (see chapter IV), and found the following model to be the best:

$$E_l = g_s D_a / P \qquad \text{(Eqn. 6.2)}$$

where P is the atmospheric pressure (kPa), considered equal to 100 for the whole period studied. This expression implies a total coupling of leaf surface (considered as an isothermal system) to surrounding bulk air conditions. The characteristics of this model and their implications have been widely discussed in the chapter IV. As is shown in Equation 6.2, the input variables to the transpiration model are g_s and D_a. The g_s was calculated from Equation 6.1. In the E_l modelling procedure, the limits of the g_s modelling were not necessary.

6.3.3. Photosynthesis sub-model

Carbon uptake at the leaf level was estimated with a mechanistically based model of C_3 leaf gas exchange (Tenhunen et al., 1990; Harley & Tenhunen, 1991) derived from Farquhar et al. (1980) and Farquhar & von Caemmerer (1982), linked with an empirical model of stomatal conductance — described above. The environmental inputs are PAR, T_a and D_a. The photosynthesis model is detailed in the Appendix 2. Table 6.3 shows the values of the parameters and constants for the leaf photosynthesis model, and parameters used to describe the temperature dependence of the model.

Parameters for the leaf photosynthesis model were set as reported by Tenhunen et al. (1990) for the scrub oak species *Quercus coccifera*. It has been shown to give good results for *Q. ilex* dense canopies in Catalonia (Spain) (Sala & Tenhunen, 1996), and south-east France (Damesin, 1996). The scaling factor (dimensionless) for the maximum carboxylation rate ($c[V_{cmax}]$) is determined as a function of the leaf nitrogen content by least squares linear regression. As we did not have enough measurements of leaf nitrogen content for our trees, the scaling factor was adjusted to obtain the best-fitting estimate of g_s and A_n (minimum difference between measured and simulated). The same value was used throughout the study period, independently of possible changes in leaf nitrogen content during the year.

Table 6.3. Values of the parameters and constants for the leaf photosynthesis model, and parameters used to describe their temperature dependence. Parameters have been described in the Appendix 2. Variables relative to each parameter are shown in brackets.

Parameter	Units	Temperature parameter	Value	Units
K_c	μmol CO_2 mol^{-1}	c (K_c)	31.95	-----
		ΔH_a (K_c)	63.50	kJ mol^{-1}
K_o	mmol O_2 mol^{-1}	c(K_o)	19.61	-----
		ΔH_a (K_o)	35.00	kJ mol^{-1}
τ	-----	c(τ)	3.9489	-----
		ΔH_a (τ)	-28.99	kJ mol^{-1}
R_d	μmol CO_2 m^{-2} s^{-1}	c(R_d)	16.5	-----
		ΔH_a (R_d)	41.5	kJ mol^{-1}
V_{cmax}	μmol CO_2 m^{-2} s^{-1}	c(V_{cmax})	14.35	-----
		ΔH_a (V_{cmax})	65.0	kJ mol^{-1}
		ΔH_a (V_{cmax})	250.0	kJ mol^{-1}
		ΔS (V_{cmax})	0.600	kJ K^{-1} mol^{-1}
J_{max}	μmol electrons m^{-2} s^{-1}	c(J_{max})	15.5	-----
		ΔH_a (J_{max})	43.4	kJ mol^{-1}
		ΔH_a (J_{max})	245.0	kJ mol^{-1}
		ΔS (J_{max})	0.805	kJ K^{-1} mol^{-1}
α	mol electrons mol photons^{-1}	-----	0.24	-----

6.3.4. Testing and combining the sub-models

Sets of stomatal conductance, transpiration and net CO_2 assimilation measurements were arranged consecutively and distributed alternately (regardless of the date) into two independent data sets: one for modelling and the other for validation of the model.

We linked the A_n model with the g_s model by the follow expression (Farquhar, 1989)

$$c_i = c_a - A_n k / g_s \qquad \text{(Eqn. 6.3)}$$

where c_i and c_a are the CO_2 concentration in the intercellular air space and the air outside the leaf boundary layer, respectively. The factor k (with a value of 1.6) corrects for the difference in diffusivity between CO_2 and H_2O (Harley et al., 1992). From this expression we calculated A_n and g_s for a difference between c_a and c_i — in absolute value, less than 1. The E_l model is linked to the g_s model by Equation 6.2.

Figure 6.1a shows g_s simulated from Equation 6.1 compared with measured values of g_s. The D_a and Ψ_p explained 73% of g_s measured ($Y = 52.8 + 0.86\ X$, $n = 98$, $p < 0.0001$). However, D_a alone explained some 70% of g_s. The low contribution of Ψ_p to g_s was due to a D_a-Ψ_p covariation phenomenon found during the study period in these trees (see chapter IV). We added Ψ_p to the g_s model in order to take into account the plant water status through the period modelled.

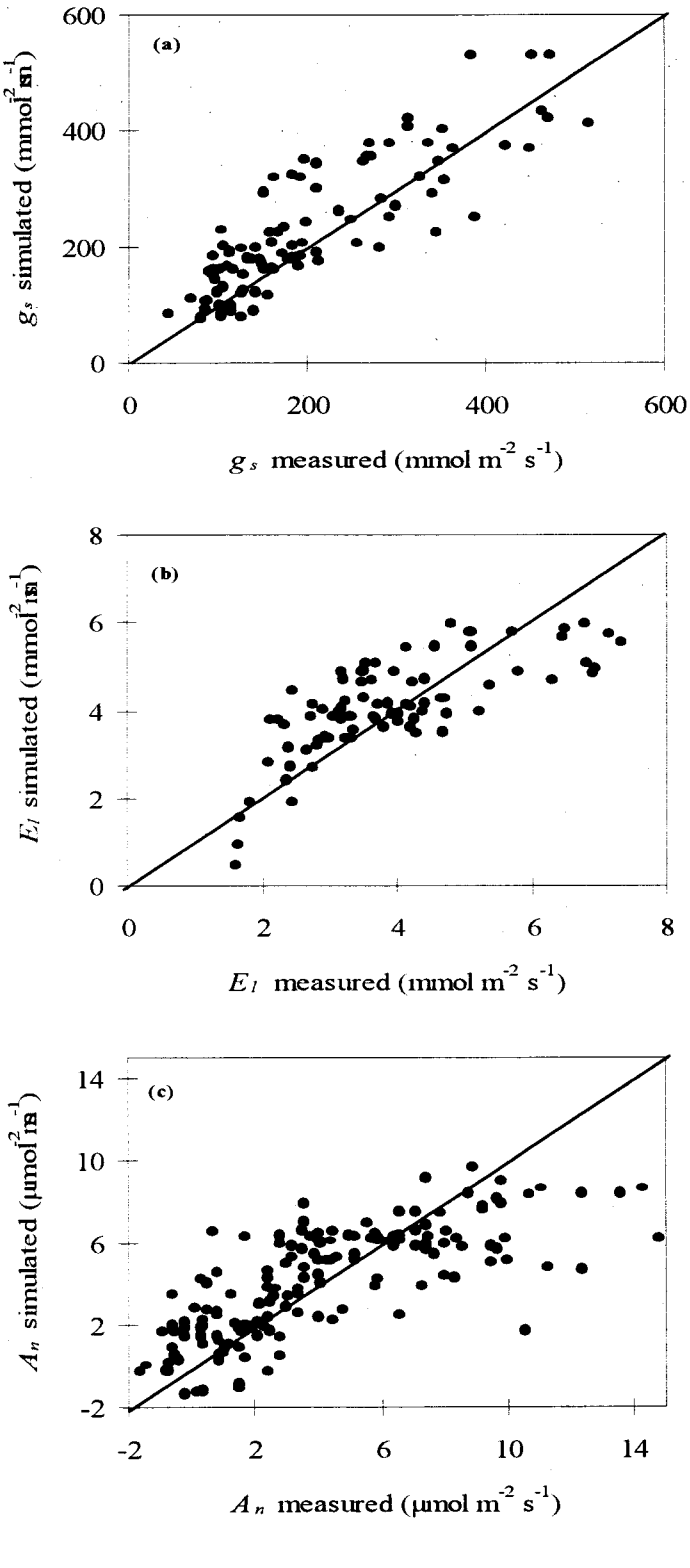

Figure 6.1. Relationships between simulated and measured values of three variables of the leaf gas exchange: stomatal conductance (g_s) values (Y = 52.8 + 0.86 X, $n = 98$, $r^2 = 0.73$, $p<0.0001$) **(a)**; leaf transpiration (E_l) values (Y = 1.82 + 0.58 X, $n = 82$, $r^2 = 0.54$, $p<0.0001$) **(b)**; net CO_2 leaf assimilation (A_n) values (Y = 1.83 + 0.55 X, $n = 84$, $r^2 = 0.59$, $p<0.0001$) **(c)**. The solid line represents the 1:1 value.

6.4. RESULTS

Fig. 6.2 shows some weather variables measured during the simulation period. The ranges of these variables used in the modelling procedure are shown in Table 6.1. The period studied was representative of a dry year. From February 1994 to January 1995, both months inclusive, the total rainfall was 509.9 mm, that is, some 70 per cent of the mean total precipitation at the study site. That year also had a severe drought period of four months — from June to September (Fig. 6.2d). However, Ψ_p varied only between -0.25 and -1.9 MPa, except for Tree 3, which was artificially disturbed, and whose Ψ_p was not less than -1.2 MPa (Fig. 6.3).

6.4.1. *Gas exchange daily patterns*

Field measurements of leaf photosynthesis ranged between 0 and 14.8 μmol m^{-2} s^{-1}, with values above 10 μmol m^{-2} s^{-1} being reached only on some days in spring and winter. The g_s measurements ranged between 65 and 531 mmol m^{-2} s^{-1}, with values between 400 and 531 mmol m^{-2} s^{-1} being found only in autumn and winter. Values lower than 100 mmol m^{-2} s^{-1} were found mainly towards the end of the drought period. Measurements of E_l ranged between 1.6 and 7.4 mmol m^{-2} s^{-1}. Values above 6 mmol m^{-2} s^{-1} were measured for Tree 3 on 15 June and 18 August, and between 5 and 6 mmol m^{-2} s^{-1} in Tree 5 on 16 June.

Figure 6.4 shows *PAR*, air temperature, and air to leaf water vapour pressure deficit measured by the ADC, and used in the simulation of those four days. The four typical days chosen were representative of the different seasons modelled (see below).

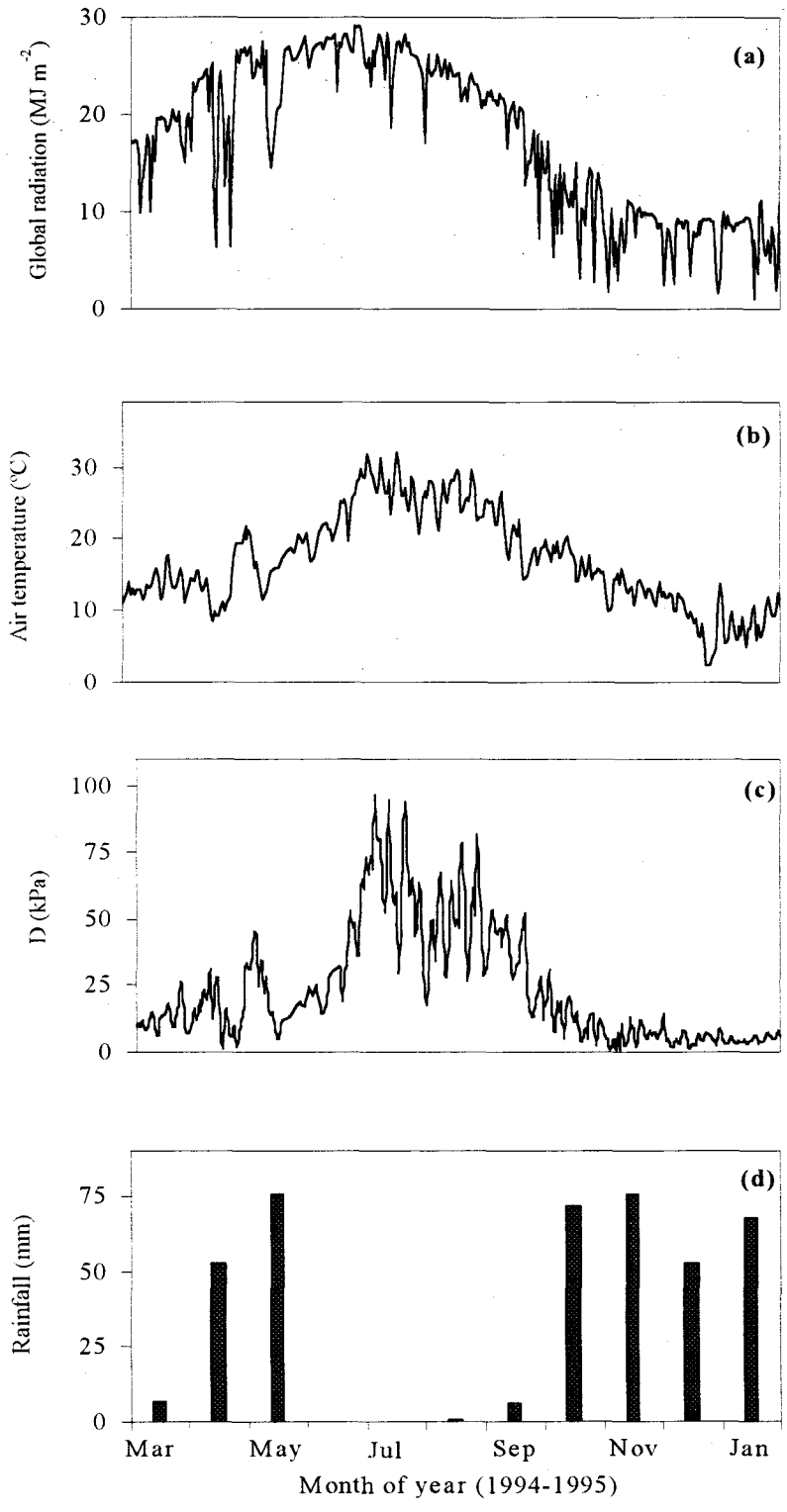

Figure 6.2. Seasonal variation of the environmental variables for the simulated period. Variables correspond to daily global accumulated radiation **(a)**, mean daily air temperature **(b)**, accumulated daily air water vapour pressure deficit (*D*) **(c)**, and total monthly rainfall **(d)**.

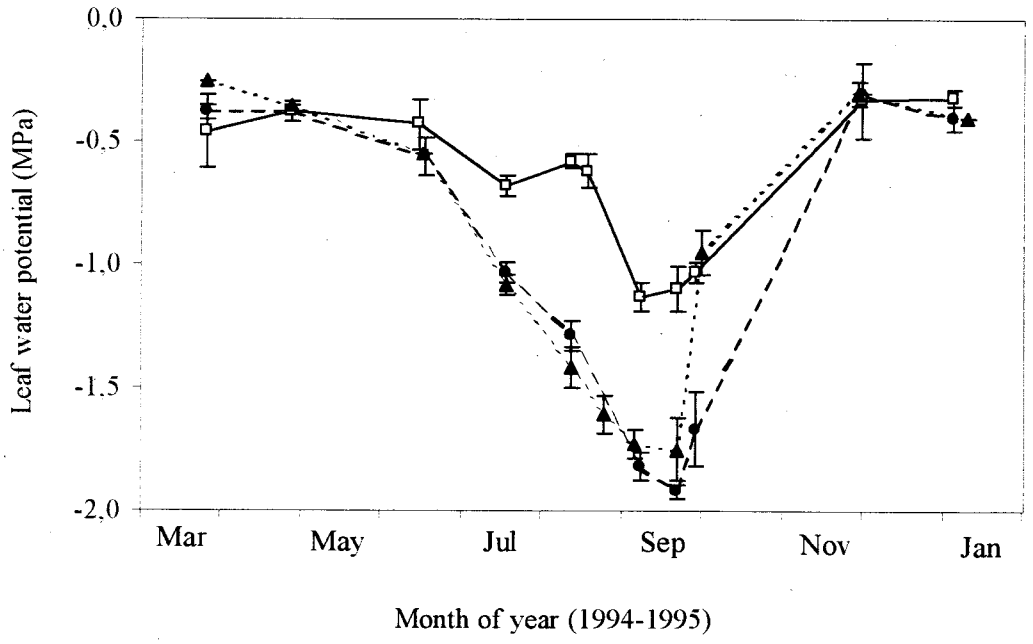

Figure 6.3. Pre-dawn leaf water potential for the 1994-95 period, measured for Trees 1 (filled circles), 3 (unfilled squares) and 5 (filled triangles). Vertical bars indicate the standard error.

Figures 6.5 to 6.8 shows comparisons between simulated and measured diurnal courses of A_n, g_s and E_l from ADC field measurements on four typical days of the different seasons of the year for Tree 5. In the spring (16 June), summer (24 August), and autumn (30 November), we found a reasonable agreement of the measured values with the model for E_l and g_s (Fig. 6.5, 6.6 and 6.7). Differences were found only in the winter period (9 January 1995) (Fig. 6.8). Simulation of A_n was comparable to measurements for the four days represented in Figures 6.5 to 6.8. The results in Tree 5 were similar to those in Trees 1 and 3.

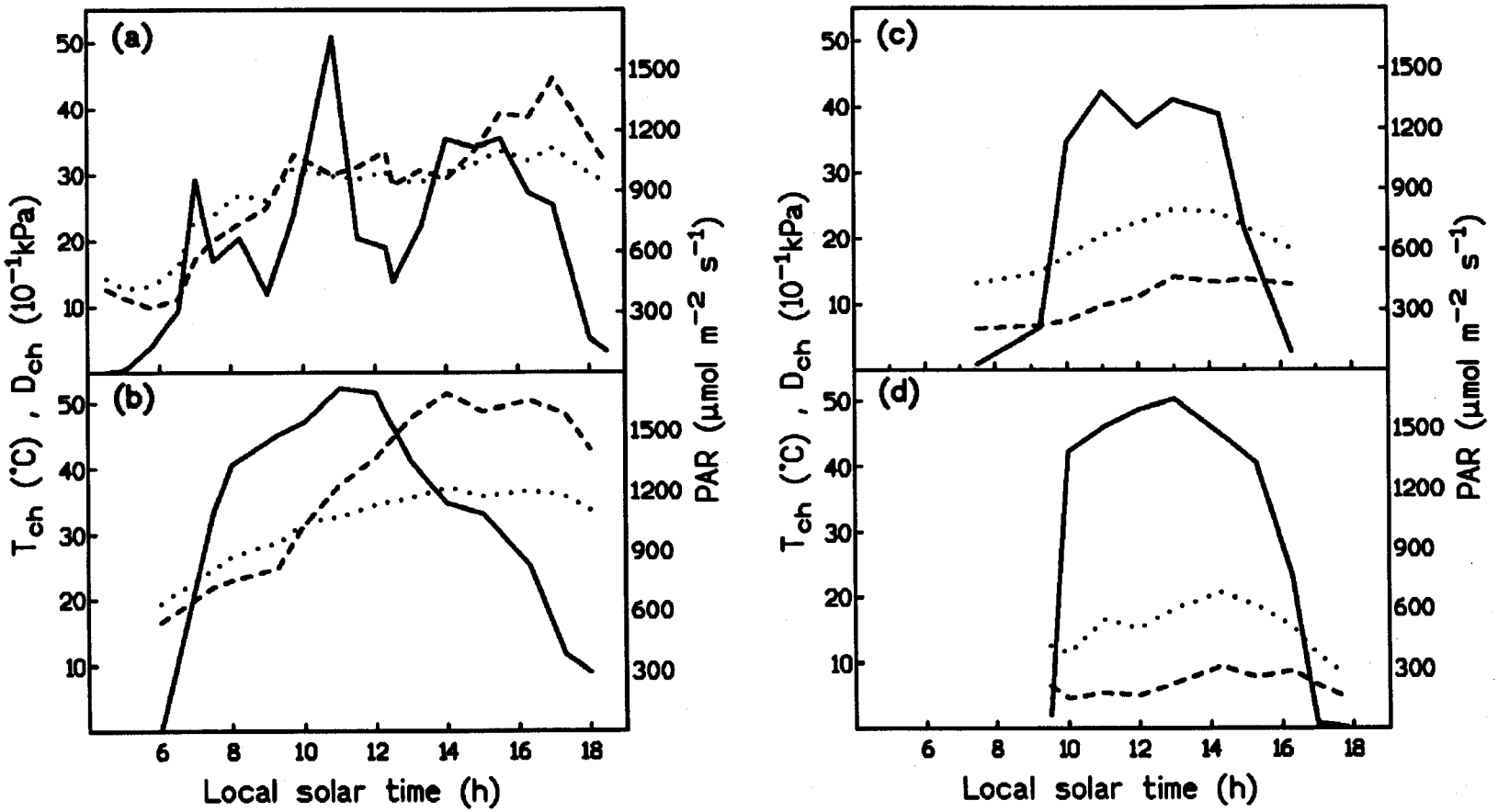

Figure 6.4. Diurnal variation of the environmental variables recorded in leaf gas-exchange measurements for Tree 5. The variables measured by the ADC were chamber air temperature (T_{ch}; in dotted line), leaf to chamber water pressure deficit (D_{ch}; in dashed line) and the photosynthetically active radiation (*PAR*; in solid line) measured. Days correspond to 16 June **(a)**, 24 August **(b)**, and 29 November **(c)**, in 1994, and 9 January 1995 **(d)**.

The small differences found between measured and simulated values of E_l, g_s and A_n were related mainly to peaks or sharp changes in the physiological response of the leaf to environmental variables, and not directly to the latter (Fig. 6.3). These small, sharp changes in response could be an artefact of the ADC measurements, particularly for A_n.

In spring and summer, E_l time courses were characterised by a rapid increase in the early morning that reached the maximum daily value. This value remained constant until sunset, when there was a sharp decrease. During the spring, the morning increase was less steep than in summer, but always reached the maximum value before midday (Fig. 6.5c); the maximum was higher in summer (Fig. 6.6c). In autumn and winter, the time courses were characterised by a gentle increase of E_l during the day, which reached the maximum daily value late in the afternoon, before sunset (Fig. 6.7c and 6.8c).

In early spring, g_s gained maximum values (also maximum values of the period) in early morning, then decreased through the day, following a negative exponential function. In late spring and for the whole summer period, g_s reached the maximum daily value just at sunrise, and decreased exponentially with time during the day (Fig. 6.5b and 6.6b). As the drought became severe, the maximum daily g_s value decreased continuously. In autumn and winter, g_s remained at maximum daily values from sunrise to sunset (Fig. 6.8b), excepting during dry days, when g_s decreased through the afternoon (Fig. 6.7b).

A_n presented a bell-shaped daytime course during most of the year, but with a wide range of maximum daily values (Fig. 6.5a, 6.7a and 6.8a). On some days, we found an increase through the day that reached the maximum value in the afternoon. During the summer, the daytime course was very different: A_n reached the daily maximum value early in the morning (just after sunrise), and immediately afterwards showed a rapid decrease that continued throughout the day (e.g., Fig. 6.6a).

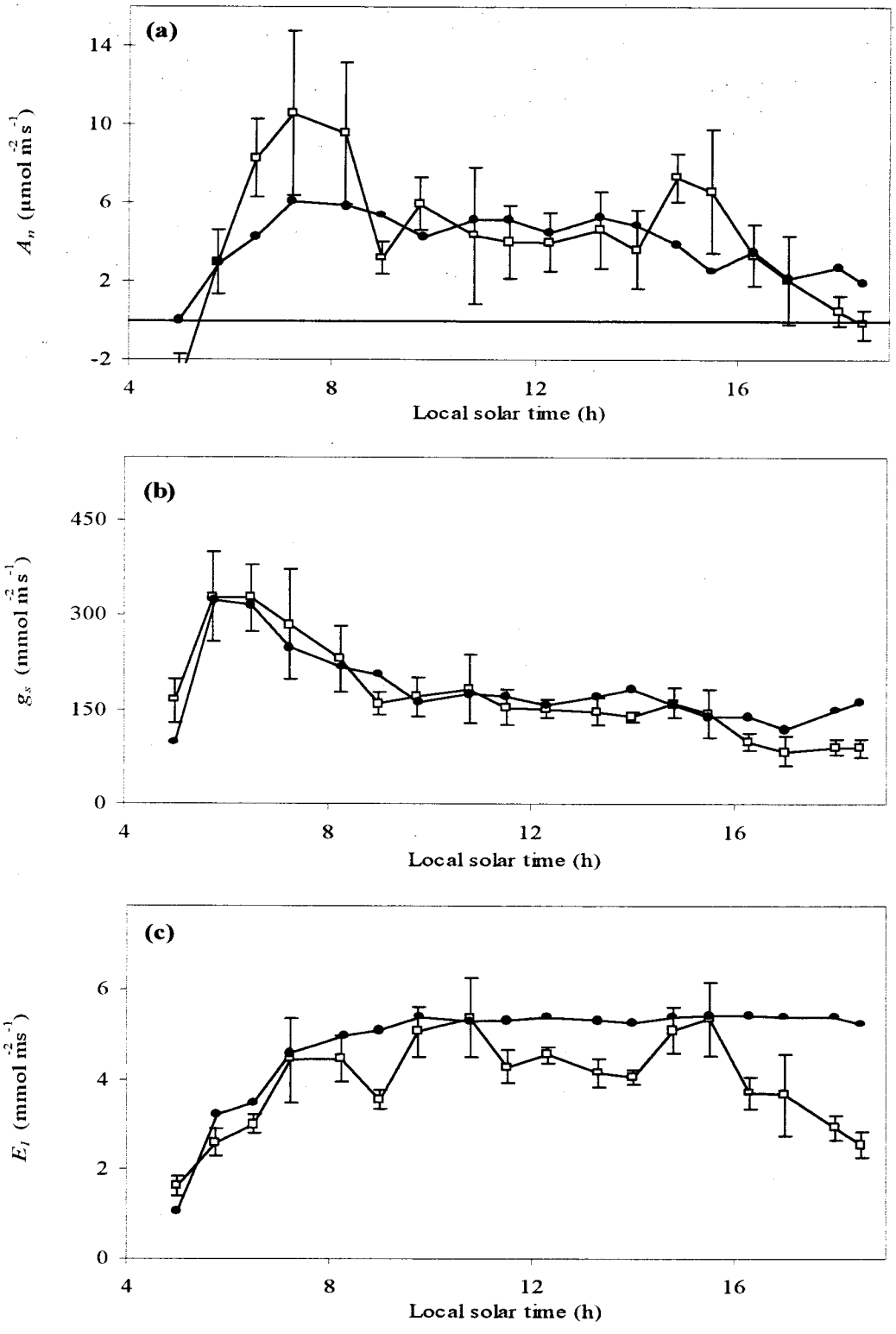

Figure 6.5. Comparison of diurnal variation of net CO_2 leaf assimilation (A_n) **(a)**, stomatal conductance (g_s) **(b)** and leaf transpiration (E_l) **(c)** measured (unfilled squares) and simulated (filled circles) for Tree 5. The day corresponds to 16 June 1994. Vertical bars indicate standard error.

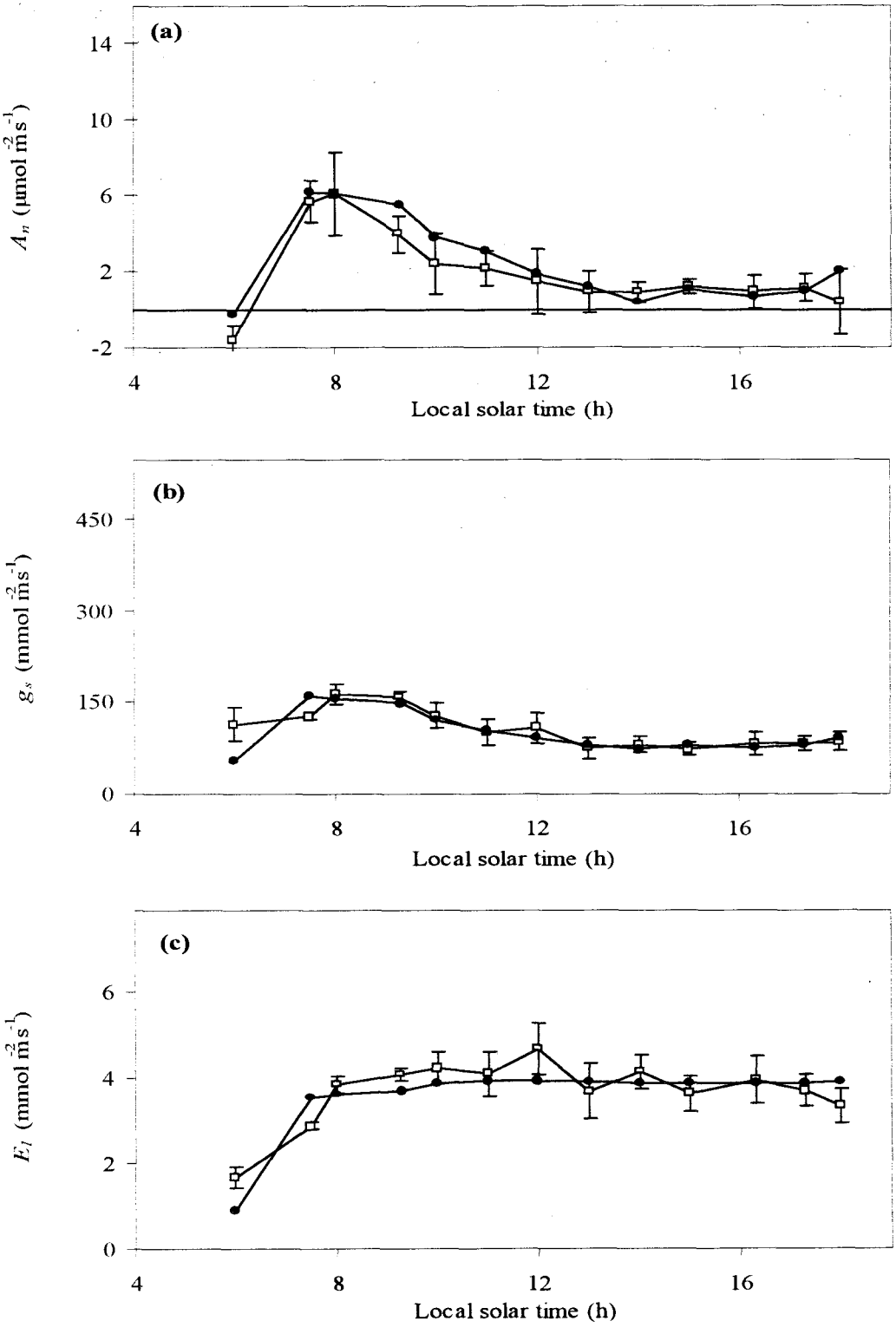

Figure 6.6. Comparison of diurnal variation of net CO_2 leaf assimilation (A_n) **(a)**, stomatal conductance (g_s) **(b)** and leaf transpiration (E_l) **(c)** measured (unfilled squares) and simulated (filled circles) for Tree 5. The day corresponds to 24 August 1994. Vertical bars indicate standard error.

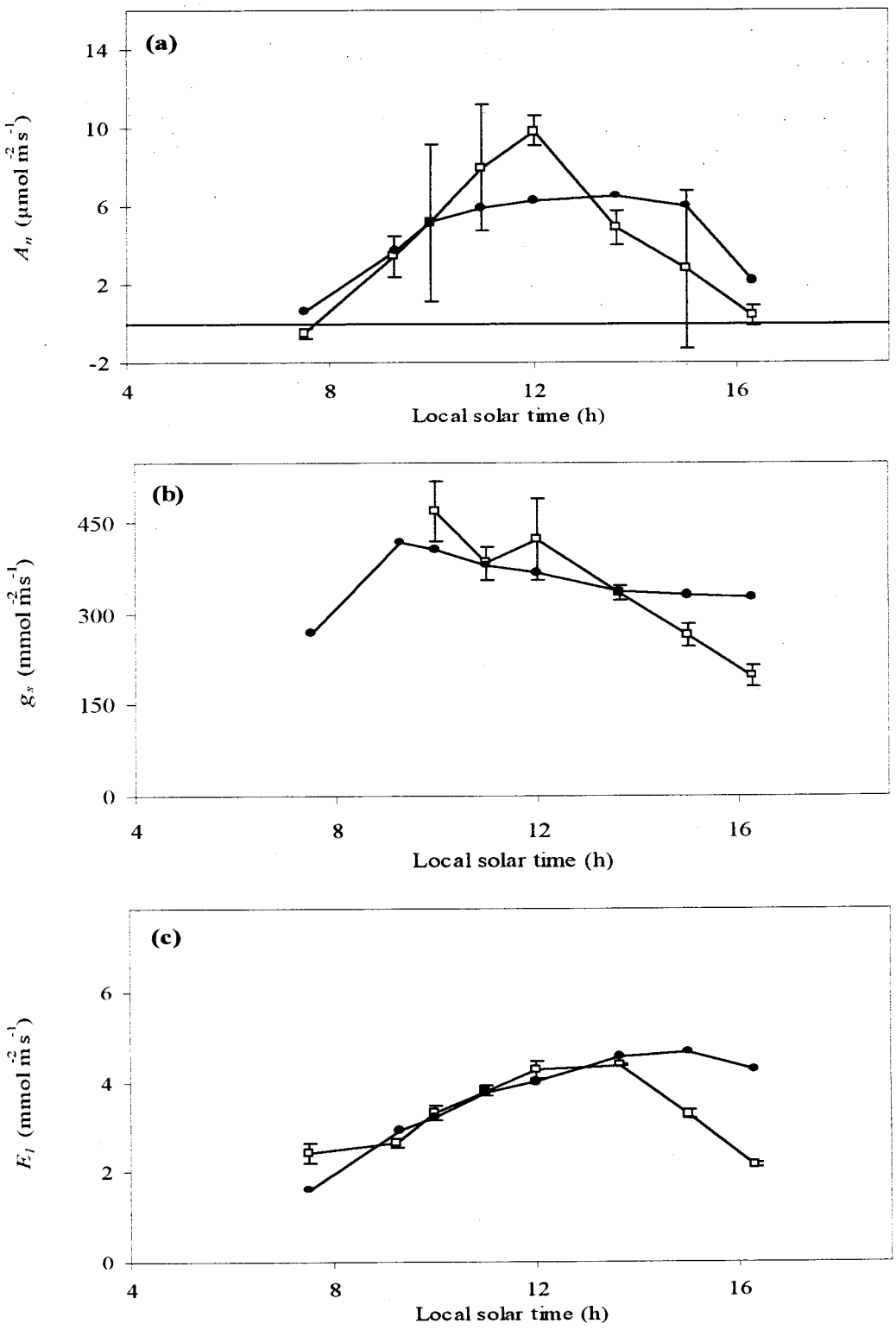

Figure 6.7. Comparison of diurnal variation of net CO_2 leaf assimilation (A_n) **(a)**, stomatal conductance (g_s) **(b)** and leaf transpiration (E_l) **(c)** measured (unfilled squares) and simulated (filled circles) for Tree 5. The day corresponds to 29 November 1994. Vertical bars indicate standard error.

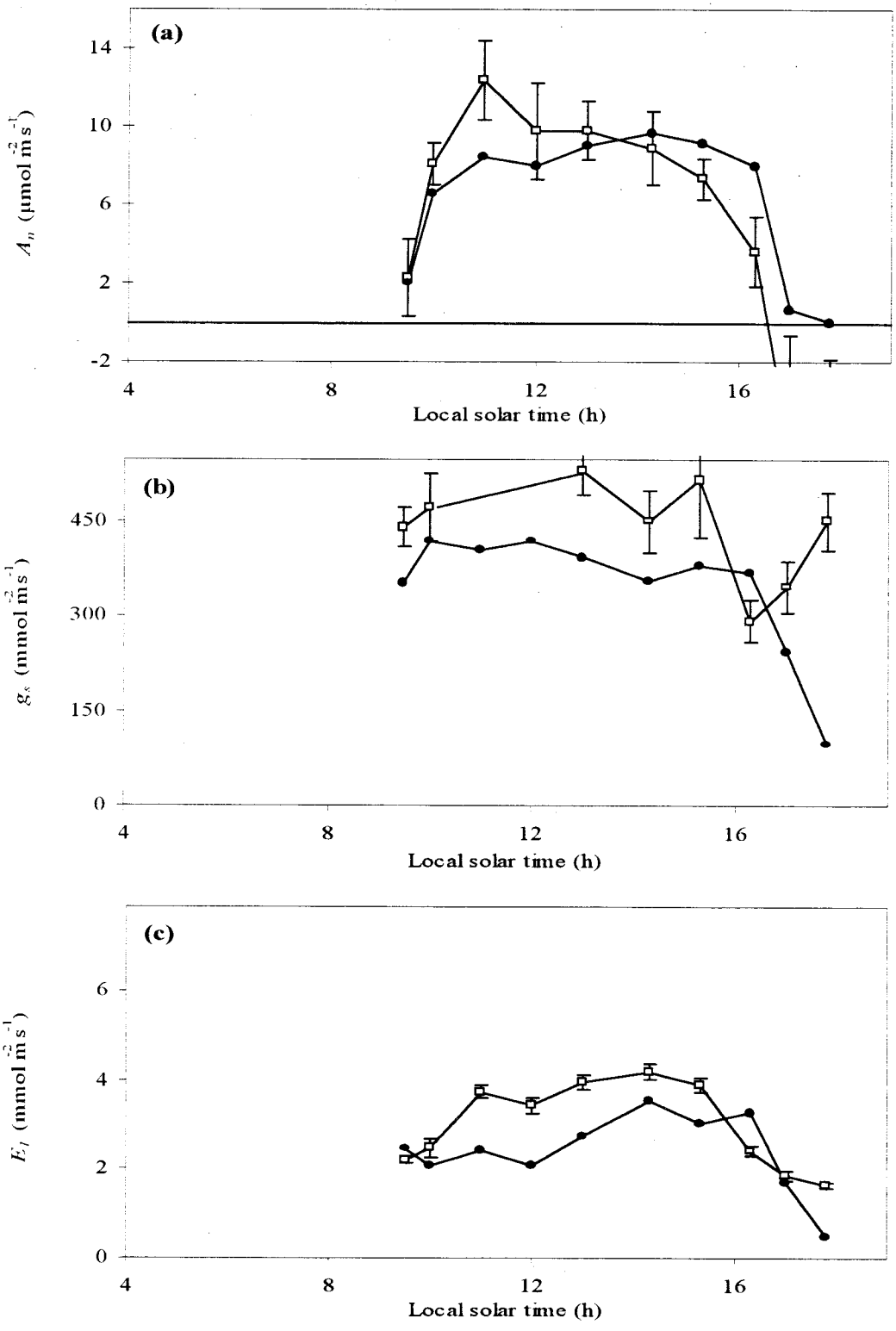

Figure 6.8. Comparison of diurnal variation of net CO_2 leaf assimilation (A_N) **(a)**, stomatal conductance (g_S) **(b)** and leaf transpiration (E_l) **(c)** measured (unfilled squares) and simulated (filled circles) for Tree 5. The day corresponds to 9 January 1995. Vertical bars indicate standard error.

Appreciable differences between A_n measured and simulated were found in the diurnal peaks, above all when it was greater than 10 μmol m^{-2} s^{-1}. In regarding g_s, this variable was modelled better in spring and summer, like E_l (Fig. 6.5 to 6.8).

6.4.2. *Water use efficiency of leaves*

Variation in the diurnal pattern of *WUE* throughout the seasons was comparable to that in photosynthesis, as shown in Figure 6.9 for Tree 5. This Figure illustrates characteristic diurnal courses of *WUE* for the different seasons of the year. The same patterns were found in both Trees 1 and 3. Instantaneous measurements of *WUE* ranged from 0 to 6 μmol CO_2 mmol H_2O^{-1} approximately. Negative values shown in Figure 6.9 correspond to net leaf respiration (negative net CO_2 assimilation).

The spring and summer diurnal *WUE* pattern showed the highest values were reached early in the morning (between 07:00 and 09:00), with a subsequent continuous decrease through the day. The peaks were about 3 and 2 μmol CO_2 mmol H_2O^{-1} in spring and summer respectively (Fig. 6.9a and b). During the summer — from July to late September — the *WUE* decreased rapidly to reach a stable value (about 0.5 μmol CO_2 mmol H_2O^{-1}) late in the morning that continued through the afternoon (Fig. 6.9b). The courses of the autumn and winter diurnal *WUE* pattern were bell-shaped, as were those of A_n (Fig. 6.9c and d). During these periods, the peaks reached higher values, ranging between 2.5 and 5 μmol CO_2 mmol H_2O^{-1}; the maximum value was measured in Tree 3, on 4th of January 1995, very early in the morning (between 09:00 and 10:00). The peaks were reached during the morning, depending on the daily weather characteristics. The differences between *WUE* measured and simulated (Fig. 6.9) were comparable to the differences in A_n measured and simulated (Fig. 6.5 to 6.8) for all days analysed.

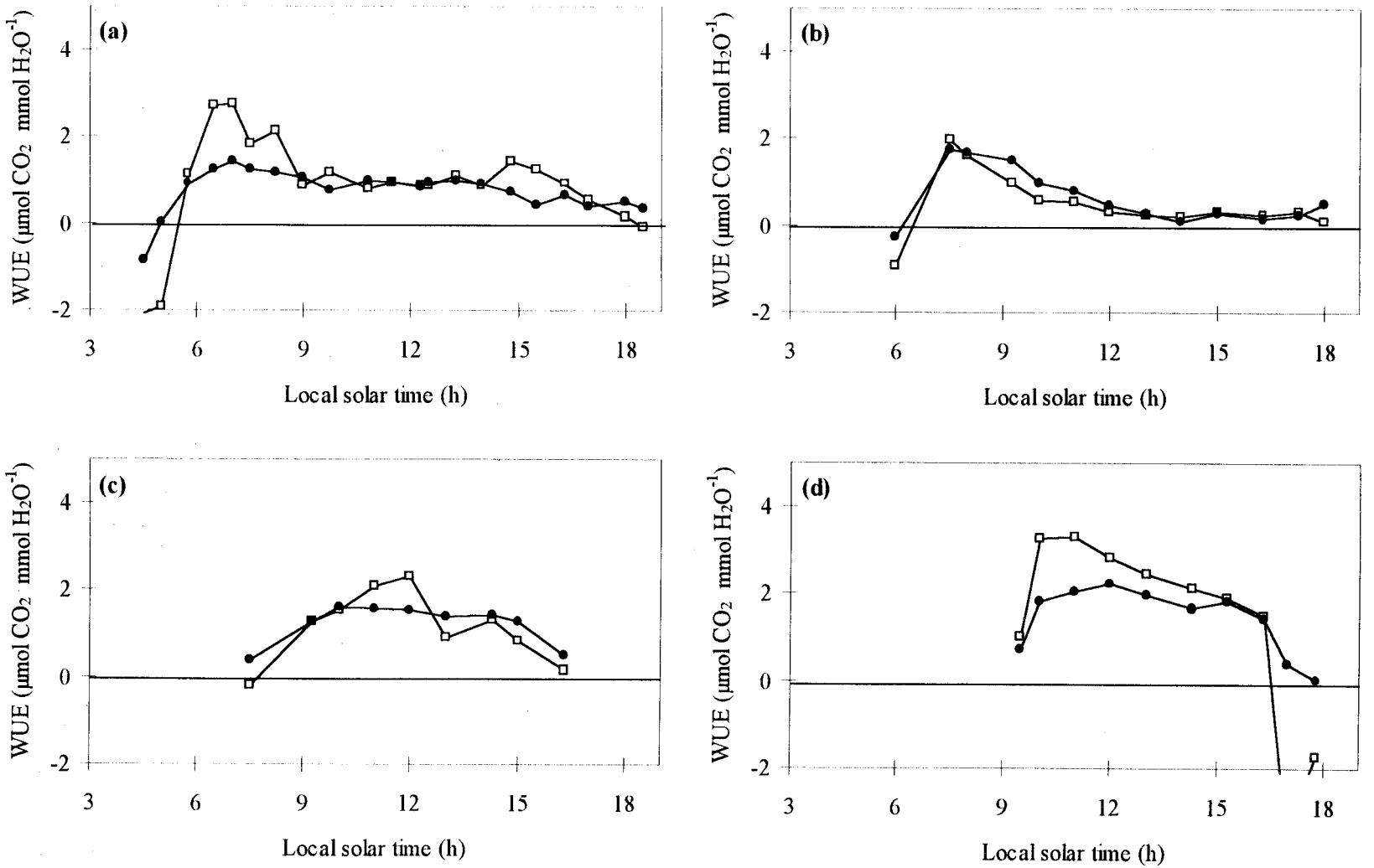

Figure 6.9. Comparison of diurnal variation of water use efficiency (*WUE*) measured (unfilled squares) and simulated (filled circles) for Tree 5. Days correspond to 16 June **(a)**, 24 August **(b)**, and 29 November **(c)**, in 1994, and 9 January 1995 **(d)**.

6.4.3. Patterns in seasonal simulations

Seasonal simulations were made from environmental variables recorded automatically by the meteorological station. From the model described, we simulated monthly net CO_2 leaf assimilation, stomatal conductance and leaf transpiration throughout a year as the sum of the daily values. Total daily net CO_2 assimilation and transpiration were estimated by integrating the daily curves of net photosynthesis and transpiration rates on time. We found, as the three trees show, close values of assimilation in all months of the year.

Seasonal patterns of simulated A_n, E_l and *WUE* are illustrated in Figure 6.10. The monthly value is the mean value of simulations for Trees 1, 3 and 5. Because of reduction in total daily radiation, minimum values of A_n were simulated in winter (December and January) (about 3 mol of CO_2 m^{-2} $month^{-1}$). The maximum simulated rates of A_n occurred in June (7 mol of CO_2 m^{-2} $month^{-1}$), when total daily radiation was at a maximum, and water availability and temperatures were not yet limiting. The seasonal leaf assimilation pattern showed a continuous decrease from June to the end of winter, and which was steeper in July and August, probably due to limiting temperatures. Maximum values of temperature were reached in those months. Increased leaf temperatures resulted in an increase of leaf respiration rates, leading to a relative decrease in leaf net assimilation. This decrease was particularly significant because the increase in air temperature implies an increase in D_a with a decrease in stomatal conductance.

The monthly leaf transpiration pattern was similar in all trees (Fig. 6.10b), but maximum values in Tree 3 were different to those in Trees 1 and 5 from June to September. The minimum values (about 30 mm $month^{-1}$) were simulated for the winter period due to low leaf air water vapour pressure deficit (D_a) values recorded. During the study period, from March 1994 to January 1995, total A_n ranged between 54.2 and 54.5 mol CO_2 m^{-2}. The total E_l in this period differed widely between trees, with values of 799.7, 807.6 and 862.6 mm for Trees 1, 5 and

3 respectively. Figure 6.10c shows monthly *WUE* simulated. The November value is unusually high. This is because some days produced lower D_a and consequently lower transpiration, but with some photosynthetic activity. The minimum monthly value simulated, about 25 mmol CO_2 mol H_2O^{-1} $month^{-1}$, was for July.

6.5. DISCUSSION

Thornley (1996) discussed the value of mechanistic (process-based) models to further understanding. He stated that it is '*desirable that the qualitative behaviour of the model be compared with observations where possible*'. A mechanistically based model of C_3 leaf CO_2 assimilation and transpiration linked to an empirical stomatal conductance model is compared with field measurements. This model estimates, using time integration, daily and seasonal changes in carbon fixation, transpiration, and water use efficiency of Mediterranean sclerophyll trees.

6.5.1. *Model performance*

Close correspondence between observed leaf gas exchange and that simulated with the model supports the idea that leaf performance is accurately predicted for different environmental conditions. It should nevertheless be remembered that most of the measurements were made in spring and summer, which implies a more accurate prediction of the model in those periods, above all for A_n and g_s. As Farquhar's model describes the photosynthetic properties of leaves in terms of the underlying biochemistry, and as species differ in their biochemical capacity to assimilate CO_2 from the atmosphere (Wullschleger, 1993), future research will have to establish the A_n/c_i curve responses of leaves in *Q. ilex*, as well as the relationships between leaf nitrogen content and Rubisco capacity, in order to improve simulations of photosynthesis in this species.

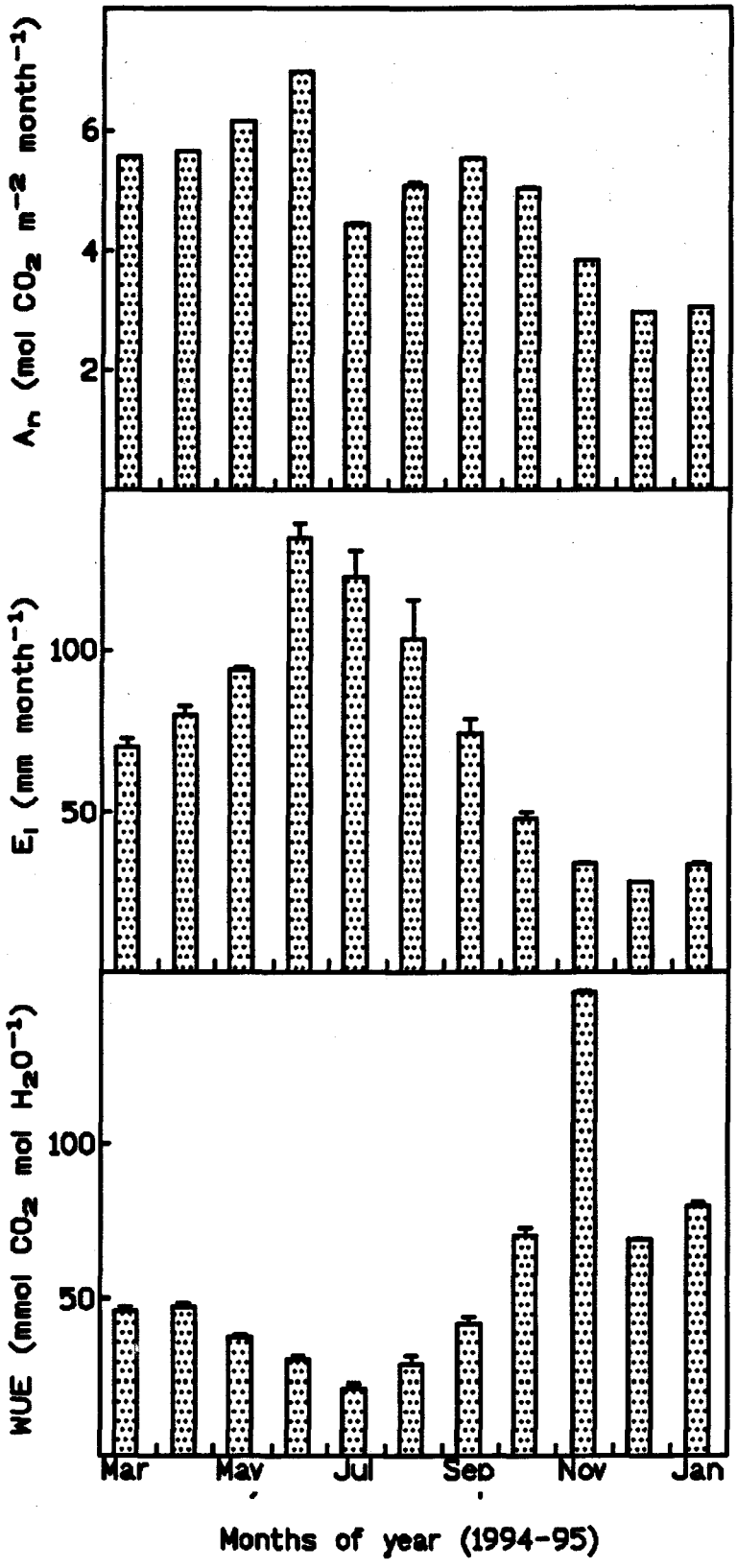

Figure 6.10. Total mean (Trees 1, 3 and 5) monthly simulations of net CO_2 leaf assimilation (A_n) **(a)**, leaf transpiration (E_l) **(b)** and water use efficiency (*WUE*) **(c)**. Vertical bars indicate the standard error.

The use of the same value of V_{cmax} at different leaf phenology time could explain the model's failure to simulate rapid peaks of A_n above 10 μmol m^{-2} s^{-1} on some days of winter and early spring, due to an upper limit of carboxylation rate. Some tests (not shown) on our data set showed that the value of A_n increased with an increase of the parameter $c[V_{cmax}]$. Various authors have reported Rubisco capacity as a function of leaf nitrogen content (Evans & Farquhar, 1991; Hollinger, 1992; Leuning et al., 1991), but at the same time this function could depend on the species and plant adaptation to the environment (Leuning et al., 1991; Wullschleger, 1993). There are no data available describing the specific relationships between photosynthetic capacity and leaf nitrogen content, and we did not have enough measurements of leaf nitrogen content for our trees, so the relationship between V_{cmax} and nitrogen content (N) was made by optimising the parameter $c[V_{cmax}]$ (as described above), which takes the same value throughout the study period. Even though changes in leaf N throughout leaf phenology have been reported in different species (Castell et al., 1994; Escudero et al., 1987), and we found perceptible differences in leaf N between summer (1.6 %, ± 0.1) and winter (2 %, ± 0.1), we did not consider changes in nitrogen content with time, since we had only two measurements of N with close values -inadequate for any correlation.

6.5.2. *Response of leaf gas exchange to water stress*

Leaf gas exchange values recorded in our study are in the range of those measured by other authors in the same species under different environmental conditions (Acherar & Rambal, 1992; Tetriach, 1993; Castell et al., 1994; Sala & Tenhunen, 1994), and in other Mediterranean evergreen sclerophyll species such as *Arbutus unedo* (Harley et al., 1986; Beyschlag et al., 1987; Castell et al., 1994), *Quercus coccifera* (Tenhunen et al., 1990), or *Q. suber* (Oliveira et al., 1992; Faria et al., 1996).

In general, the diurnal patterns of leaf gas exchange changed between well-watered and drought periods. In the first period — from early October to the beginning of June — g_s reached high values early in the morning and remained nearly constant throughout the afternoon. The A_n was bell-shaped, with a maximum value near midday, limited only by light intensity. At the beginning of the drought period — from mid-June to the end of September—, the diurnal pattern of g_s showed a midday decrease, reported as midday stomatal closure by various authors in Mediterranean *Quercus* species in natural conditions (Tenhunen et al., 1981, 1982; Rhizopoulou & Mitrakos, 1990; Acherar & Rambal, 1992; Sala & Tenhunen, 1994) (see also Faria et al., 1996). As water stress became severe and D_a reached high values, stomatal closure occurred earlier in the morning, and g_s remained at minimal values throughout the day (Fig. 6.6b). A similar diurnal pattern were shown by A_n, as it was limited by g_s in the drought period. In that period, E_l increased rapidly early in the morning, parallel to the increase in D_a. High values were reached before midday, and remained constant in the afternoon, when stomatal closure counteracted the continuous increase of D_a. In the well-watered period, the slow increase of E_l during the morning was related to low values of D_a. Comparable leaf gas exchange diurnal patterns were reported by Tenhunen et al. (1990) in *Q. coccifera*, and by Tetriach (1993) in *Q. ilex* and *Q. pubescens*. However, in all cases maximum values of g_s and E_l were lower than those reported in our study. Sala & Tenhunen (1996) also found low maximum values of g_s and E_l in *Q. ilex*. Higher g_s and E_l values for trees in open (our site of study) as opposed to closed (those cited above) sites were reported by Abrams (1986). Moreover, the high values of D_a measured in our ecosystem, compared with the ecosystems cited, contributed to high values of E_l even when g_s decreased.

Analysis of the daily maximum simulated values of A_n showed no significant differences between trees. Significant differences were observed between stressed (Trees 1 and 5) and non-stressed (Tree 3) trees in daily maximum values of g_s and

E_l. These differences were due to the difference in Ψ_p between trees. The absence of differences in maximum and monthly values of A_n between trees in the drought period, when the differences in g_s were significant, could be explained by the fact that during this period, A_n reached diurnal maximum values early in the morning, when stomatal closure was still small, and that moderate water stress has little or no effect on photosynthetic capacity, as suggested by Kaiser (1987) in Mediterranean sclerophyll species, Epron & Dreyer (1993) in deciduous oaks, and Sala & Tenhunen (1996) in *Quercus ilex*. The minimum Ψ_p measured in this work was approximately half those recorded in dense canopies of *Q. ilex* by different authors (Table A1.1, Appendix 1), from which we deduce the measured values of Ψ_p are representative of moderate water stress in relation to A_n activity.

Constant rates of maximum daily net CO_2 assimilation were exhibited throughout the year studied, including the water stress period. These values were slightly lower but more constant over time than those reported by Tetriach (1993), Castell et al. (1994), or Sala & Tenhunen (1996) in closed canopies of *Q. ilex*. However those studies presented only occasional daily values, whereas our model simulated results under varying environmental conditions during a whole month.

The seasonal pattern of monthly net CO_2 assimilation was comparable to that shown by Sala & Tenhunen (1996) in dense canopies of *Q. ilex*, with the maximum rate in late spring and minimum rate in winter, though the latter was significantly lower in the cited work. Since those authors did not measure A_n, but only simulated it, it is not possible to know the accuracy of their A_n simulations. Nor can the differences between our results and those of Sala & Tenhunen (1996) be explained by the upper limit of carboxylation rate found in the A_n model. The differences between months were more marked in dense forests of *Q. ilex* (Sala & Tenhunen, 1996) than in the patterns simulated in the present work. This is possibly due to milder climatic conditions through the year, resulting in high assimilation rates in autumn and winter. Such an idea is supported by the monthly patterns reported by Tenhunen et al. (1990) in *Q. coccifera* near Lisbon,

Portugal. This site is at a latitude very close to that of our experimental site, and the climates are very similar. The pattern of assimilation in *Q. coccifera* shows small differences between months, although the pattern is not very similar to the one we found in *Q. ilex*.

The daily pattern of *WUE* remained quite constant throughout the study period. The *WUE* was at its highest level early in the morning, when cool, humid air reduced transpiration to a minimum. In the drought period, it decreased rapidly, reaching a stable value later in the morning when the transpiration rate was at a maximum (Zine El Abidine et al, 1995). In the watered period it decreased slowly through the day. At the seasonal time-scale, *WUE* was lowest in July, when A_n decreased considerably but E_l remained high. It seems that the plant adapts to the drought, so that E_l decreased while A_n remained high. This increases the *WUE* with severity of the drought. Nevertheless, the highest values were found in winter, since the plant maintains high values of A_n throughout the year. Comparable seasonal patterns of *WUE* were found by Sala & Tenhunen (1996) in dense forests of *Quercus ilex* in NE Spain. However, Tenhunen et al. (1990), in *Q. coccifera*, near Lisbon, Portugal, report a monthly pattern of *WUE* very different from ours. In theirs, maximum annual values extend to the end of the dry period (September), and then decrease substantially, reaching values similar to those of the rest of the year.

6.5.3. Canopy transpiration

Seasonal leaf transpiration simulation showed that from winter to the end of spring there was a continuous increase in E_l, which reached the maximum value in June (beginning of the dry period). This pattern is related with the continuous increase in D_a. From late June to the end of the drought (early October), E_l decreased continuously due to stomatal closure and soil water stress. From that month on, E_l continued to decrease, due to low D_a. The seasonal leaf transpiration

pattern was comparable to that simulated by Sala & Tenhunen (1996) in the same species, but significantly higher because they integrated within canopy variability (as discussed below).

In the trees studied, whole-tree transpiration was calculated from sap flow measurements (see chapter III). Similar canopy transpiration patterns throughout the year were found for simulated leaf transpiration and measured canopy transpiration. The pattern of sap flow was repeated in years 1993 and 1994. Total annual transpiration simulated for isolated sun leaves was about 800 and 862 mm in stressed and non-stressed trees, respectively. From sap flow measurements made in these trees (see chapter III), was estimated an annual tree transpiration (from October 1993 to September 1994) of approximately 200 mm. These high values of leaf transpiration simulated are not in accord with tree transpiration measured, because certain factors concerning the single, tree-canopy level were not considered. Firstly, there is a sun-shade functional differentiation of leaves for CO_2 assimilation to transpiration, as pointed out by various authors (Abrams & Kubiske, 1990; Sala, 1992; Sala & Tenhunen, 1996; Faria et al., 1996), related with a decrease in transpiration of shade leaves compared with that of sun leaves. Another functional differentiation is due to leaf age. Decreases in transpiration due to ageing have been observed in herbaceous species (Whitehead & Singh, 1995), conifer and deciduous species (Hinckley et al., 1978), and evergreen oaks such as *Q. ilex* (Castell et al., 1994).

Finally, an environmental factor that could explain some differences in tree transpiration between estimated (from leaf transpiration) and measured sap flow is rain interception by the canopy. This was not considered in the leaf-level simulation, but its value can be comparable to the annual tree transpiration in this type of ecosystem with isolated trees (Calabuig et al., 1978; Haworth & McPherson, 1995). Thus there are particular problems in integrating spatial leaf photosynthesis and transpiration from leaf to tree-canopy level in these trees.

6.6. CONCLUDING REMARKS

Confirmed by field measurements, our results demonstrate that the modelling approach, compared to field measurements, provides a realistic description of diurnal and seasonal patterns of leaf gas exchange response to different environmental conditions, and as affected by water availability. The simulations we describe depict the responses of a single leaf. However, the results could be discussed in terms of canopy response, assuming that canopy processes can be approximated as 'a big leaf'. Such assumption is a lot more realistic for trees in oak savannahs (isolated trees) than for those in dense canopies, because the isolated tree can be considered a single-layer system of evaporation from the plant canopy, as pointed out in chapter IV. This eliminates an important problem, that of multilayer approximations. However, this single layer in isolated trees consists of two leaf populations: sun and shade leaves.

Sun-shade functional differentiation of leaves (Hollinger, 1989; Green, 1993; Sala & Tenhunen, 1996) must be considered in any whole-tree modelling of canopy gas exchange, and particularly of canopy assimilation. Unfortunately, no data were available describing the specific functional differentiation of sun-shade leaves in isolated *Quercus ilex* trees. Furthermore, it is necessary to know the sun leaf/shade leaf proportion in the tree-canopy. This ratio cannot be estimated from the leaf area index alone, as pointed out by Green (1993) for isolated walnut trees, because the self-shading canopy, which changes with solar angle through the day and the year, has not been taken into account.

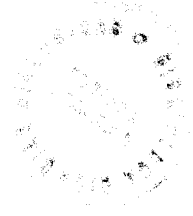

VII. CONCLUSIONES

1.- La dinámica del flujo de savia medida en el tronco es comparable al patrón de transpiración foliar, tanto en la forma como en la duración; tan solo se aprecia un retraso de una hora y media entre la transpiración foliar y el flujo de savia a nivel del tronco del árbol; este retraso lo crea el agua acumulada en los tejidos conductores. En este sentido, se ha constatado un flujo de savia nocturno (entre 0.5 y 1 $L.h^{-1}$) correspondiente a la recarga de los tejidos conductores; este flujo fue mayor cuanto mayor fue la transpiración del día precedente, llegando a ser significativo incluso en invierno.

2.- En el año hidrológico 1993-94, el consumo total anual de agua por árbol osciló entre los 13.000 y los 20.000 litros. De este consumo, la mitad correspondió a los cuatro meses de la estación seca (junio-septiembre). La otra mitad se reparte a partes iguales entre el periodo otoño-invierno (octubre-febrero) y la primavera (marzo-mayo). Estos porcentajes fueron idénticos en los tres árboles estudiados. La transpiración máxima diaria se alcanzó entre finales de mayo y principios de junio, oscilando entre los 80 y los 120 $L.día^{-1}$, según el árbol.

3.- El potencial hídrico de la planta al amanecer nunca fue inferior a los -2.5 MPa, aún habiéndose medido en dos años muy secos (421 y 503 mm respectivamente). Este potencial es mucho menos negativo que el medido en esta especie y en otras del género Quercus en la cuenca mediterránea.

4.- La transpiración anual por árbol osciló entre los 169 y los 205 $mm.año^{-1}$. En términos de transpiración por hectárea el valor estimado fue de 65.2 $mm.año^{-1}$. Si se expresa el consumo en función de la superficie foliar, la transpiración fue de 98.6 mm por unidad de LAI, valor comparable al estimado en bosques cerrados de Quercus ilex (87.5 - 98.5 $mm.LAI^{-1}$).

5.- En la evolución estacional del agua acumulada en el suelo se observaron los valores máximos en el mes de marzo (309-426 mm), correspondiendo con la recarga invernal del

suelo. Los valores mínimos se registraron en los meses de agosto y septiembre (196-281 mm). No se observaron diferencias significativas entre el agua perdida en los perfiles del suelo fuera de la proyección de la copa de los árboles y bajo ésta en los meses de verano, cuando la hierba está seca, lo que indicaría un sistema radicular que tiende a ocupar toda la superficie libre disponible, más allá de la proyección de la copa del árbol.

6.- Se ha modelado la conductancia estomática en función de la demanda evaporativa del aire (D_a). La respuesta de la conductancia estomática frente a la humedad, considerada como D_a, es no lineal, siendo ésta una función exponencial negativa. Esta respuesta sugiere un control de la conductancia estomática por parte de D_a, en forma de "feedback".

7.- Se ha obtenido un modelo simplificado de transpiración en base a dos características principales de la vegetación en estudio: de una parte, un coeficiente de desconexión (Ω) próximo a cero; y de otra, una conductancia superficial dependiente de la demanda evaporativa del aire. Este modelo se ha inferido, en igualdad de condiciones, para la hoja y el árbol entero, y se ajusta bien a los valores observados. El modelo de transpiración desarrollado para los árboles estudiados propone una sensibilidad de la transpiración a la conductancia superficial similar para la hoja y el árbol, en contra de la hipótesis de otros autores, que observan una disminución de la sensibilidad a medida que se sube en el nivel de organización.

8.- Cuando se representa la transpiración frente a la demanda evaporativa del aire, se pone de manifiesto un proceso de histéresis en función del potencial hídrico de la planta. Este proceso de histéresis vendría determinado por una adaptación del flujo de agua a través de los estomas a las condiciones de estrés hídrico.

9.- El análisis del flujo de savia muestra diferencias significativas en la densidad de flujo de savia entre distintas orientaciones del tronco: sur (S), noreste (NE) y noroeste (NW). Estas diferencias se aprecian a una escala de tiempo diaria y estacional. La orientación NE muestra una mayor actividad a lo largo de la mañana, mientras que la orientación NW la presenta a la largo de la tarde. La orientación S dos máximos de actividad con una disminución mas o menos acusada al mediodía. Las diferencias en la dinámica diaria

fueron menos acusadas en días nublados y hacia el final del periodo de sequía, cuando la disponibilidad hídrica de la planta fue menor. Las orientaciones NE y NW presentan un flujo de savia significativamente mayor que la orientación S, exceptuando el final del periodo seco, en el cual se hacen comparables. Estas diferencias no pueden ser explicada por diferencias la cantidad de radiación interceptada por distintos sectores de la copa del árbol, sino por otros factores que no han sido estimados en este estudio.

10.- El modelo de asimilación de CO_2 en plantas C_3 de Farquhar, junto a los modelos de conductancia estomática y transpiración desarrollados en este trabajo, permiten obtener muy buenas estimaciones del intercambio gaseoso foliar en los árboles estudiados. Las pequeñas diferencias encontradas entre los valores medidos y simulados se deben principalmente a picos y cambios bruscos en las condiciones ambientales alrededor de la hoja, que el modelo no llega a simular bien, debido a la escala de tiempo a la que se ha desarrollado; por ejemplo, diferencias apreciables entre la asimilación neta medida y simulada se dieron en picos superiores a los 10 $\mu mol.m^{-2}.s^{-1}$.

11.- La asimilación neta total mensual presenta un máximo en junio, y otro mínimo en diciembre, oscilando los valores entre 3 y 7 mol de $CO_2.m^{-2}.mes^{-1}$. El patrón de transpiración mensual sigue la misma dinámica encontrada en el flujo de savia. Así, éste posee un máximo en junio, y un mínimo en diciembre. El patrón mensual de la eficiencia en la utilización del agua presenta una tendencia inversa a la de la transpiración; los valores mínimos se alcanzan en el periodo seco, y los máximos en noviembre-enero.

VII.bis CONCLUSIONS

1.- The diurnal course of sap flow density was comparable to the pattern of leaf transpiration in form and duration, but with a delay of approximately one hour and a half between leaf transpiration and tree transpiration peaks. This delay is explained by the water stock in the living tissues of the tree. In this way, we noted a night water flow in the trunk every day (between 0.5 and 1 L h^{-1}) during the study period that depended on the climatic conditions of the previous day. This *night water flow was even significant in the winter period.*

2.- During the hydrological year 1993-94, annual water consumption per tree was between 13,000 and 20,000 litres, depending on the tree size. From June to September the tree consumed half of the annual tree water consumption. The rest was consumed during autumn-winter period (October-February) (50%) and the spring period (March-May) (50%). The seasonal percentages of consumption were similar among trees. Maximum daily tree transpiration measured was 80-120 L $year^{-1}$. Values were reached between last May and early June.

3.- Pre-dawn leaf water potential never was lower than –2.5 MPa. The leaf water potential was less negative to those measured in this and others species of genus Quercus in the Mediterranean basin.

4.- Annual tree transpiration was about 169-205 mm $year^{-1}$. The transpiration per hectare was about 65.2 mm $year^{-1}$. Transpiration per leaf area index (LAI) unit on isolated trees was 98.6. This value was similar to those found in dense canopies of the same species. (87.5 - 98.5 mm LAI^{-1}).

5.- The maximum values of soil water content were recorded in March (309-426 mm), in agreement with the winter soil replenishment. The minimum values were recorded in August and September (196-281 mm). The soil water contents inside and outside of the

tree canopy showed no significant differences. Consequently, we can assume a root system extended beneath of the tree canopy.

6.- The air water vapour pressure deficit (D_a) was found to be the best predictor of stomatal conductance (g_s) behaviour, at both hourly and daily time scales. The response of stomatal aperture to D_a follows a negative exponential. Here, D_a exhibited a feedback control on g_s, that is, D_a controls stomatal aperture via leaf water flow.

7.- Two main characteristics of the vegetation under study allowed us to obtain a simplified model of transpiration: a near zero decoupling coefficient (Ω), and a surface conductance modelled by D_a. This model was found appropriate at both leaf and tree levels, with a different behaviour as a function of plant water status. The Ω explains the sensitivity of transpiration to changes in surface conductance, which we found did not change with the increased spatial-scale in the dehesa ecosystems. This is contrary to the thesis of other authors, which suggests a diminished sensitivity of transpiration to surface conductance with increasing areal scale.

8.- We found a hysteresis process in the relationship between transpiration and D_a as a function of the plants' water status. The hysteresis of transpiration through the drought period may be explained by an acclimation of the plant's stomatal flow to water stress conditions.

9.- The sap flow analysis demonstrated significant differences in sap flow density among tree orientations, particularly among S orientation and NE and NW orientations. These differences were noted at daily and seasonal time scale. The NE oriented sector showed a diurnal sap flow density course with main activity in the morning. In the NW oriented sector the main activity was in the afternoon. The S oriented sector showed a lower activity than other sectors, with a more or less accentuated midday decrease. The diurnal differences were less pronounced in cloudy days and at the end of the drought period, when leaf water request was strongly low. Similar differences among orientations were found in daily sap flow density. The NE and NW orientations showed higher sap flow density than

S orientation, excepting to the end of the drought period were values become comparable among orientations. The within-tree transpiration variability founded can not be explained only by the amount of radiation intercepted by the canopy. Other factors, such as tree architecture (xylem conductivity, leaf area index) or leaf gas exchanges, have to be considered.

10.- We use a mechanistically based C_3 leaf CO_2 assimilation model linked with an empirical stomatal model to simulate Quercus ilex leaf net photosynthesis and transpiration. The modelling approach, compared to field measurements, provides a realistic description of diurnal and seasonal patterns of leaf gas-exchange response to different environmental conditions, as affected by water availability. The small differences found between measured and simulated values were related mainly to peaks or rapid changes in the physiological response of the leaf to environmental variables. Appreciable differences between leaf CO_2 assimilation measured and simulated were found in the diurnal peaks, above all when it was greater than 10 $\mu mol\ m^{-2}\ s^{-1}$.

11.- The maximum simulated rates of monthly net CO_2 assimilation changed between June and December, about 7 and 3 mol of $CO_2\ m^{-2}\ month^{-1}$, respectively. Similar canopy transpiration patterns throughout the year were found for simulated leaf transpiration and measured canopy transpiration, with maximum values in June and minimum values in December. The monthly water use efficiency (WUE) pattern was inverse to monthly transpiration pattern. Monthly WUE was lowest in July and higher in winter period (November-January).

VIII. REFERENCES

Abrams, M.D., 1986. Physiological plasticity in water relations and leaf structure of understory versus open-grown *Cercis canadensis* in northeastern Kansas. *Can. J. For. Res.* **16**, 1170-1174.

Abrams, M.D., 1990. Adaptations and responses to drought in *Quercus* species of North America. *Tree Physiol.*, **7**: 227-238.

Abrams, M.D. & Kubiske, M.E., 1990. Leaf structural characteristics of 31 hardwood and conifer tree species in Central Wisconsin: influence of light regime and shade-tolerance rank. *For. Ecol. Manag.*, **31**: 245-253.

Abtew, W., Gregory, J.M. & Borrelli, J., 1989. Wind profile: estimation of displacement height and aerodynamic roughness. *Transactions of the ASAE*, **32**: 521-527.

Acherar, M. & Rambal, S., 1992. Comparative water relations of four Mediterranean oak species. *Vegetatio*, **99-100**: 177-184.

Alvino, A., Centritto, M. & De Lorenzi, F., 1994. Photosynthesis response of sunlit and shade pepper (*Capsicum annuum*) leaves at different positions in the canopy under two water regimes. *Aust. J. Plant. Physiol.*, **21**: 377-391.

Anfodillo, T., Sigalotti, G.B., Tomasi, M., Semenzato, P. & Valentini, R., 1993. Applications of a thermal imaging technique in the study of the ascent sap in woody species. *Plant Cell Environ.*, **16**: 997-1001.

Aphalo, P.J. & Jarvis, P.G., 1991. Do stomata respond to relative humidity? *Plant Cell Environ.*, **14**: 127-132.

Aphalo, P.J. & Jarvis, P.G., 1993. An analysis of Ball's empirical model of stomatal conductance. *Ann. Bot.*, **72**: 321-327.

Aussenac, G. & Valette, J.C., 1982. Comportement hydrique estival de *Cedrus atlantica* Manetti, *Quercus ilex* L. et *Quercus pubescens* Willd. este de divers pins dans le Mont Ventoux. *Ann. Sci. For.*, **39**: 41-62.

Bahari, Z.A., Pallardy, S.G. & Parker, W.C., 1985. Photosynthesis, water relations, and drought adaptations in six woody species of oak-hickory forests in Central Missouri. *Forest Sci.*, **31**: 557-569.

Baldocchi, D.D., Mat, D.R., Hutchison, B.A. & McMillen, R.T., 1984. Solar radiation within an oak-hickory forest: an evaluation of the extinction coefficients for several

radiation components during fully-leafed and leafless periods. *Agric. For. Meteorol.*, **32**: 307-322.

Ball, J.T., Woodrow, I.E. & Berry, J.A., 1987. A model predicting stomatal conductance and its contribution to the control of photosynthesis under different environmental conditions. **In**: Biggins, J. (Ed.). Progress in photosynthesis research. Dordrecht: Martinus Nijhoff Publisher, pp: 221-224.

Barrantes, O., 1986. Influencia de la encina sobre el pasto en la Sierra Norte de Sevilla: una aproximación experimental. Tesina de Licenciatura. Universidad de Sevilla. Sevilla. 71 p. + apéndices.

Beyschlag, W., Lange, O.L. & Tenhunen, J.D., 1986. Photosynthesis and water relations of the mediterranean evergreen sclerophyll *Arbutus unedo* L. throughout the year at a site in Portugal. *Flora*, **178**: 409-444.

Biron, P., 1994. Le cycle de l'eau en foret de moyenne montagne: flux de sève et bilans hydriques stationnels (bassin versant du Strengbach a Aubure-Hautes Vosges). Thèse Univ. Louis Pasteur, Strasbourg I, Strasbourg, pp: 61-71.

Blake-Jacobson, M.E., 1987. Stomatal conductance and water relations of shrubs growing at the chaparral-desert ecotone in California and Arizona. In: Plant response to stress. Functional analysis in Mediterranean ecosystems. Tenhunen, J.D., Catarino, F.M., Lange, O.L.& Oechel, W.D. (Eds.). NATO ASI series, Series G, Ecological Sciences 15, Springer-Verlag, Berlin, pp: 223-245.

Breda, N., 1994. Analyse du fonctionnement hydrique des chênes sessile (*Quercus petraea*) et pédonculé (*Q. robur*) en conditions naturelles; effets des facteurs du milieu et de l'éclaircie. Thèse Univ. Nancy, Nancy.

Breda, N., Cochard, H., Dreyer, E. & Granier, A., 1993a. Field comparison of transpiration, stomatal conductance and vulnerability to cavitation of *Quercus petraea* and *Quercus robur* under water stress. *Ann. Sci. For.*, **50**: 571-582.

Breda, N., Cochard, H., Dreyer, E. & Granier, A., 1993b. Water transfer in a mature oak stand (*Quercus petraea*): seasonal evolution and effects of a severe drought. *Can. J. For. Res.*, **23**: 1136-1143.

Brough, D.W., Jones, H.G. & Grace, J., 1986. Diurnal changes in water content of the stems of apple trees, as influenced by irrigation. *Plant Cell Environ.*, **9**: 1-7.

Brown, M.J. & Parker, G.G., 1994. Canopy light transmitance in a chronosequence of mixed-species deciduous forests. *Can. J. For. Res.*, **24**: 1694-1703.

Bulla, L., Fragoso, C., Haridasan, M., Lamotte, M., Montes, R.A., San José, J., Sarmiento, G., Scholes, R.J. & Spetch, R.L., 1995. El funcionament ecològic de la sabana. **In:** Biosfera, Vol. III, Sabanes. Editorial Fundaciò Enciclopedia Catalana. pp: 93-107.

Burton, A.J., Pregitzer, K.S. & Reed, D.D., 1991. Leaf area and foliar biomass relationships in northern hardwood forest located along an 800 km acid deposition gradient. *Forest Sci.*, **37**: 1041-1059.

Calabuig, E.L., Gago Gamallo, M.L. & Gómez Gutiérrez, J.M., 1978. Influencia de la encina (*Quercus rotundifolia* Lam.) en la distribución del agua de lluvia. Centro de Edafología y Biología Aplicada del CSIC. *Anuario 1977*, Vol. **IV**: 143-159.

Carlson, T.N. & Lynn, B., 1991. The effect of plant water storage on transpiration and radiometric surface temperature. *Agric. For. Meteorol.*, **57**: 171-186.

Castell, C., Terradas, J. & Tenhunen, J.D., 1994. Water relations, gas exchange, and growth of reprousts and mature plants shoots of *Arbutus unedo* L. and *Quercus ilex* L. *Oecologia*, **98**: 201-211.

Castro-Díez, P., 1996. Variaciones estructurales y funcionales de los fanerófitos dominantes en las comunidades de encinar a lo largo de un gradiente climático atlántico-mediterráneo. Tesis Univ. de León, León. 207 p.

Castro-Díez, P., Villar-Salvador, P., Pérez-Rontomé, C., Maestro-Martinez, C., Montserrat-Martí, G., 1997. Leaf morphology and leaf chemical composition in three *Quercus* (*Fagaceae*) species along a climatic gradient in NE Spain. *Trees*, **11**: 127-134.

Castroviejo, S., Laínz, M., López González, G., Montserrat, P., Muñoz Garmendia, F., Paiva, J. & Villar, L., (Eds.) 1990. *Flora Ibérica*. Real Jardín Botánico, CSIC, Madrid. Vol. **II**, pp: 19-20.

Chaves, M.M. & Pereira, J.S., 1992. Water stress, CO_2 and climate change. *J. Exp. Bot.*, **43**: 1131-1139.

Chaves, M.M., Pereira, J.S., Cerasoli, S., Clifton-Brown, J., Miglietta, F. & Raschi, A., 1995. Leaf metabolism during summer drought in *Quercus ilex* trees with lifetime exposure to elevated CO_2. *J. Biogeogr.*, **22**: 255-259.

Cochard, H. & Tyree, M.T., 1990. Xylem dysfunction in *Quercus*: vessel sizes, tyloses, cavitation and seasonal changes in embolism. *Tree Physiol.*, **6**: 393-407.

Damesin, C., 1996. Relations hydriques, photosynthèses et efficacité d'utilisation de l'eau chez deux chênes méditerranéens caduc et sempervirent cooccurrents. Thèse Univ. De Paris-Sud, UFR Scientifique d'Orsay, Paris, 99 p. + annexes.

De Lillis, M. & Fontanella, A., 1992. Comparative phenology and growth in different species of the Mediterranean maquis of central Italy, *Vegetatio*, **99-100**: 83-96.

Duhme, F. & Hinckley, T.M., 1992. Daily and seasonal variation in water relations of macchia shrubs and tress in France (Montpellier) and Turkey (Antalya). *Vegetatio*, **99-100**: 185-198.

Dye, P.J., & Olbrich, B.W., 1993. Estimating transpiration from 6-year-old *Eucalyptus grandis* trees: development of a canopy conductance model and comparison with independent sap flux measurements. *Plant Cell Environ.*, **16**: 45-53.

Epron, D. & Dreyer, E., 1993. Photosynthesis of oak leaves under water stress: maintenance of high photochemical efficiency of photosystem II and occurrence of non-uniform CO_2 assimilation. *Tree Physiol.*, **13**: 107-117.

Escudero, A., Manzano, J.J. & Del Arco, J.M., 1987. Nitrogen concentrations in the leaves of different mediterranean woody species. *Ecologia Mediterranea*, **13**: 11-17.

Evans, J.R. & Farquhar, G.D., 1991. Modelling canopy photosynthesis from the biochemistry of the C_3 chloroplast. **In**: K.J. Boote & R.S. Loomis (Eds.). Modelling Crop photosynthesis -from Biochemistry to Canopy. ASA, Madison, Wisconsin, pp: 1-15.

Faria, T., García-Plazaola, J.I., Abadía, A., Cerasoli, S., Pereira, J.S. & Chaves, M.M., 1996. Diurnal changes in photoprotective mechanisms in leaves of cork oak (*Quercus suber*) during summer. *Tree Physiol.*, **16**: 115-123.

Farquhar, G.D., 1978. Feedforward responses of stomata to humidity. *Aust. J. Plant Physiol.*, **5**: 787-800.

Farquhar, G.D.,1989. Models of integrated photosynthesis of cells and leaves. *Phil. Trans. R. Soc. Lond. B*, **323**: 357-367.

Farquhar, G.D. Von Caemmerer, S. & Berry, J.A., 1980. A biochemical model of photosynthesis CO_2 assimilation in leaves of C_3 species. *Planta*, **149**: 78-90.

Farquhar, G.D. & Von Caemmerer, S., 1982. Modelling of photosynthesis response to environment. **In**: Lange, O.L., Nobel, P.S., Osmond, C.B. & Ziegler, H. (Eds.). Encyclopedia of Plant Physiology. Vol. 12B, Physiological Plant Ecology II, Water relations and carbon assimilation. Springer-Verlag, Berlin, pp: 549-587.

Farrington, P., Bartle, G.A., Watson, G.D. & Salama, R.B., 1994. Long-term transpiration in two eucalyptus species in a native woodland estimated by the heat-pulse technique. *Aust. J. Ecol.*, **19**: 17-25.

Field, C.B., Ball, J.T. & Berry, J.A., 1991. Photosynthesis: principles and field techniques. **In**: Pearcy, Ehleringer, Mooney & Rundel (Eds.). Plant physiological ecology. Field methods and instrumentation. Chapman & Hall, London, pp: 209-253.

Gallego, H.A., Rico, M., Moreno, G: & Santa Regina, I., 1994. Leaf water potential and stomatal conductance in *Quercus pyrenaica* Willd. forests: vertical gradients and response to environmental factors. *Tree Physiol.*, **14**: 1039-1047.

Gallego-Fernández, J.B., 1989. Aproximaciones a la biología reproductiva de *Quercus rotundifolia* L. Departamento de Biología Vegetal y Ecología. University of Seville.

Gibbs, R.D., 1958. Patterns in the seasonal water content of trees. **In**: Thimann, K.V, (Ed.). The physiology of forest tree. Ronald Press, New York, pp: 43-69.

Goulden, M.L. & Field, C.B., 1994. Three methods for monitoring the gas exchange of individual tree canopies: ventilated-chamber, sap-flow and Penman-Monteith measurements on evergreen oaks. *Funct. Ecol.*, **8**: 125-135.

Granier, A., 1985. Une nouvelle méthode pour la mesure de flux de sève brute dans le tronc des arbres. *Ann. Sci. For.*, **42**: 193-200.

Granier, A., 1987. Evaluation of transpiration in a Douglas-fir stand by means of sap flow measurements. *Tree Physiol.*, **3**: 309-320.

Granier, A., Bobay, V., Gash, J.H.C., Gelpe, J., Saugier, B. & Shuttleworth, W.J., 1990. Vapour flux density and transpiration rate comparisons in a stand of maritime Pinus (*Pinus pinaster* Ait.) in Les Landes forest. *Agric. For. Meteorol.*, **51**: 309-319.

Granier, A. & Loustau, D., 1994. Measuring and modelling the transpiration of a maritime pine canopy from sap-flow data. *Agric. For. Meteorol.*, **71**: 61-81.

Granier, A., Anfodillo, T., Sabatti, M., Cochard, H., Dreyer, E., Tomasi, M., Valentini, R. & Breda, N., 1994. Axial and radial water flow in the trunks of oak trees: a quantitative and qualitative analysis. *Tree Physiol.*, **14**: 1383-1396.

Grantz, D.A. & Meinzer, F.C., 1990. Stomatal response to humidity in a sugarcane field: simultaneous porometric and micrometeorological measurements. *Plant Cell Environ.*, **13**: 27-37.

Green, S.R., 1993. Radiation balance, transpiration and photosynthesis of an isolated tree. *Agric. For. Meteorol.*, **64**: 201-221.

Griffin, J.R., 1973. Xylem sap tension in three woodland oaks of central California. *Ecology*, **54**: 152-159.

Harley, P.C., Tenhunen, J.D. & Lange, O.L., 1986. Use of an analytical model to study limitations on net photosynthesis in *Arbutus unedo* under field conditions. *Oecologia,* **70**: 393-401.

Harley, P.C. & Tenhunen, J.D., 1991. Modelling the photosynthesis response of C_3 leaves to environmental factors. **In**: Boote, K.J. & Loomis, R.S.(Eds.). Modelling Crop photosynthesis -from Biochemistry to Canopy. ASA, Madison, Wisconsin, pp: 17-39.

Harley, P.C., Thomas, R.B., Reynolds, J.F. & Strain, B.R., 1992. Modelling photosynthesis of cotton grown in elevated CO_2. *Plant Cell Environ.,* **15**: 271-282.

Hasting, S.J., Oechel, W.C. & Sionit, N., 1989. Water relations and photosynthesis of chaparral reproust and seedlings following fire and hand clearing. **In:** The California Chaparral. Paradigms reesamined. Keeley, S. C. (Ed.). Natural History Museum of Los Angeles County, Science Series, 34, pp: 107-113.

Haworth, K. & McPherson, G.R., 1995. Effects of *Quercus emoryi* trees on precipitation distribution and microclimate in a semi-arid savanna. *J. Arid Environ.,* **31**: 153-170.

Heiman J. & Stickan, W., 1993. Heat pulse measurements on beech (*Fagus sylvatica* L.) in relation to weather conditions. **In**: Borghetti, M., Grace, J. & Raschi, A. (Eds.). Water transport in plants under climatic stress. Cambridge University Press, UK, pp: 174-180.

Herzog, K.M., Häsler, R. & Thum, R., 1995. Diurnal changes in the radius of a subalpine Norway spruce stem: their relation to the sap flow and their use to estimate transpiration. *Trees,* **10**: 94-101.

Hinckley, T.M., Lassoie, J.P. & Running, S.W., 1978. Temporal and spatial variations in the water status of forest trees. *Forest Sci. Monograph,* **20**: 72 pp.

Hinckley, T.M., Duhme, F., Hinckley, A.R. & Richter, H., 1983. Drought relations of shrub species: assessment of the mechanisms of drought resistance. *Oecologia,* **59**: 344-350.

Hollinger, D.Y., 1989. Canopy organization and foliage photosynthetic capacity in a broad-leaved evergreen montane forest. *Func. Ecol.,* **3**: 53-62.

Hollinger, D.Y., 1992. Leaf and simulated whole-canopy photosynthesis in two co-occurring tree species. *Ecology,* **73**: 1-14.

Jarvis, P.G., 1976. The interpretation of the variations in leaf water potential and stomatal conductance found in canopies in the field. *Phil. Trans. R. Soc. London Ser. B,* **273**: 593-610.

Jarvis, P.G., 1995. Scaling processes and problems. *Plant Cell Environ.*, **18**: 1079-1089.

Jarvis, P.G. & Morison, J.I.L., 1981. The control of transpiration and photosynthesis by the stomata. **In**: Jarvis,, P.G. & Mansfield, T.A. (Eds.). Stomatal physiology. Cambridge University Press, Cambridge, pp: 247-279.

Jarvis, P.G. & McNaughton, K.G., 1986. Stomatal control of transpiration: scaling up from leaf to region. *Adv. Ecol. Res.*, **15**: 1-49.

Joffre, R., 1987. Contraintes du milieu et réponses de la végétation herbacée dans les dehesas de la Sierra Norte (Andalousie, Espagne). Thèse Univ. Sciences et Techniques du Languedoc, Montpellier, 186 p. + annexes.

Joffre, R., Leiva-Morales, M.J., Rambal, S., & Fernández-Alés, R., 1987. Dynamique racinaire et extraction de l'eau du sol par des graminées pérennes et annuelles méditerranéennes. *Acta Oecol., Oecol. Plant.*, **8**: 181-194.

Joffre, R. & Rambal, S., 1988. Soil water improvement by trees in the rangelands of Southern Spain. *Acta Oecol., Oecol. Plant.*, **9**: 405-422.

Joffre, R., Vacher, J., De los Llanos, C. & Long, G., 1988. The dehesa: an agrosilvopastoral system of the mediterranean region with special reference to the Sierra Morena area of Spain. *Agroforest. Syst.*, **6**: 71-96.

Joffre, R., Hubert, B. & Meuret, M., 1991. Les systèmes agro-sylvo-pastoraux méditerranéens: enjeux et réflexions pour une gestion raisonnée. MAB Digest n°10, UNESCO, Paris.

Joffre R. & Rambal S., 1993. How tree cover influences the water balance of mediterranean rangelands. *Ecology*, **74**: 570-582.

Johnson, J.D. & Ferrell, W.K., 1983. Stomatal response to vapour pressure deficit and the effect of plant water stress. *Plant Cell Environ.*, **6**: 451-456.

Jones, H.G., 1992. Plants and microclimate. Cambridge University Press, Cambridge.

Jones, H.G. & Sutherland, R.A., 1991. Stomatal control of xylem embolism. *Plant Cell Environ.*, **14**: 607-612.

Kaiser, W., 1987. Effects of water deficit on photosynthetic capacity. *Physiol. Plant.* **71**: 142-149.

Kaufmann, M.R. & Troendle, C.A., 1981. The relationships of leaf area and foliage biomass to sapwood conducting area in four subalpine forest tree species. *Forest Sci.*, **27**: 477-482.

Kirschbaum, M.U.F., 1994. The sensitivity of C_3 photosynthesis to increasing CO_2 concentration: a theoretical analysis of its dependence on temperature and background CO_2 concentration. *Plant Cell Environ.*, **17**: 747-754.

Körner, Ch., 1994. Leaf diffusive conductances in the major vegetation types of the globe. **In**: Schulze, E.D. & Caldwell, M.M. (Eds.). Ecophysiology of photosynthesis. Ecological Studies 100, Springer, New York, pp: 463-490.

Körner, Ch. & Cochrane, P.M., 1985. Stomatal responses and water relations of *Eucalyptus pauciflora* in summer along an elevational gradient. *Oecologia*, **66**: 443-455.

Köstner, B.M.M., Schulze, E-D., Kelliher, F.M., Hollinger, D.Y., Byers, J.N., Hunt, J.E., McSeveny, T.M., Meserth, R. & Weir, P.L., 1992. Transpiration and canopy conductance in a pristine broad-leaved forest of *Nothofagus*: an analysis of xylem sap flow and eddy correlation measurements. *Oecologia*, **91**: 350-359.

Krause, D. & Kummerow, J., 1977. Xeromorphic structure and soil moisture chaparral. *Oecologia Plantarum*, **12**: 133-148.

Leiva, M.J., 1991. Factores que limitan a las comunidades de gramíneas perennes en los pastos mediterráneos de la Sierra Norte de Sevilla. Tesis Univ. de Sevilla, Sevilla. 146 pp.

Leuning, R., Cromer, R.N. & Rance, S., 1991. Spatial distributions of foliar nitrogen and phosphorus in crowns of *Eucalyptus grandis*. *Oecologia*, **88**: 504-510.

Lindroth, A., 1985. Canopy conductance of coniferous forest related to climate. *Water Resour. Res.*, **21**: 297-304.

Lloyd, J. 1991 Modelling stomatal responses to environment in *Macadamia integrifolia*. *Aust. J. Plant Physiol.*, **18**: 649-660.

Lo Gullo, M.A. & Salleo, S., 1993. Different vulnerabilities of *Quercus ilex* L. to freeze- and summer drought-induced xylem embolism: an ecological interpretation. *Plant Cell Environ.*, **16**: 511-519.

Lösch, R. & Tenhunen, J.D., 1981. Stomatal responses to humidity-phenomenon and mechanism. **In**: Jarvis, P.G. & Mansfield, T.A.(Eds.). Stomatal physiology. Cambridge University Press, Cambridge, pp: 137-161.

Lostau, D., Granier, A. & El Hadj Moussa, F., 1990. Evolution saisonnière du flux de sève dans un peuplement de pins maritimes. *Ann. Sci. For.*, **21**: 599-618.

Lucot, E. & Bruckert, S., 1992. Organisation du système racinaire du chêne pédonculé (*Quercus robur*) développé en conditions édaphiques non contraignantes (sol brun lessivé colluvial). *Ann. Sci. For.*, **49**: 465-479.

Mapas provinciales de suelos. Sevilla. 1975. Ministerio de Agricultura. Madrid. 282 p. + mapas.

Marshall, J.D. & Waring, R.H., 1986. Comparison of methods of estimating leaf-area index in old-growth Douglas-fir. *Ecology*, **67**: 975-979.

Marsteau, C., 1979. Structure, dynamique et mise en valeur forestière d'une zone à chêne pubescent. Mémoire de L'Ecole National des Ingénieurs des Travaux des Eaux et Forêst, INRA, Recherches Forestières. Station de Sylviculture Méditerrannéenne. Avignon, 92p. + annexes.

Martin, P., 1989. The significance of radiative coupling between vegetation and the atmosphere. *Agric. For. Meteorol.*, **49**: 45-53.

Matthews, M.A., Van Volkenburgh, E. & Boyer, J.S., 1984. Acclimation of leaf growth to low water potentials in sunflower. *Plant Cell Environ.*, **7**: 199-206.

McMurtrie R.E., Leuning, R., Thompson, W.A. & Wheeler, A.M., 1992. A model of canopy photosynthesis and water use incorporating a mechanistic formulation of leaf CO_2 exchange. *For. Ecol. Manag.*, **52**: 261-278.

McNaughton, K.G. & Jarvis, P.G., 1983. Predicting effects of vegetation changes on transpiration and evaporation. **In**: Kozlowski, T.T.(Ed.). Water deficits and plant growth. Vol. VII, Academic Press Inc., New York, pp: 1-47.

McNaughton, K.G. & Jarvis, P.G., 1991. Effects of spatial scale on stomatal control of transpiration. *Agric. For. Meteorol.*, **54**: 279-301.

Meinzer, F.C., 1993. Stomatal control of transpiration. *Trees*, **8**: 289-294.

Meinzer, F.C. & Grantz, D.A., 1989. Stomatal control of transpiration from a developing sugarcane canopy. *Plant Cell Environ.*, **12**: 635-642.

Meinzer, F.C., Goldstein, G., Holbrook, N.M., Jackson, P. & Cavelier, J., 1993. Stomatal and environmental control of transpiration in a lowland tropical forest tree. *Plant Cell Environ.*, **16**: 429-436.

Michaud, H., Lumaret, R. & Romane, F., 1992. Variation in the genetic structure and reproductive biology of holm oak populations. *Vegetatio*, **99-100**: 107-113.

Miller, D.R., Vavrina, C.A. & Christensen, T.W., 1980. Measurement of sap flow and transpiration in ring-porous oaks using a heat pulse velocity technique. *Forest Sci.*, **26**: 485-494.

Monteith, J.L., 1965. Evaporation and environment. *Symp. Soc. Exp. Biol.*, **19**: 205-234.

Monteith, J.L. & Unsworth, M.H., 1990. Principles of environmental physics. Edward Arnold, London.

Mott, K.A. & Parkhurst, D.F., 1991. Stomatal responses to humidity in air and helox. *Plant Cell Environ.*, **14**: 509-515.

Nel, E.M. & Wessman, C.A., 1993. Canopy transmitance models for estimating forest leaf area index. *Can. J. For. Res.*, **23**: 2579-2586.

Nizinski, J. & Saugier, B., 1989. Dynamique de l'eau dans une chênaie (*Quercus petraea* (Matt.) Liebl.) en forêt de Fontainebleau. *Ann. Sci. For.*, **46**: 173-186.

Norman, J.M., 1993. Scaling process between leaf and canopy levels. **In**: Ehleringer, J.R. & Field, C.B.(Eds.). Scaling physiological process. Leaf to globe. Academic Press Inc., San Diego, pp: 41-76.

Nygren, P., Rebottaro, S. & Chavarria, R., 1993. Application of the pipe model theory to non-destructive estimation of leaf biomass and leaf area of pruned agroforestry trees. *Agroforest. Sys.*, **23**: 63-77.

Oliveira, G., 1995. Autoecologia do sobreiro (*Quercus suber* L.) em montados portugueses. Thèse Dissertação, Facultade de Ciências da Universidade de Lisboa, Lisboa, 162 p.

Oliveira, G., Correia, O.A., Martins-Loução, M.A. & Catarino, F.M., 1992. Water relations of cork-oak (*Quercus suber* L.) under natural conditions. *Vegetatio*, **99-100**: 199-208.

Ortega, F., 1987. Cambios temporales de los pastos anuales mediterráneos de la Sierra Norte de Sevilla, en relación con el régimen de precipitación. Tesis Univ. de Sevilla. Sevilla. 184 p.

Piñol, J., Avila, A., Escarré, A., Lledó, M.J. & Rodà, F., 1992. Comparison of the hydrological characteristics of three small experimental holm oak forested catchments in the NE Spain in relation to larger areas. *Vegetatio*, **99-100**: 169-176.

Pitacco, A., Gallinaro, N., & Giulivo, C., 1992. Evaluation of actual evpotranspiration of a *Quercus ilex* L. stand by the bowen ratio-energy budget method. *Vegetatio*, **99-100**: 163-168.

Poole, D.K. & Miller, P.C., 1981. The distribution of plant water stress and vegetation characteristics in southern californian chaparral. *Am. Mid. Nat.*, **105**: 32-43.

Rambal, S., 1992. *Quercus ilex* facing water stress: a functional equilibrium hypothesis. *Vegetatio*, **99-100**: 147-153.

Rambal, S., 1993. The differential role of mechanisms for drought resistance in a Mediterranean evergreen shrub: a simulation approach. *Plant Cell Environ.*, **16**: 35-44.

Rambal, S. & Debussche, G., 1995. Water balance of Mediterranean ecosystems under a changing climate. **In:** Global change and Mediterranean-type ecosystems. Moreno,

J.M. & Oechel, W.C. (Eds.). Ecological Studies 117, Springer, New York, pp: 386-407.

Reich, P.B. & Hinckley, T.M., 1989. Influence of pre-dawn water potential and soil-to-leaf hydraulic conductance on maximum daily leaf diffusive conductance in two oak species. *Funct. Ecol.*, **3**: 719-726.

Rennolls, K., 1994. Pipe-model theory of stem-profile development. *Forest Ecol. Manag.*, **69**: 41-55.

Rhizopoulou, S. & Mitrakos, K., 1990. Water relations of evergreen sclerophylls. I. Seasonal changes in the water relations of eleven species from the same environment. *Ann. Bot.*, **65**: 171-178.

Ritchie, J.T., 1972. Model for predicting evaporation from a row crop with incomplete cover. *Water Resour. Res.*, **8**: 1204-1212.

Rogers, R. & Hinckley, T.M., 1979. Foliar weight and area related to current sapwood area in oak. *Forest Sci.*, **25**: 298-303.

Roldan, I., 1993. Estudio de la organización espacial de los pastos mediterráneos. Tesis Univ. de Sevilla. Sevilla. 235 p. + apéndices.

Rundel, P.W., 1980. Adaptations of Mediterranean-climate oaks to environmental stress. **In**: Plumb, T.R. (Ed.). Proceedings of the Symposium on the Ecology, management and utilization of Californian oaks. Pacific Southwest Forest and Range Experiment Station, Berkeley, pp: 43-54.

Sala, A., 1992. Water relations, canopy structure, and canopy gas exchange in a *Quercus ilex* L. forest: variation in the time and space. Tesis. Univ. de Barcelona. Barcelona. 151 p.

Sala, A. & Tenhunen, J.D., 1994. Site-specific water relations and stomatal response of *Quercus ilex* in a Mediterranean watershed. *Tree Physiol.*, **14**: 601-617.

Sala, A., Sabaté, S., Gracia, C. & Tenhunen, J.D., 1994. Canopy structure within a *Quercus ilex* forested watershed: variations due to location, phenological development, and water availability. *Trees*, **8**: 254-261.

Sala, A. & Tenhunen, J.D., 1996. Simulations of canopy net photosynthesis and transpiration in *Quercus ilex* L. under the influence of seasonal drought. *Agric. For. Meteorol.*, **78**: 203-222.

Salleo, S. & Lo Gullo, M.A., 1990. Sclerophylly and plant water relations in three Mediterranean *Quercus* species. *Ann. Bot.*, **65**: 259-270.

Scholander, P.F., Hammel, H.T., Bradstreet, E.D. & Hemmingsen, E.A., 1965. Sap pressure in vascular plants. *Science*, **148**: 339-346.

Schulze, E-D., Cermák, J., Matyssek, Penka, M., Zimmermann, R., Vasícek, F., Gries, W. & Kucera, J., 1985. Canopy transpiration and water fluxes in the xylem of the trunk of *Larix* and *Picea* trees -a comparison of xylem flow, porometer and cuvette measurements. *Oecologia*, **66**: 475-483.

Schulze, E-D., Turner, N.C., Gollan, T. & Shackel, K.A., 1987. Stomatal response to air humidity and to soil drought. **In**: Zeiger, E., Farquhar, G.D. & Cowan, I.R.(Eds.). Stomatal function. Stanford University Press, Stanford, pp: 311-320.

Sharkey, T.D., 1985. Photosynthesis in intact leaves of C_3 plants: physics, physiology and rate limitations. *Bot. Rev.*, **51**: 53-106.

Shelburne, V.B., Hedden, R.L. & Allen, R.M., 1993. The effects of site, stand density, and sapwood permeability on the relationships between leaf area and sapwood area in loblolly pine (*Pinus tadea* L.). *Forest Ecol. Manag.*, **58**: 193-209.

Sheriff, D.W., 1984. Epidermal transpiration and stomatal responses to humidity: some hypotheses explored. *Plant Cell Environ.*, **7**: 669-677.

Shinozaki, K., Yoda, K., Hozumi, K. & Kira, T. 1964a. A quantitative analysis of plant form - the pipe model theory. I: Basic analyses. *Jap. J. Ecol.*, **14**: 97-105.

Shinozaki, K., Yoda, K., Hozumi, K. & Kira, T. 1964b. A quantitative analysis of plant form - the pipe model theory. II: Further evidences of the theory ant its application in forest ecology. *Jap. J. Ecol.*, **14**: 133-139.

Sokal, R.R. & Rohlf, F.J., 1981. Biometry. 2nd Ed., W H Freeman and Co. New York.

Sprugel, D.G., Hynckley, T.M. & Schaap, W., 1991. The theory and practice of branch autonomy. *Annu. Rev. Ecol. Syst.*, **22**: 309-334

Steinberg, S.L., McFarland, M.J. & Worthington, J.W., 1990. Comparison of trunk and branch sap flow with canopy transpiration in Pecan. *J. Exp. Bot.*, **41**: 653-659.

Stewart, J.B., 1988. Modelling surface conductance of pine forest. *Agric. For. Meteorol.*, **43**: 19-35.

Stockle, C.O., 1992. Canopy photosynthesis and transpiration estimates using radiation interception models with different level of details. *Ecol. Model.*, **60**: 31-44.

Stone, E.L. & Kalisz, P.J., 1991. On the maximum extent of tree roots. *Forest Ecol. Manag.*, **46**: 59-102.

Strahler, A.N., 1986. Geografía física. 7ª Edición. Editorial Omega. Barcelona.

Swanson, R.H., 1994. Significant historical developments in thermal methods for measuring sap flow in trees. *Agric. For. Meteorol.*, **72**: 113-132.

Tenhunen, J.D., Lange, O.L. & Braun, M., 1981. Midday stomatal closure in mediterranean type sclerophylls under simulated habitat conditions in an environmental chamber. II. Effect of the complex of leaf temperature and air humidity on gas exchange of *Arbutus unedo* and *Quercus ilex*. *Oecologia*, **50**: 5-11.

Tenhunen, J.D., Lange, O.L. & Jahner, D., 1982. The control by atmospheric factors and water stress of midday stomatal closure in *Arbutus unedo* growing in a natural macchia. *Oecologia*, **55**: 165-169.

Tenhunen, J.D., Lange, O.L., Gebel, J., Beyschlag, W. & Weber, J.A., 1985. Changes in the photosynthetic capacity, carboxylation efficiency and CO_2 compensation point associated with midday stomatal closure and midday depression of net CO_2 exchange of leaves of *Quercus suber*. *Planta*, **162**: 193-203.

Tenhunen, J.D., Pearcy, R.W. & Lange, O.L., 1987. Diurnal variations in leaf conductance and gas exchange in natural environments. **In**: Zeiger, E., Farquhar, G.D. & Cowan, I.R.(Eds.). Stomatal function. Stanford University Press, Stanford, pp: 321-351.

Tenhunen, J.D., Sala, A., Harley, P.C., Dougherty, R.L. & Reynolds, J.F., 1990. Factors influencing carbon fixation and water use by mediterranean sclerophyll shrubs during summer drought. *Oecologia*, **82**: 381-393.

Terradas, J. & Savé, R., 1992. The influence of summer and winter stress and water relationships on the distribution of *Quercus ilex* L. *Vegetatio*, **99-100**: 137-145.

Tetriach, M., 1993. Photosynthesis and transpiration of evergreen Mediterranean and deciduous trees in an ecotone during a growing season. *Acta Oecol.*, **14**: 341-360.

Thornley, J.H.M., 1996. Modelling water in crops and plant ecosystems. *Ann. Bot.*, **77**: 261-275.

Tutin, T.G., Heywood, V.H., Burges, N.A., Valentine, D.H., Walters, S.M. & Webb, D.A., (Eds.) 1964. Flora Europaea. Cambridge University Press, Cambridge. Vol. **I**, pp: 62.

Tyree, M.T., 1988. A dynamic model for water flow in a single tree: evidence that models must account for hydraulic architecture. *Tree Physiol.*, **4**: 195-217.

Vacher, J., 1984. Analyse phyto et agro-écolgique des dehesas pastorales de la Sierra Norte. Thèse U.S.T.L., Montpellier, 195 p.

Valentini, R., Epron, D., De Angelis, P., Matteucci, G. & Dreyer, E. 1995. *In situ* estimation of net CO_2 assimilation, photosynthetic electron flow and photorespiration in

Turkey oak (*Q. cerris* L.) leaves: diurnal cycles under different levels of water supply. *Plant Cell Environ.*, **18**: 631-640.

Valette, J.C., 1981. Comportements hydriques du cèdre, des chênes et des pins méditerranéens. INRA. . Station de Sylviculture Méditerrannéenne. Avignon. Document interne, 81-1, 43p.

Vankat, J.L., 1989. Water stress in chaparral shrubs in summer-rain *versus* summer-drought climates. **In:** The California Chaparral. Paradigms reesamined. Keeley, S.C. (Ed.). Natural History Museum of Los Angeles County, *Science Series*, **34**, pp: 117-124.

Villar-Salvador, P., Castro-Díez, P., Pérez-Rontomé, C. & Montserrat-Martí, G., 1997. Stem xylem features in three *Quercus* (*Fagaceae*) species along a climatic gradient in NE Spain. *Trees*, **12**: 90-96.

Waring, R.H., Gholz, H.L., Grier, C.C. & Plummer, M.L., 1977. Evaluating stem conducting tissue as an estimator of leaf area in four woody angiosperms. *Can. J. Bot.*, **55**: 1474-1477.

Waring, R.H. & Running, S.W. 1978. Sapwood water storage: its contribution to transpiration and effect upon water conductance through the stems of old-growth Douglas-fir. *Plant Cell Environ.*, **1**: 131-140.

Waring, R.H., Schroeder, P.E. & Oren, R., 1982. Application of the pipe model theory to predict canopy leaf area. *Can. J. For. Res.*, **12**: 556-560.

Whitehead, W.F. & Singh, B.P., 1995. Leaf age affects gas exchange in Okra. *HortScience*, **30**: 1017-1019.

Wullschleger, S.D., 1993. Biochemical limitations to carbon assimilation in C_3 plants. A restrospective analysis of the A/c_i curves from 109 species. *J. Exp. Bot.* **44**. 907-920.

Zimmermann, M.H. & Brown, C.L., 1971. Trees. Structure and function. Springer-Verlang New York.

Zimmermann, M.H., 1983. *Xylem structure and the ascent of sap*. Springer-Verlang, New York.

Zine El Abidine, A., Stewart, J.D., Bernier, P.Y. & Plamondon, A.P. 1995. Diurnal and seasonal variations in gas exchange and water relations of lowland and upland black spruce ecotype. *Can. J. Bot.*, **73**: 716-722.

IX. APPENDIXES

APPENDIX 1

Table A1.1. Literature review of minimum values of pre-dawn (Ψ_p) and noon leaf (Ψ_m) water potentials measured on mature plants of different *Quercus* species.

Specie	Ψ_p	Ψ_m	Site	Reference
Quercus ilex[e]	-3.2	-3.8	Mont Ventoux, SE France	Aussenac & Valette (1982)**
Q. ilex	-1.3	---	Camp Redon, SE France	Acherar & Rambal (1992)
Q. ilex	-2.5	-3.0	Barcelone, NE Spain	Castell et al. (1994)
Q. ilex	-3.6	-4.1	Rome, Italy	De Lillis & Fontanella (1992)*
Q. ilex	-3.1	-3.9	Puechabon, SE France	Rambal (1992)
Q. ilex	-3.2	-4.1	Camp Redon, SE France	Rambal (1992)
Q. ilex	-3.6	-4.0	Prades Mountain, NE Spain	Sala & Tenhunen (1994)
Q. ilex	-3.5	-3.8	near Montpellier, SE France	Damesin (1996)**
Q. ilex	-4.5	---	near Montpellier, SE France	Damesin (1996)**
Q. ilex	-2.5	-3.0	near Sevilla, SW Spain	Our study
Q. agrifolia[e]	≈-4.3	---	California, W USA	Griffin (1973)*
Q. alba[d]	-1.3	-2.9	Missouri, central USA	Bahari et al. (1985)
Q. cerris[d]	-3.0	---	Central Italy	Valentini et al. (1995)**
Q. chrysolepis[e]	≈-5.3	≈-5.4	California, W USA	Rundel (1980)**
Q. coccifera[e]	---	-4.4	near Montpellier, SE France	Duhme & Hinckley (1992)*
Q. coccifera	-2.9	-3.7	near Lisbon, W Portugal	Tenhunen et al. (1985)*
Q. coccifera	-3.7	---	near Montpellier, SE France	Duhme & Hinckley (1992)**
Q. coccifera	-3.4	---	St.Gély du Fesc, SE France	Rambal (1992)
Q. dougasii[d]	-5.0	---	California, W USA	Griffin (1973)*
Q. dougasii	≈-5.2	≈-5.3	California, W USA	Rundel (1980)**

Table A1.1. (Continued)

Specie	Ψ_p	Ψ_m	Site	Reference
Q. dumosa[e]	---	≈-4.2	California, W USA	Krause & Kummerow (1977)**
Q. dumosa	---	-4.2	South California, W USA	Poole & Miller (1981)
Q. dumosa	≈-4.9	≈-5.9	South California, W USA	Hastings et al. (1989)*
Q. kelloggii[d]	≈-2.7	≈-4.0	California, W USA	Rundel (1980)**
Q. pubescens[d]	-2.5	-3.7	Gardiole Forest, S France	Marsteau (1979)**
Q. pubescens	-3.3	-3.7	Mont Ventoux, SE France	Valette (1981)**
Q. pubescens	-3.0	-3.5	near Montpellier, SE France	Damesin (1996)**
Q. pubescens	-4.6	---	near Montpellier, SE France	Damesin (1996)**
Q. pubescens	-2.3	- 3.1	near Vienna, Austria	Hinckley et al (1983)
Q. pyrenaica[d]	---	-3.3	Salamanca, W Spain	Gallego et al. (1994)
Q. rubra[d]	-1.0	-2.7	Missouri, central USA	Bahari et al. (1985)
Q. suber[e]	≈-1.7	≈-3.4	Santiago do Cacém, SW Portugal	Oliveira et al. (1992)
Q. suber	-3.7	---	Camp Redon, SE France	Acherar & Rambal (1992)
Q. turbinella[e]	-3.4	-4.2	California & Arizona, USA	Blake-Jacobson (1987)*
Q. turbinella	-3.3	-4.0	Arizona, W USA	Vankat (1989)**
Q. velutina[d]	-1.0	-2.9	Missouri, central USA	Bahari et al. (1985)
Q. wislizenii[e]	≈-4.7	≈-4.8	California, W USA	Rundel (1980)**

[e] Evergreen species

[d] Deciduous species

* From Rambal & Debussche (1995)

** From Damesin (1996)

APPENDIX 2

Stomatal conductance model

The D_a function used was

if $D_a < 0.6$ then $f(D_a) = 1$

if $D_a > 0.6$ then $f(D_a) = k_0 \exp[-k_1 (D_a - 0.6)] + k_2$ (Eqn. A2.1)

The Ψ_p function used was

if $\Psi_p < 0.3$ then $f(\Psi_p) = 1$

if $\Psi_p > 0.3$ then $f(\Psi_p) = k_3 \exp[-k_4 (\Psi_p - 0.3)] + k_5$ (Eqn. A2.2)

The *PAR* function used was

$f(PAR) = 1 - \exp(-PAR / k_6)$ (Eqn. A2.3)

Photosynthesis model

The net CO_2 assimilation (A_n) was expressed as

$A_n = V_c (1 - (0.5\, o_i / \tau\, c_i) - R_d$ (Eqn. A2.4)

where V_c is the rate of carboxylation, c_i and o_i are the intercellular CO_2 and O_2 concentrations respectively, τ is the substrate specificity factor for the Rubisco (CO_2/O_2-specific ratio), and R_d is the rate of non-photorespiratory respiration.

The rate of carboxylation was assumed to be limited by two factors

$$V_c = \min \{ W_c, W_j \} \qquad \text{(Eqn. A2.5)}$$

where min { } means the minimum of { }, W_c is the Rubisco and W_j is the RuBP-regeneration limited rate of carboxylation. Here, inorganic phosphate regeneration is not considered, as indicated by Sharkey (1985).

These functions are expressed as

$$W_c = (V_{cmax}\, c_i) / (c_i + K_c\,(1 + o_i / K_o)) \qquad \text{(Eqn. A2.6)}$$

and

$$Wj = (J\, c_i) / (4\,(c_i + o_i / \tau) \qquad \text{(Eqn. A2.7)}$$

where V_{cmax} is the maximum rate of carboxylation, K_c and K_o are the Michaelis constants. J is the potential rate of electron transport, which is calculated as

$$J = (\alpha\, I) / (1 + (\alpha^2\, I^2 / J_{max}^2))^{0.5} \qquad \text{(Eqn. A2.8)}$$

where α is the intrinsic quantum efficiency for CO_2 uptake, I is the photon flux density (PPFD) and J_{max} is the rate of electron transport at saturated irradiance.

The temperature dependence of V_{cmax} and J_{max} is given by

$$V_{cmax} = \exp [c-\Delta H_a / (R\, T_k)] / [1 + \exp [(\Delta S\, T_k - \Delta H_d) / (R\, T_k)]] \qquad \text{(Eqn. A2.9)}$$

$$J_{max} = T_k \exp [c-\Delta H_a / (R\, T_k)] / [1 + \exp [(\Delta S\, T_k - \Delta H_d) / (R\, T_k)]] \qquad \text{(Eqn. A2.10)}$$

where T_k is the absolute leaf temperature, R is the universal gas constant, c is a (dimensionless) scaling constant, ΔH_a and ΔH_d are the energy of activation and deactivation respectively, and ΔS is an entropy term.

MAIN SYMBOLS AND ABBREVIATIONS

This table contain the main symbols and abbreviations used throughout the text.

Symbol & Abbreviation	Unit	Description
Ω	dimensionless	Decoupling coefficient
Ω_c	dimensionless	Canopy to air decoupling coefficient
Ω_l	dimensionless	Leaf to air decoupling coefficient
λ	J kg^{-1}	Latent heat of vaporisation of water
τ	dimensionless	Substrate specificity factor for the Rubisco (CO_2/O_2-specific ratio)
α	mol electron mol $photon^{-1}$	Intrinsic quantum efficiency for CO_2 uptake
γ	66.1 Pa	Psychrometric constant
ρ_a	Kg m^{-3}	Density of air saturated with water vapour
Ψ_m	MPa	Noon leaf water potential
Ψ_p	MPa	Pre-dawn leaf water potential
A_n	µmol m^{-2} s^{-1}	Net CO_2 assimilation
ASW	mm	Available soil water
c_a	µmol m^{-2} s^{-1}	Air CO_2 concentration
c_i	µmol m^{-2} s^{-1}	Intercellular CO_2 concentration
c_p	J Kg^{-1} K^{-1}	Molar heat capacity of dry air at constant pressure
D_a	kPa	Leaf to air water vapour pressure deficit
D_{ch}	kPa	Leaf to chamber water vapour pressure deficit
D_l	kPa	Leaf to boundary layer water vapour pressure deficit
DSWS	mm	Driest soil water storage

Symbol & Abbreviation	Unit	Description
e_a	kPa	Air water vapour pressure
e_s	kPa	Surface water vapour pressure
E_c	mol m^{-2} s^{-1}	Canopy transpiration
E_l	mmol m^{-2} s^{-1}	Leaf transpiration
ETP	mm	Potential evapotranspiration
ETR	mm	Real evapotranspiration
g_a	mmol m^{-2} s^{-1}	Canopy boundary layer conductance
g_b	mmol m^{-2} s^{-1}	Leaf boundary layer conductance
g_c	mmol m^{-2} s^{-1}	Canopy conductance
g_r	mmol m^{-2} s^{-1}	Radiative conductance
g_s	mmol m^{-2} s^{-1}	Leaf stomatal conductance
g_{sm}	mmol m^{-2} s^{-1}	Maximum leaf stomatal conductance
H_g	MJ m^{-2}	Daily accumulated solar global radiation
I	µmol m^{-2} s^{-1}	Photon flux density (PPFD)
J	µmol electrons m^{-2} s^{-1}	Potential rate of electron transport
J_{max}	µmol electrons m^{-2} s^{-1}	Rate of electron transport at saturated irradiance
K_c	dimensionless	Michaelis constants
K_o	dimensionless	Michaelis constants
LAI	m^2 m^{-2}	Leaf area index
$MSWS$	mm	Maximum soil water storage
o_i	µmol m^{-2} s^{-1}	Intercellular O_2 concentrations
P	KPa	Air pressure
PAR	µmol m^{-2} s^{-1}	Photosynthetically active radiation (400-700 nm)
R	dimensionless	Universal gas constant
R_d	µmol m^{-2} s^{-1}	Rate of non-photorespiratory respiration
R_g	W m^{-2}	Solar global radiation
R_n	W m^{-2}	Solar net radiation

Symbol & Abbreviation	Unit	Description
s	Pa $^{o}C^{-1}$	Slope of the saturation vapour pressure curve to temperature
T_a	^{o} C	Air temperature
T_c	^{o} C	Canopy temperature
T_{ch}	^{o} C	Chamber air temperature
T_d	^{o} C	Dew point temperature
T_k	^{o} K	Absolute leaf temperature
T_l	^{o} C	Leaf temperature
TRh	mm	Transpiration per hectare
TRt	mm	Transpiration per tree
u	m s^{-1}	Windspeed
v	m^3 m^{-2} h^{-1}	Sap flow density
V_c	µmol CO_2 m^{-2} s^{-1}	Rate of carboxylation
V_{cmax}	µmol CO_2 m^{-2} s^{-1}	Maximum rate of carboxylation
W_c	µmol CO_2 m^{-2} s^{-1}	Rubisco limited rate of carboxylation
W_j	µmol CO_2 m^{-2} s^{-1}	RuBP-regeneration limited rate of carboxylation
WUE	µmol CO_2 mmol H_2O^{-1}	Water use efficiency

FIGURE CAPTIONS

TABLES CAPTIONS